Appendix A: Figures[1]

Note Regarding Restricted content

The "Figures" section of this thesis, separated as Appendix A, is under embargo until publication permits will be granted for material therein (e.g. photographs of finds, archival cards), produced by rescue excavations conducted by Ephorates of Antiquities in Greece, which is the property of the Hellenic Ministry of Culture. The only exception to this are thirteen figures essential to the thesis that were incorporated in-text, five of which were created by and are the property of the author—Figure 15, Figure 16, Figures 193-195—and eight of which are maps kindly made by Dr Hallvard Indgjerd to be used in this thesis—Figure 2, Figure 5, Figure 14, Figure 40, Figure 102, Figure 130, Figure 132, and Figure 190. To maintain the original order of the "Figures" section, these thirteen figures are also kept in their original places herein.

[1] All pictures and charts by the Author unless otherwise specified. All finds illustrated without a scale have been reduced in scale proportionately to other finds shown on the same page. The maps were made by Hallvard Indgjerd, using a base map originally developed by the Author by adapting a map of the Copernicus Land Monitoring Service; we have extended the area filled by the Ambracian Gulf to the north of its present-day shores in order to reflect its extent in antiquity.

Figure 1. Approaching Epirus from the Ionian Sea (Photo: Hallvard Indgjerd)

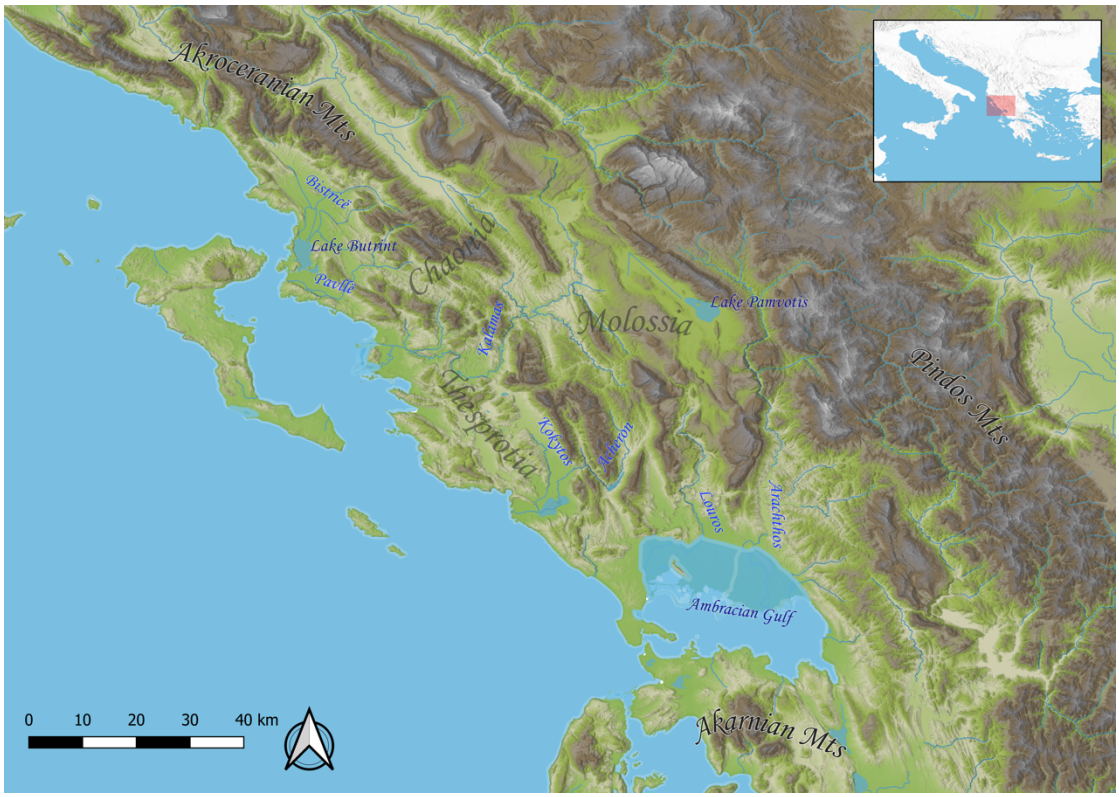

Figure 2. Map of the landscape of Epirus, showing natural features and the approximate locations of the regions of Molossia, Thesprotia and Chaonia (Map made by Hallvard Indgjerd)

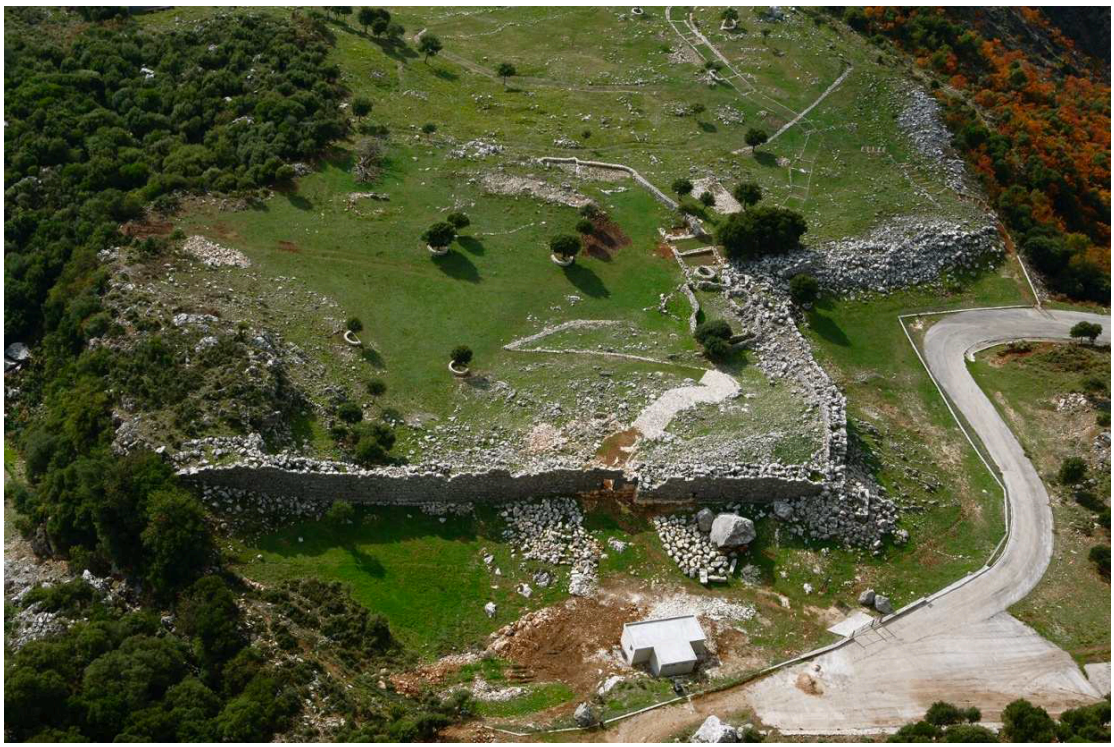

Figure 3. Elea, eastern segment, northern fully collapsed fortifications (the stretch at the centre of the picture restored during modern times; Spanodimos 2014, fig. 53)

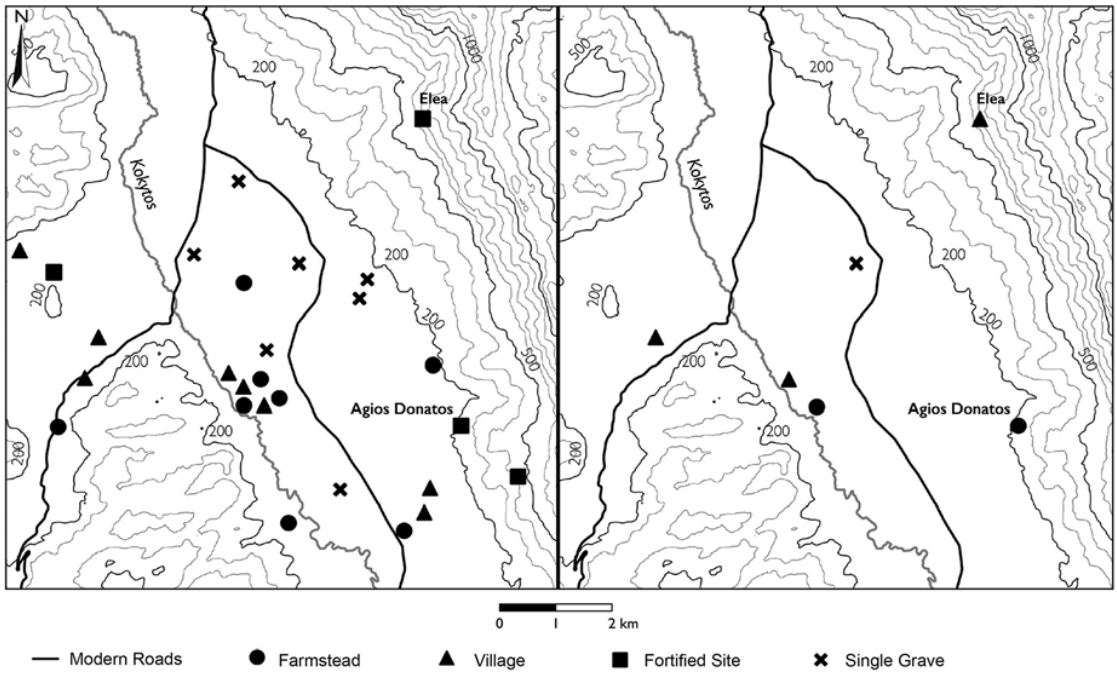

Figure 4. Maps showing the Late Classical to Early Hellenistic sites (left) and the Late Hellenistic to Early Roman sites (right) of the Kokytos valley (Forsen 2021, fig. 10.1)

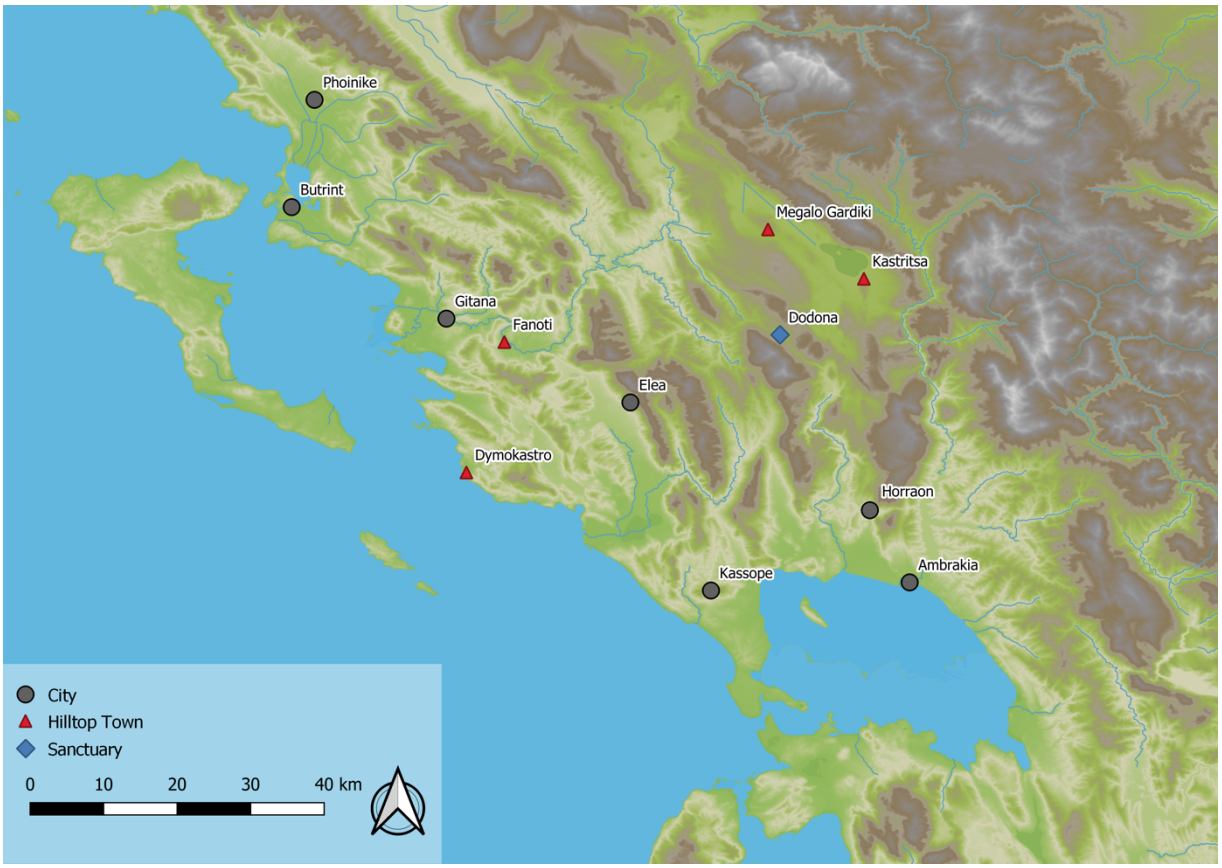

Figure 5. Map showing the location of cities and towns in Epirus inhabited both in Hellenistic and early Roman times (Map made by Hallvard Indgjerd)

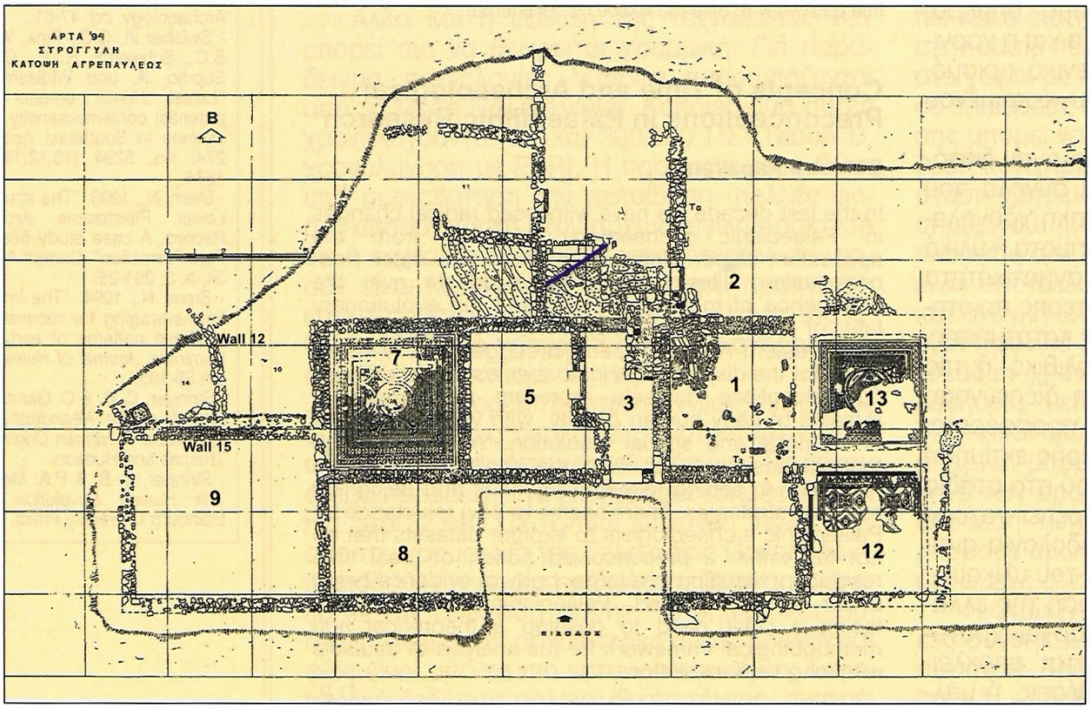

Figure 6. Strongyli, plan of the villa residential quarters (after Ntouzougli 1998, fig. 2)

Figure 7. Strongyli, oilery

Figure 8. The south-eastern projecting arm of the Kerasonas Valley, where the villa near Agios Georgios was located

Figure 9. The valley of Kerasonas, with the villa near Agios Georgios located immediately below the road seen in the foreground

Figure 10. The still-bubbling spring near the Agios Georgios villa. Notice the concentric circles created by the bubble rings as they reach the surface

Figure 11. Malathrea, approach to a fortified rural structure

Figure 12. Malathrea, view of central courtyard from the south-eastern tower (Çondi 1984, fig. 3.)

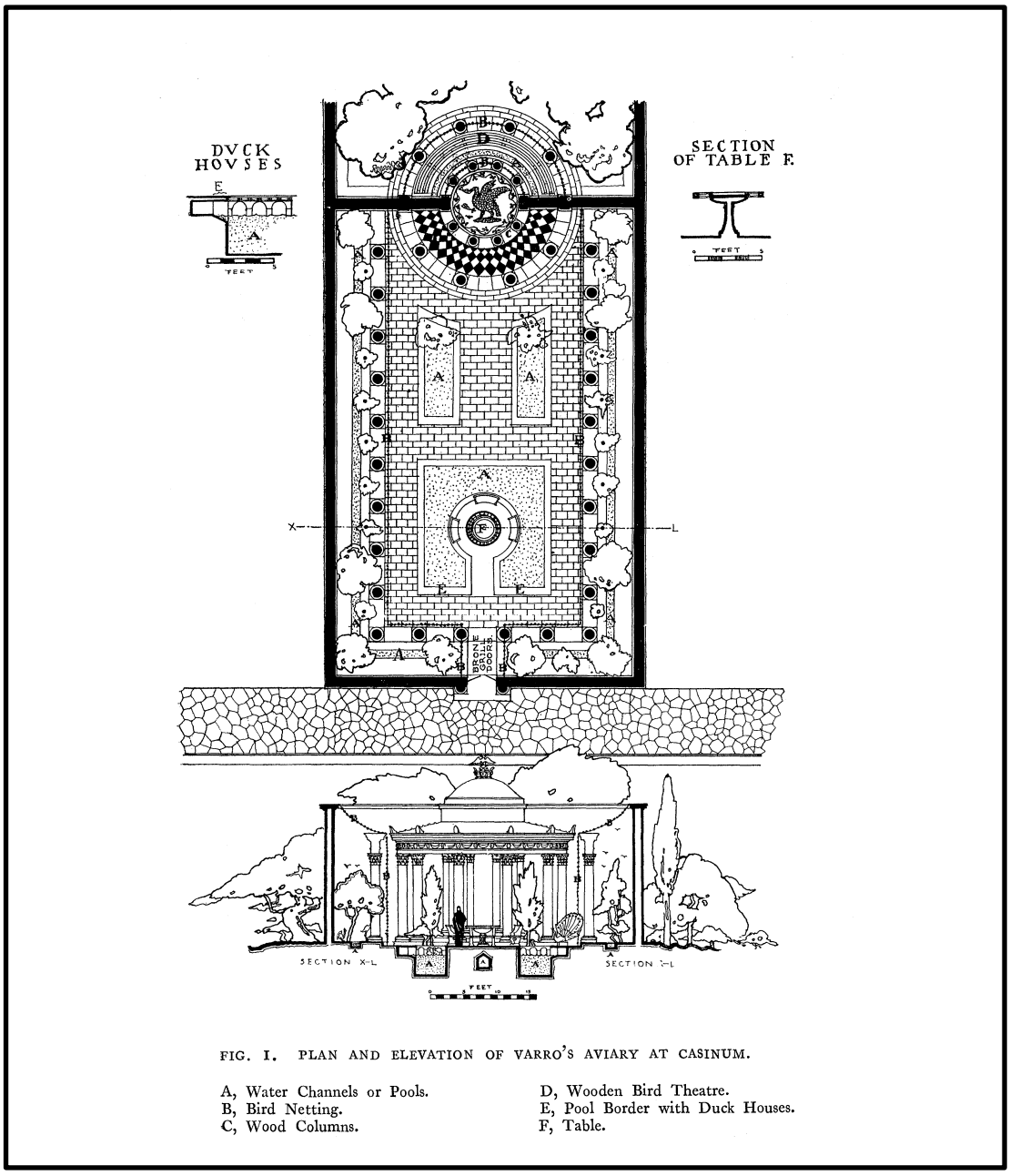

FIG. I. PLAN AND ELEVATION OF VARRO'S AVIARY AT CASINUM.

A, Water Channels or Pools.
B, Bird Netting.
C, Wood Columns.
D, Wooden Bird Theatre.
E, Pool Border with Duck Houses.
F, Table.

Figure 13. Hypothetical reconstruction of the Ornithon *of Varro's* villa *near* Casinum *by Buren and Kennedy (1919, fig. 1)*

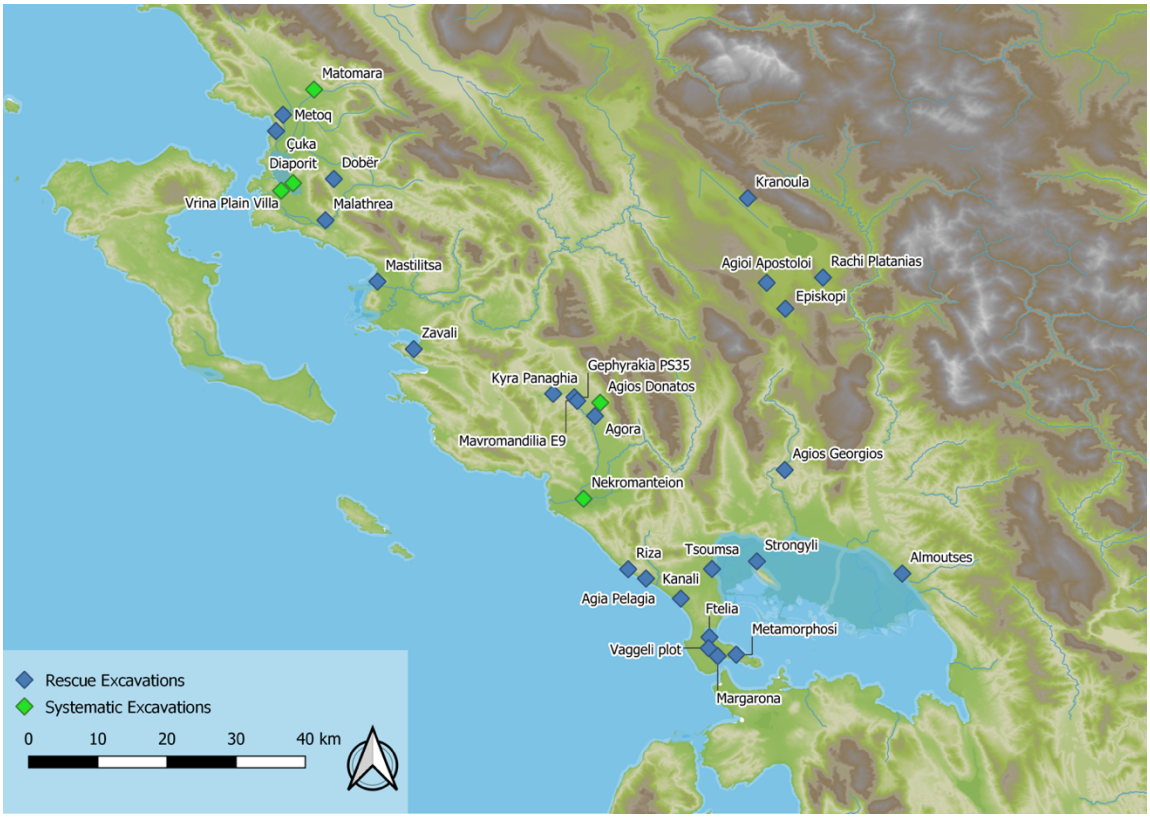

Figure 14. Map of main rural sites discussed in the thesis, systematically excavated (the five rhombi) and excavated in salvage projects (the circles). They are primarily located (from south to north) around the Ambracian Gulf, in the Kokytos valley near modern-day Paramythia, in the Ioannina basin, and in coastal Chaonia (Map made by Hallvard Indgjerd)

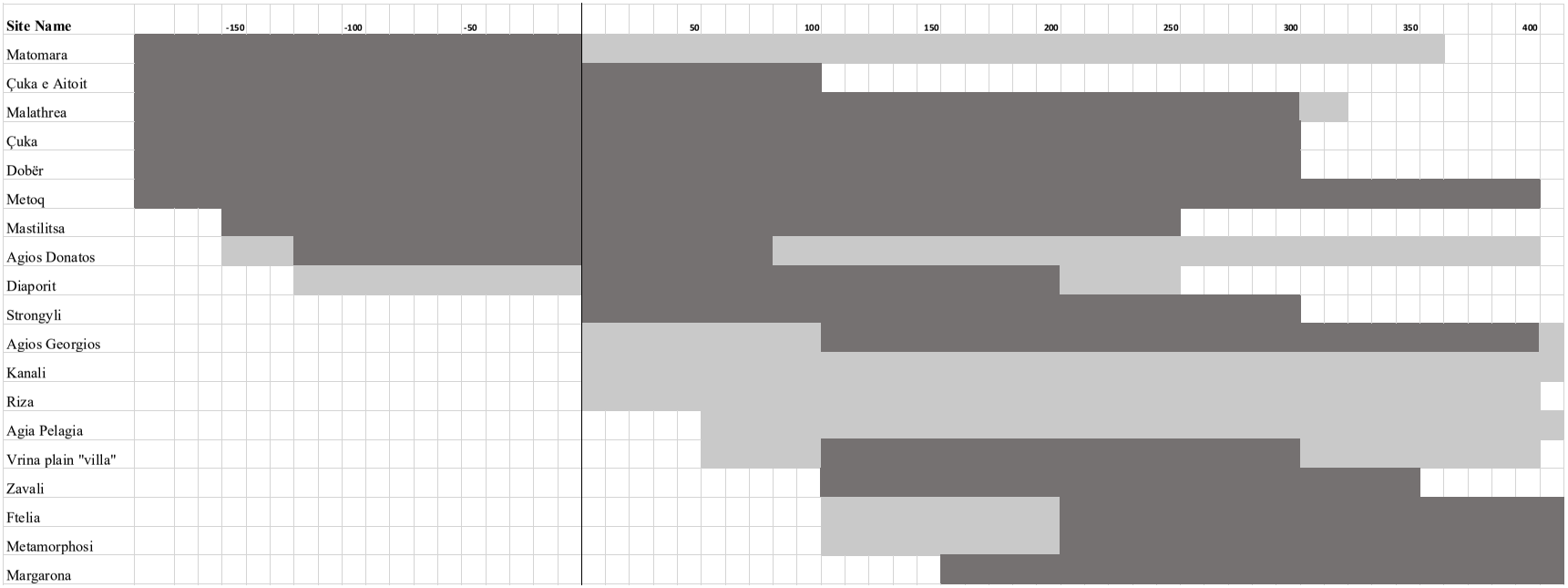

Figure 15. Chronology for supposed villa sites.
Light grey corresponds to possible occupation and dark grey to definite occupation, suggested before the work undertaken for this thesis.

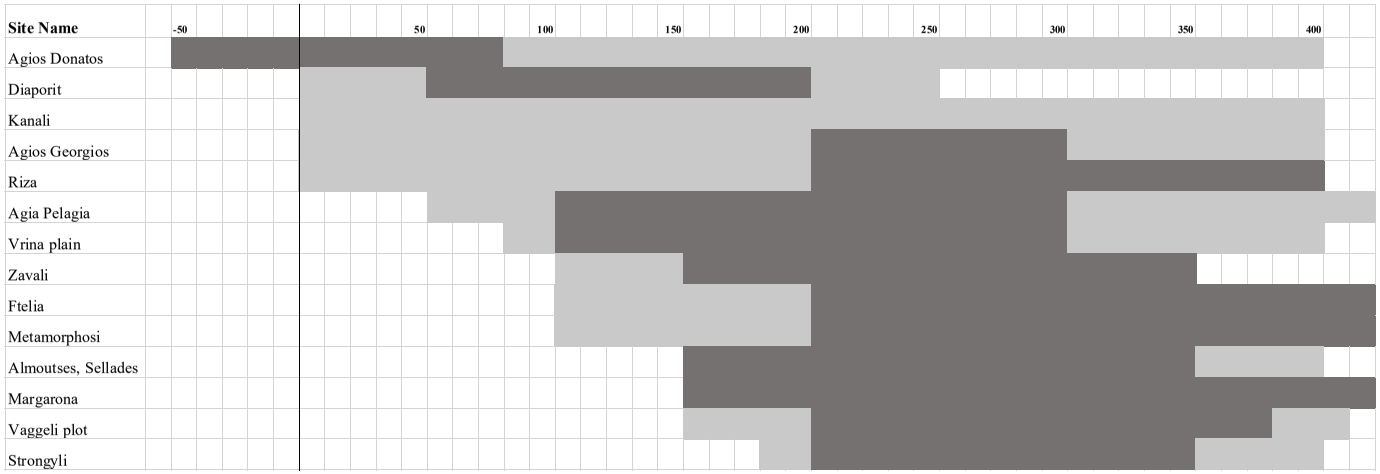

Figure 16. My chronology for villas in Epirus.
Light grey corresponds to possible occupation and dark grey to definite occupation.

Figure 17. Strongyli, mosaic 7 (Chiotis 1998, fig. 8)

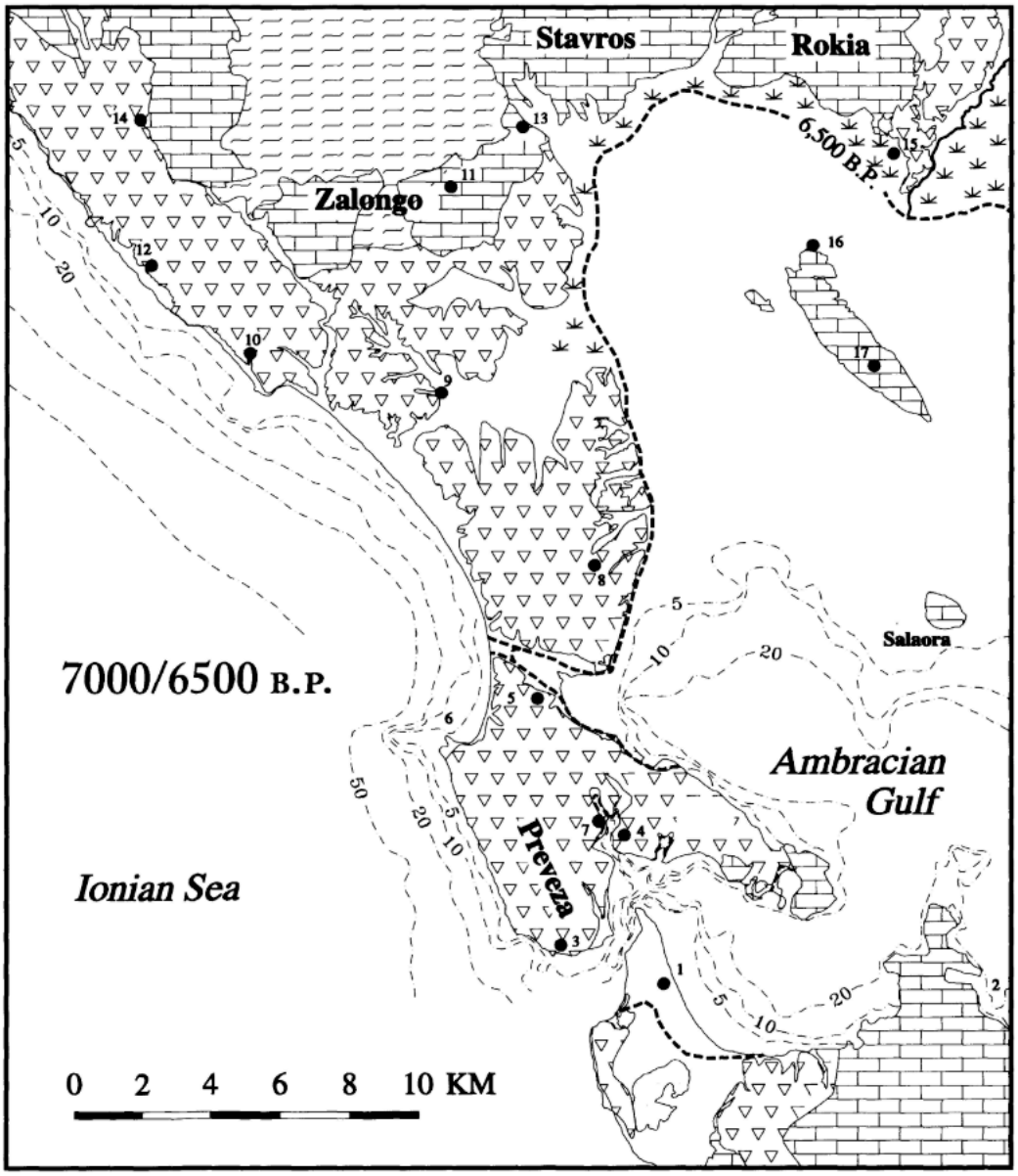

Figure 18. Palaeographic reconstruction of the western Ambracian embayment and the Preveza peninsula: 5,050/4,550 BCE (Jing and Rapp 2003, fig. 5.21a)

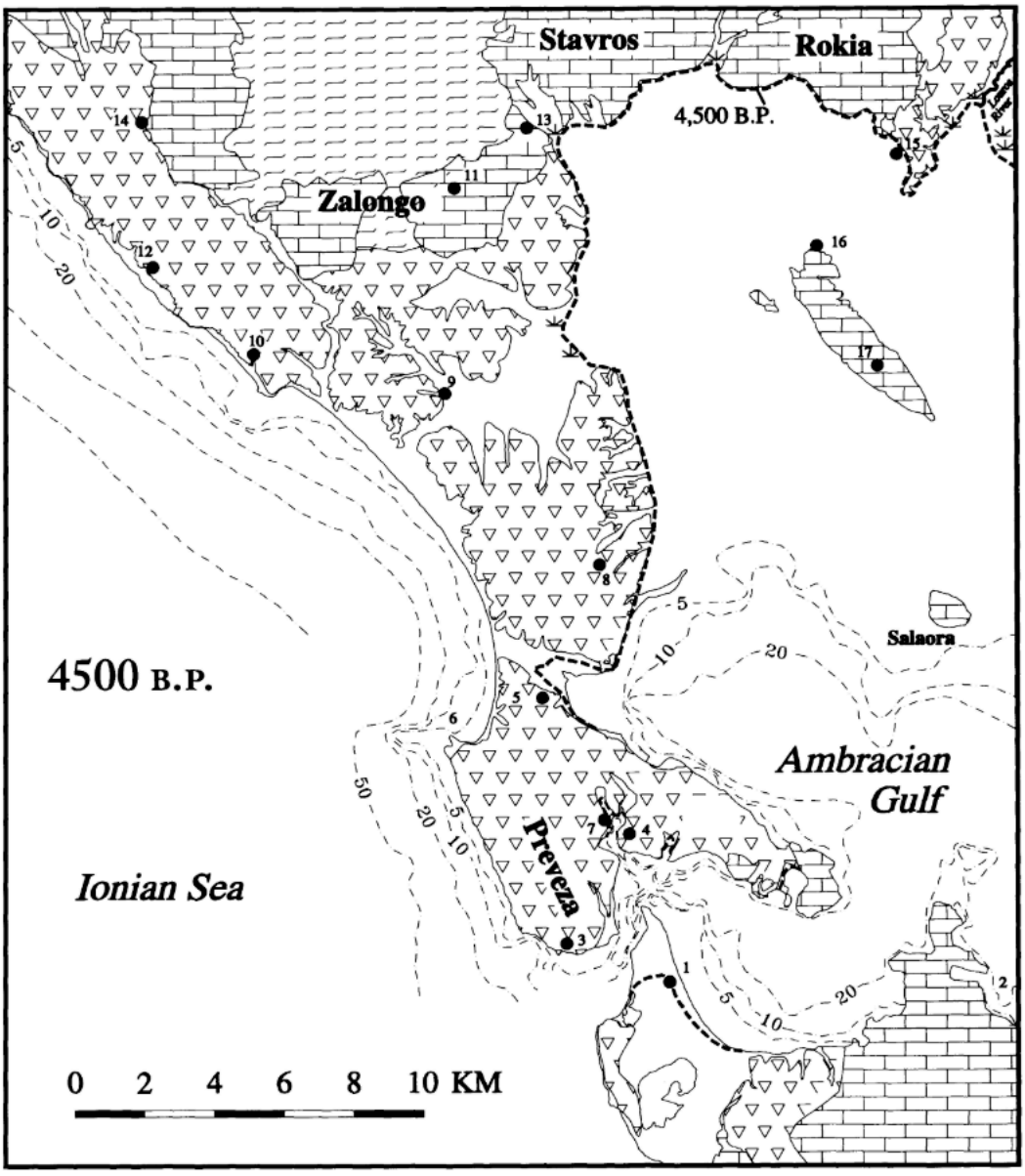

Figure 19. Palaeographic reconstruction of the western Ambracian embayment and the Preveza peninsula: 2,550 BCE (Jing and Rapp 2003, fig. 5.21b)

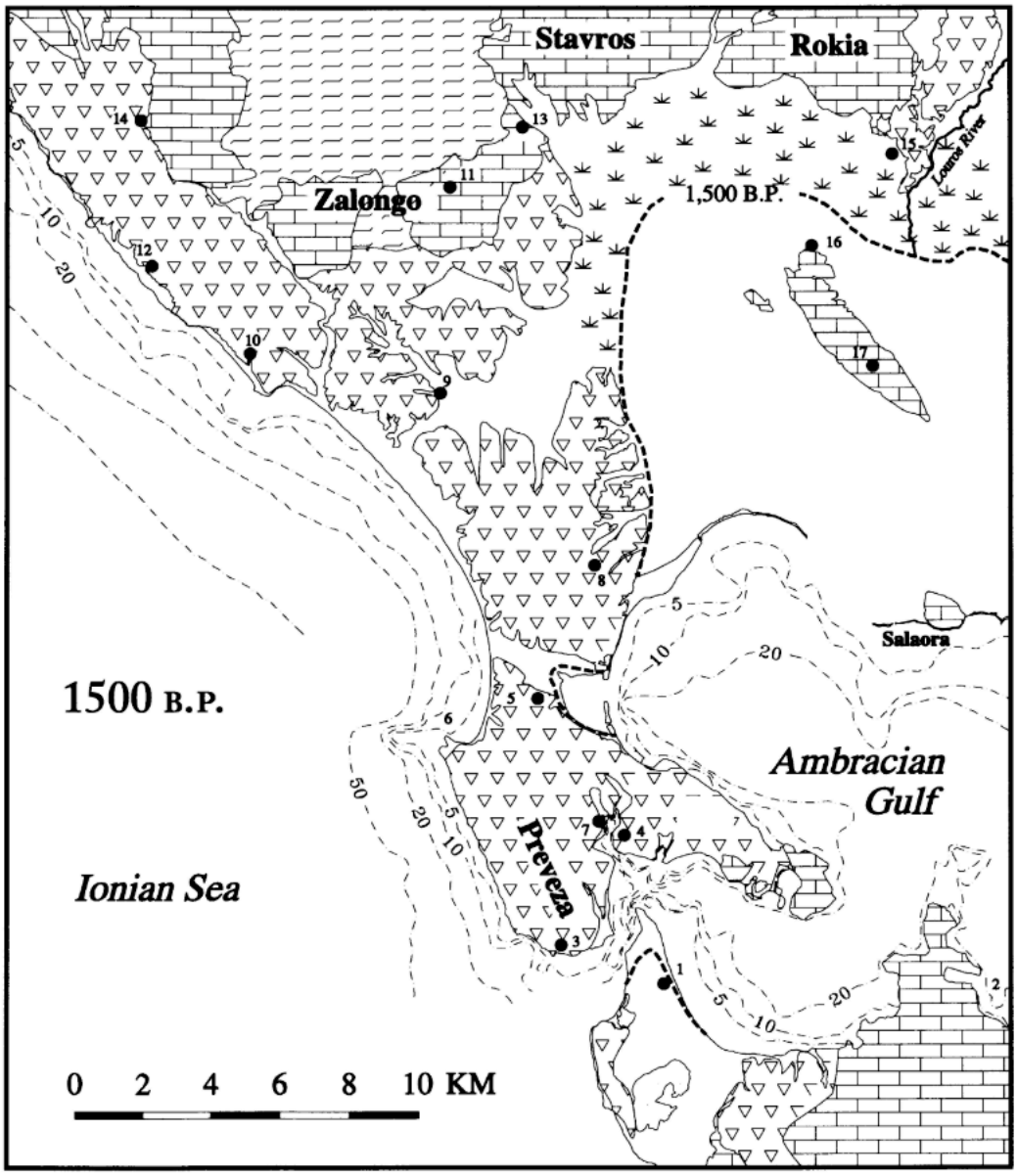

Figure 20. Palaeographic reconstruction of the western Ambracian embayment and the Preveza peninsula: 450 CE (Jing and Rapp 2003, fig. 5.21c)

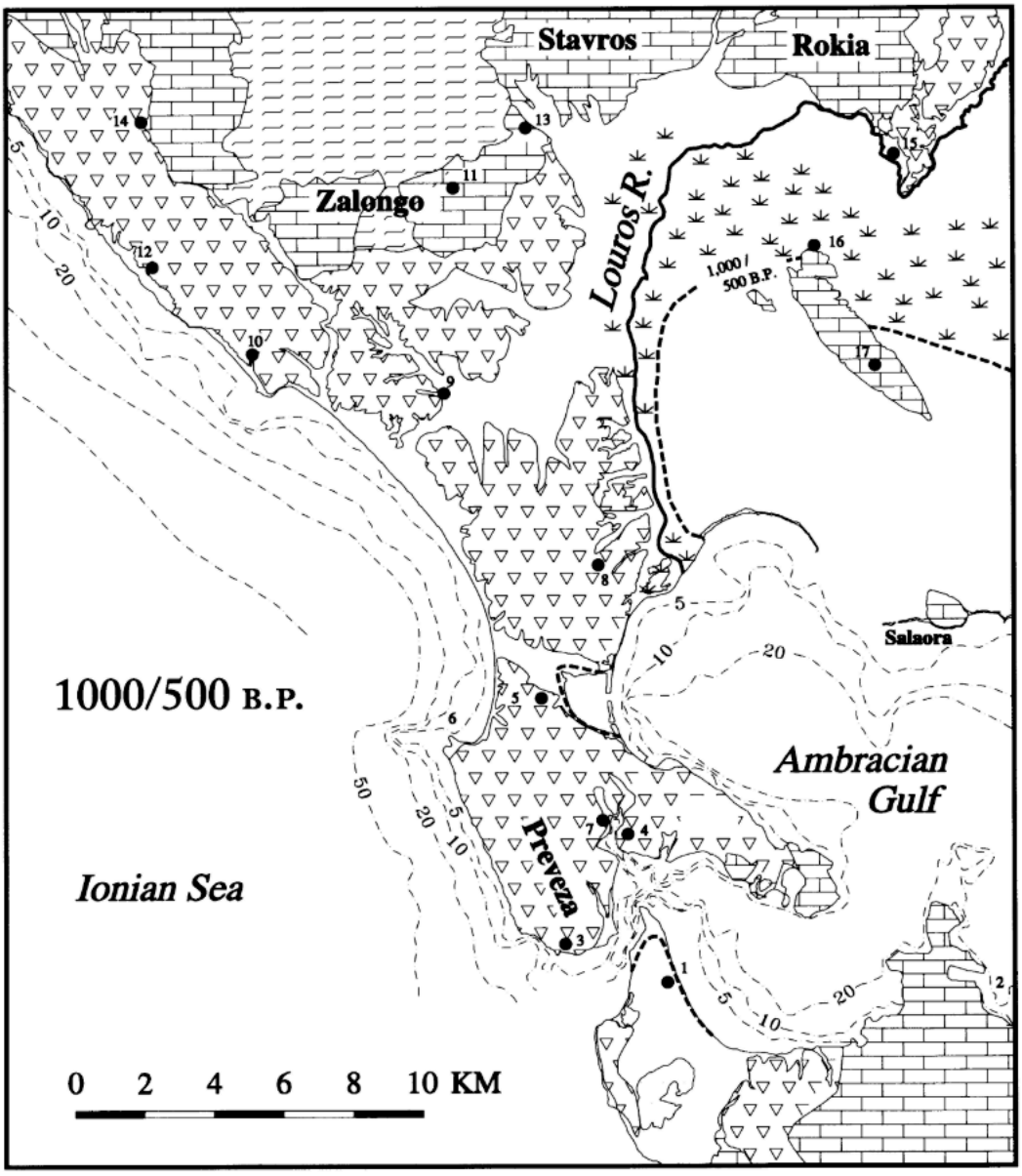

Figure 21. Palaeographic reconstruction of the western Ambracian embayment and the Preveza peninsula: 950/1450 CE (Jing and Rapp 2003, fig. 5.21d)

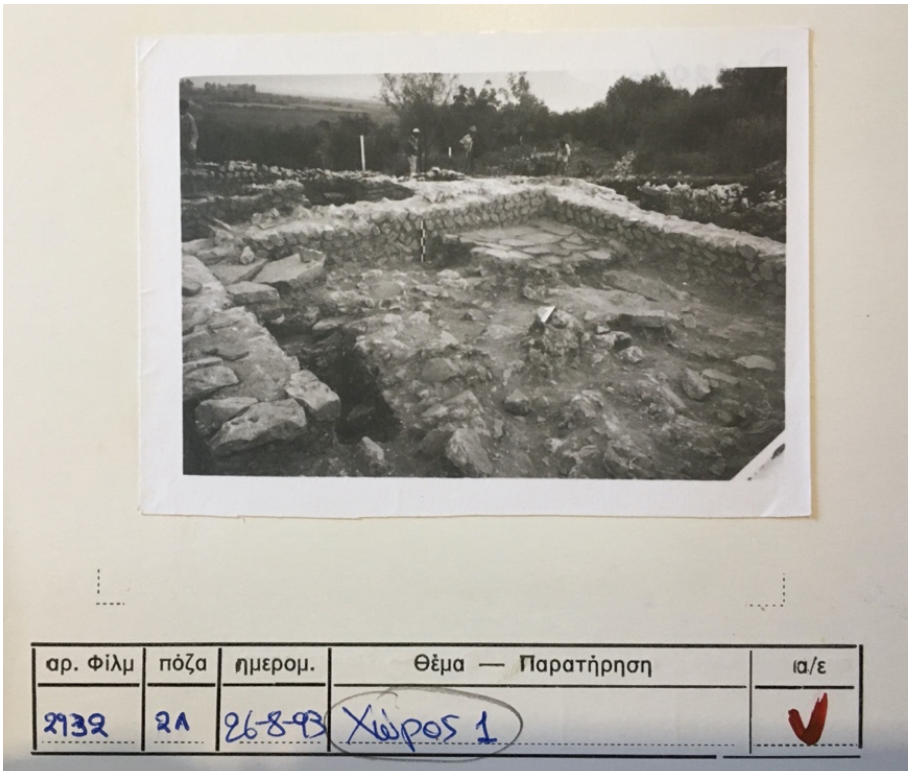

Figure 22. Strongyli, pars urbana *room 1, filled with rubble and collapsed pieces probably of an upper-storey mosaic floor, later haphazardly re-assembled in a corner of the room (Ephorate of Antiquities of Arta, Photocard)*

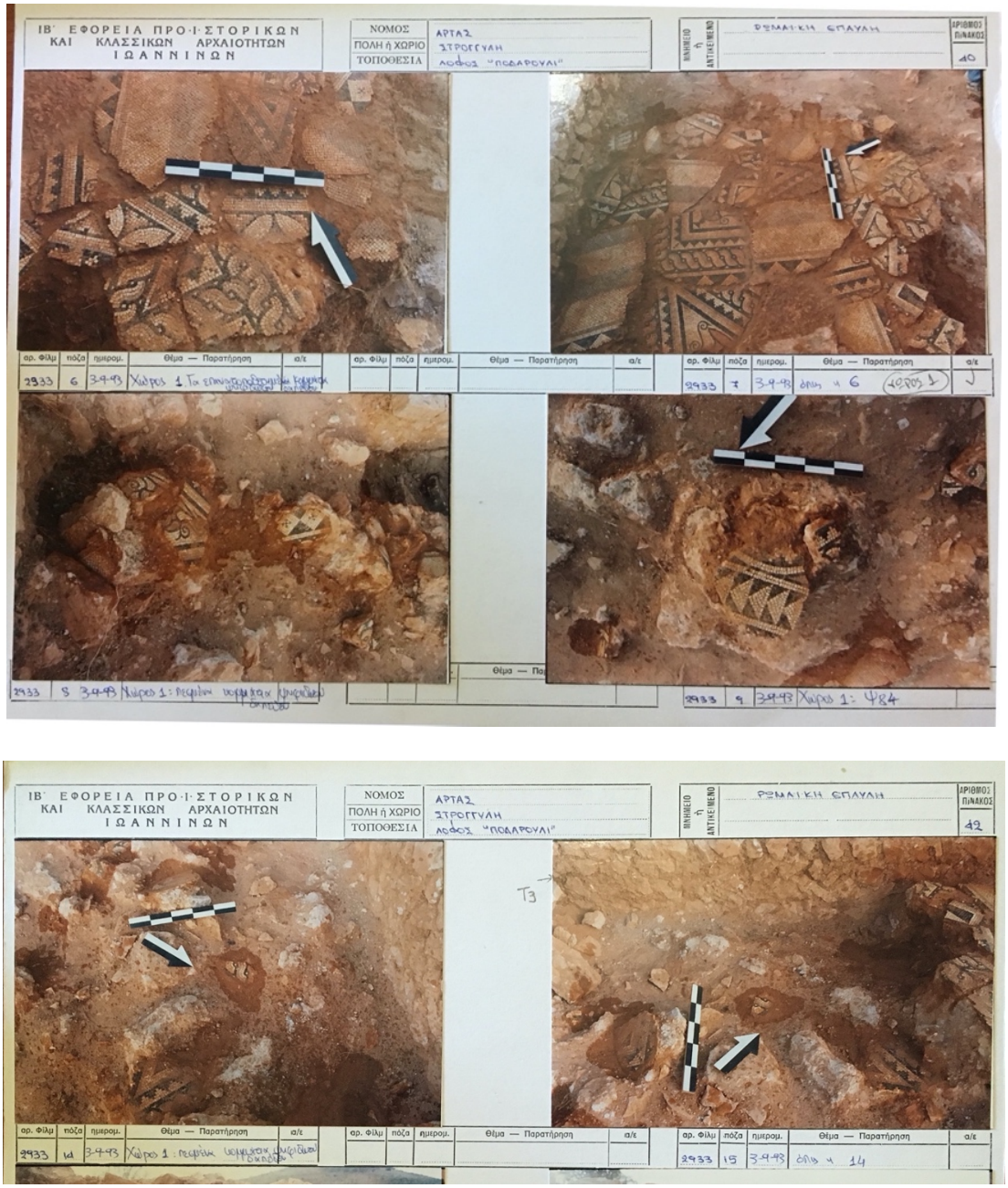

Figure 23. Strongyli, pars urbana *room 1, details of re-assembled and overturned mosaic pieces (Ephorate of Antiquities of Arta, Photocards)*

Figure 24. Utica, House of the Grand Oecus, room with collapsed upper storey mosaic floor (Fentress and Wilson 2021)

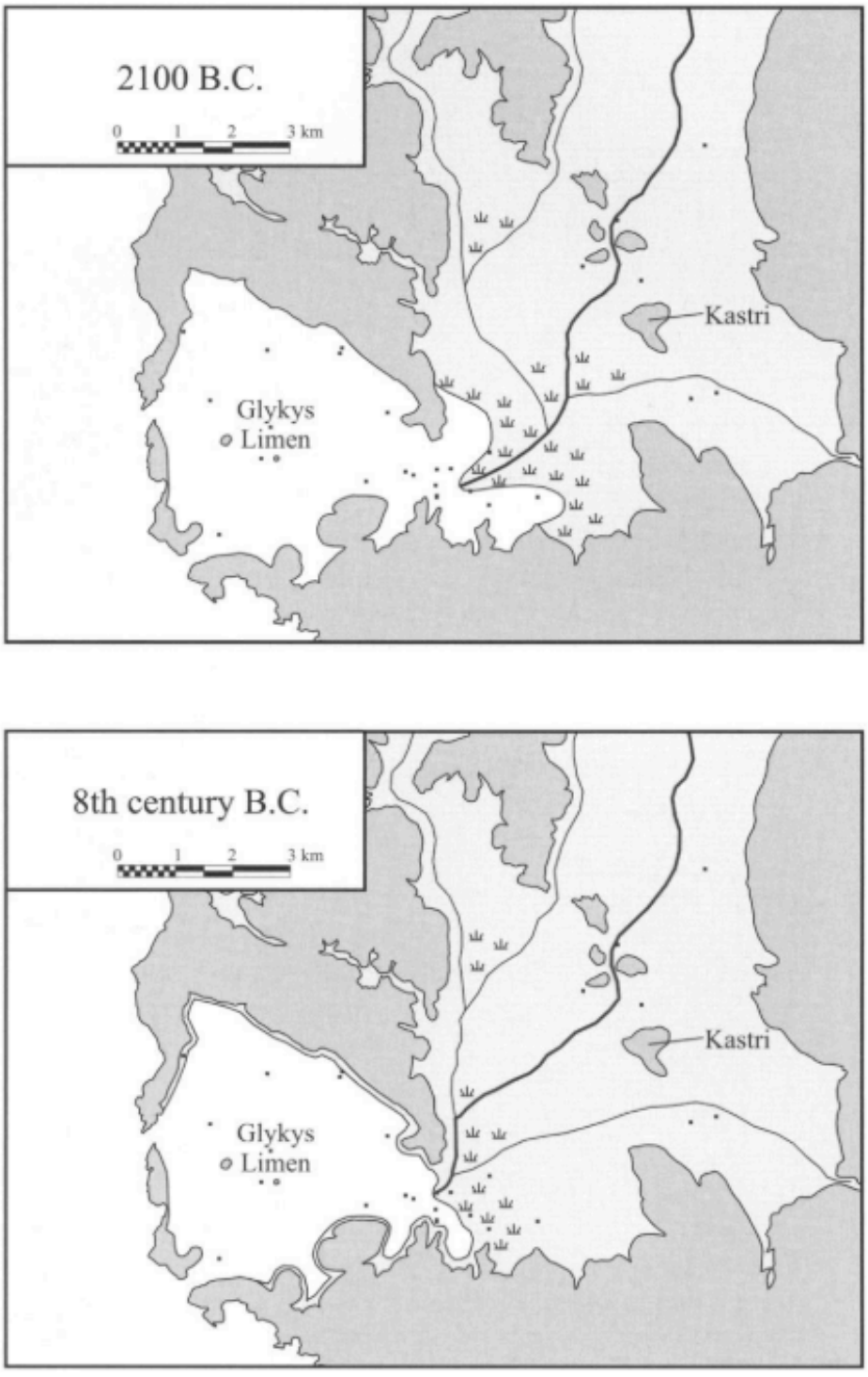

Figure 25. Paleogeographic reconstructions of the lower Acheron river valley at 2,100 BCE and in the 8th century BCE, with the small black squares pinpointing core locations (Besonen et al 2003, fig. 6.12)

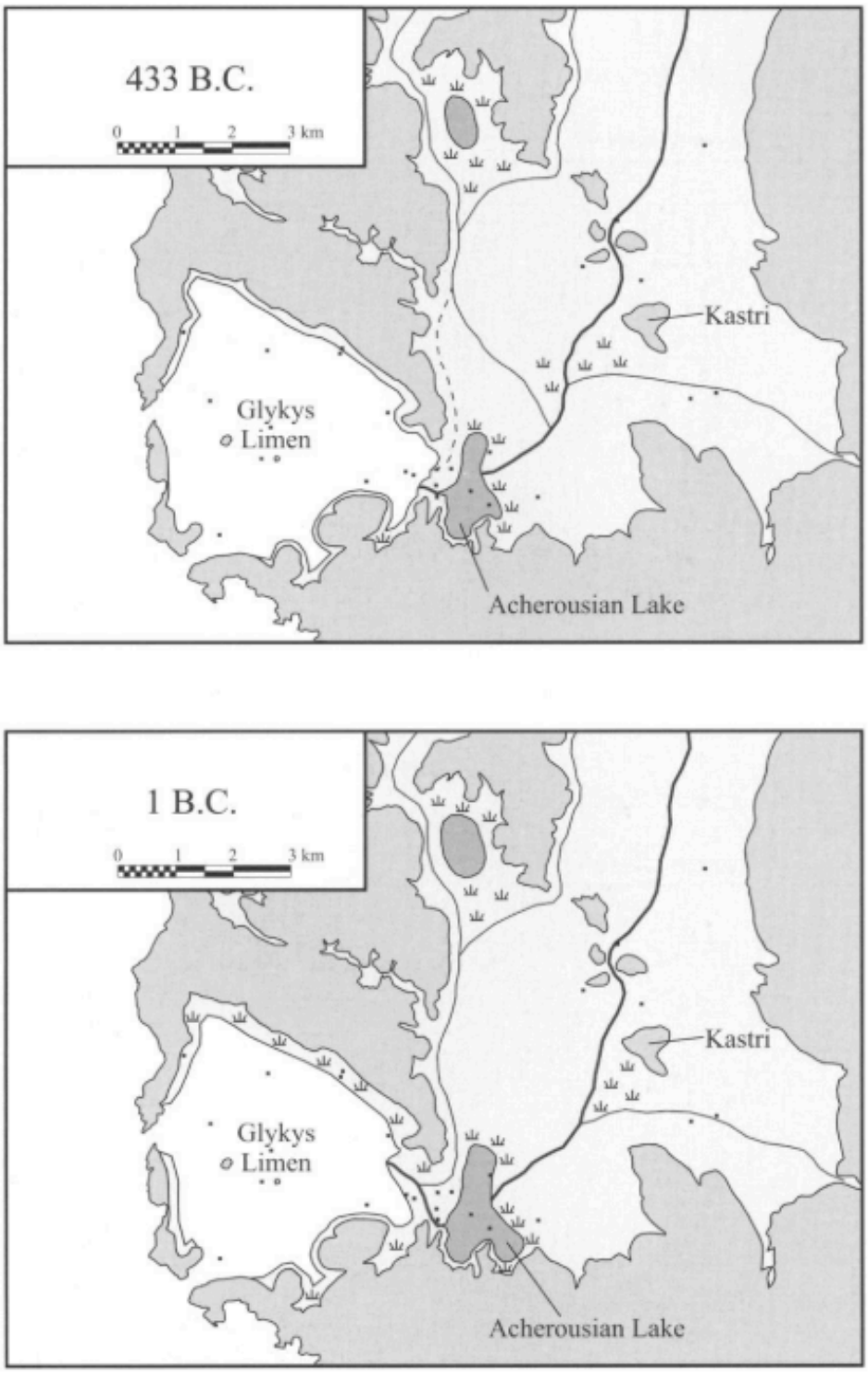

Figure 26. Paleogeographic reconstructions of the lower Acheron river valley at 433 and 1 BCE (Besonen et al 2003, fig. 6.13)

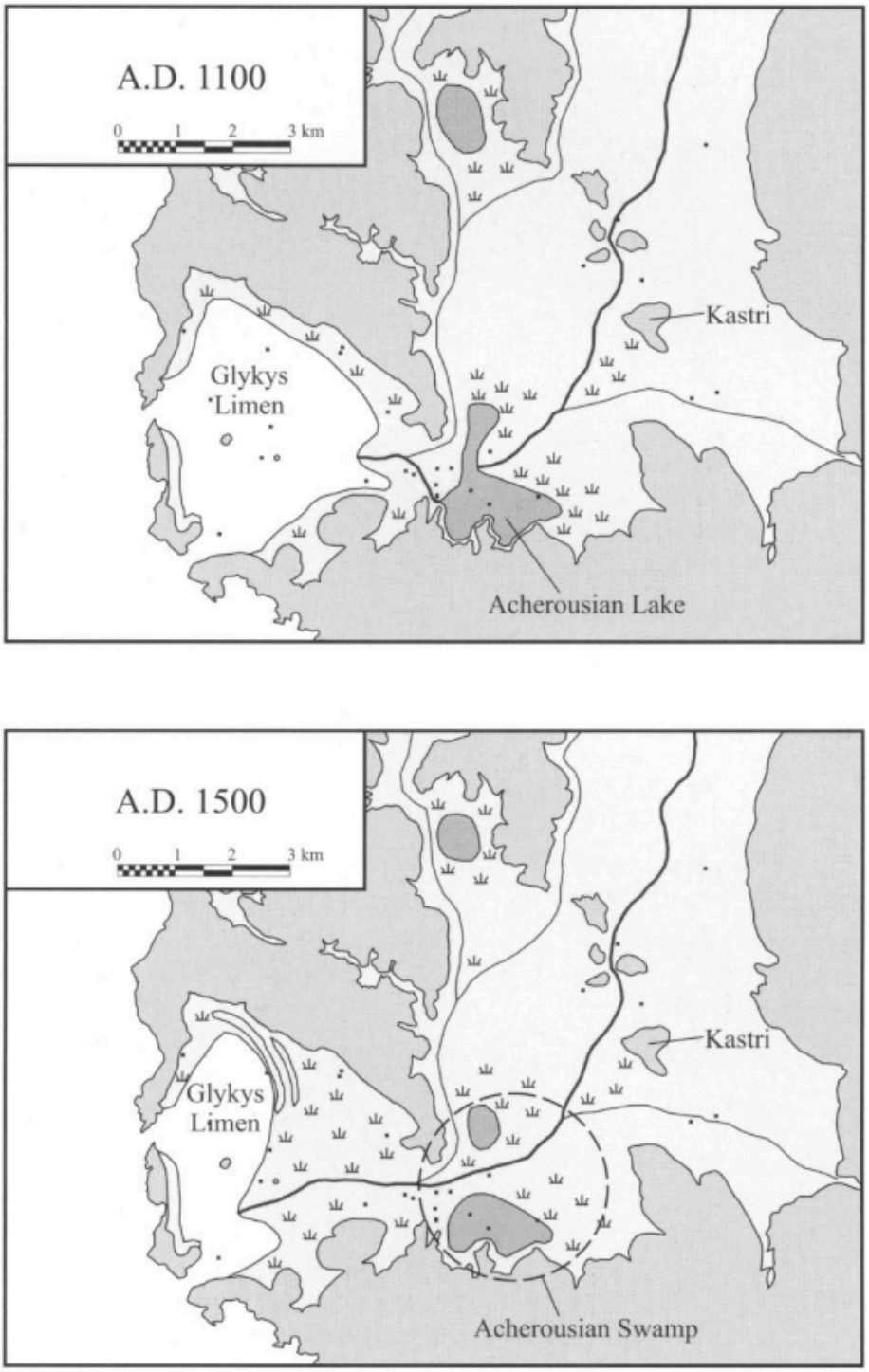

Figure 27. Paleogeographic reconstructions of the lower Acheron river valley at 1,100 CE and 1,500 CE (Besonen et al 2003, fig. 6.14)

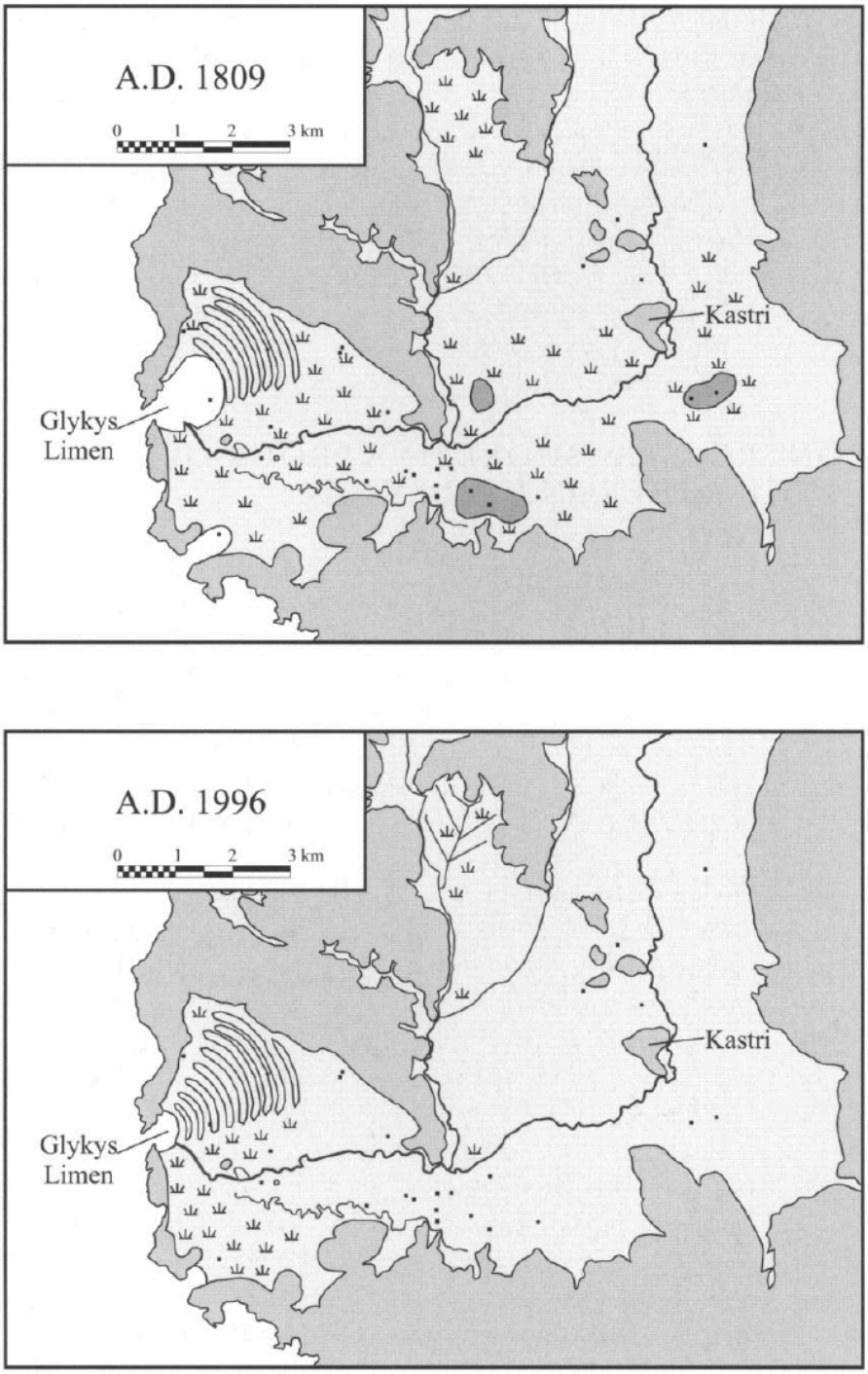

Figure 28. Paleogeographic reconstructions of the lower Acheron river valley at 1,809 CE and 1,996 CE (Besonen et al 2003, fig. 6.15)

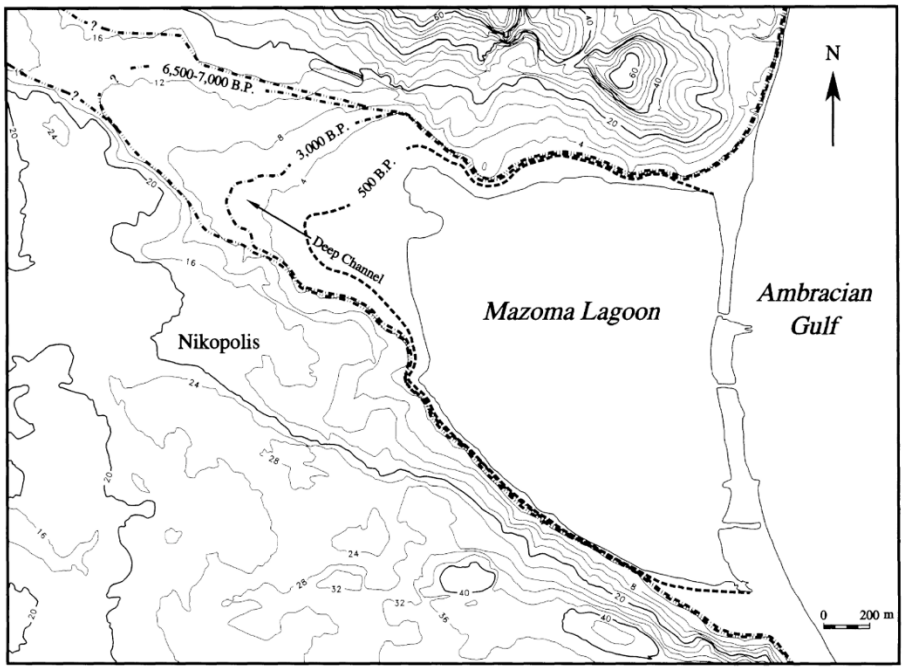

Figure 29. The marine regression of the eastern shoreline of the so-called "Nikopolis isthmus", with marked dates Before Present corresponding to 5,050/4,550 BCE, 1,050 BCE and 1450 CE (Jing and Rapp 2003, fig. 5.10)

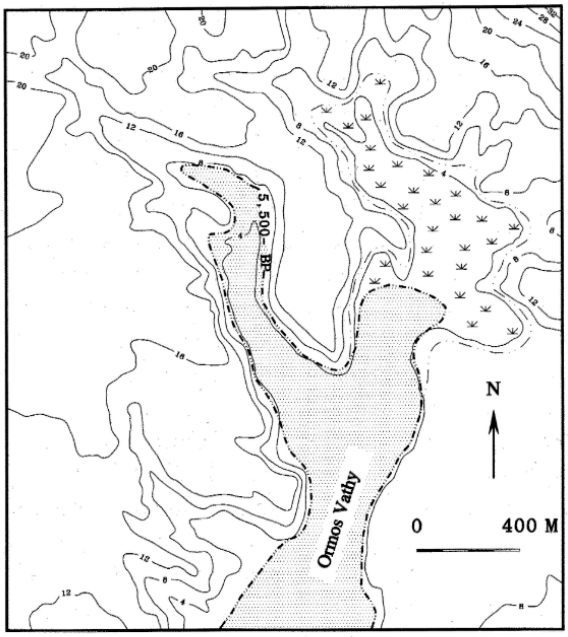

Figure 30. Ormos Vathy shoreline progradation in the Neolithic Period (after Jing and Rapp 2003, fig. 5.12)

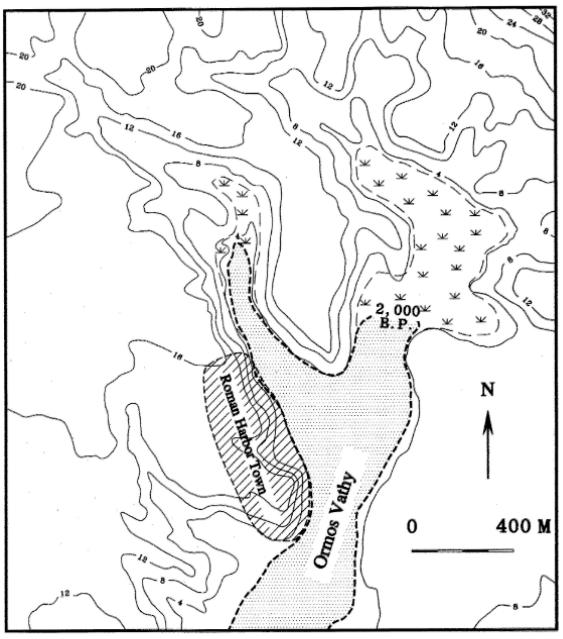

Figure 31. Ormos Vathy shoreline progradation in the Roman period (after Jing and Rapp 2003, fig. 5.12)

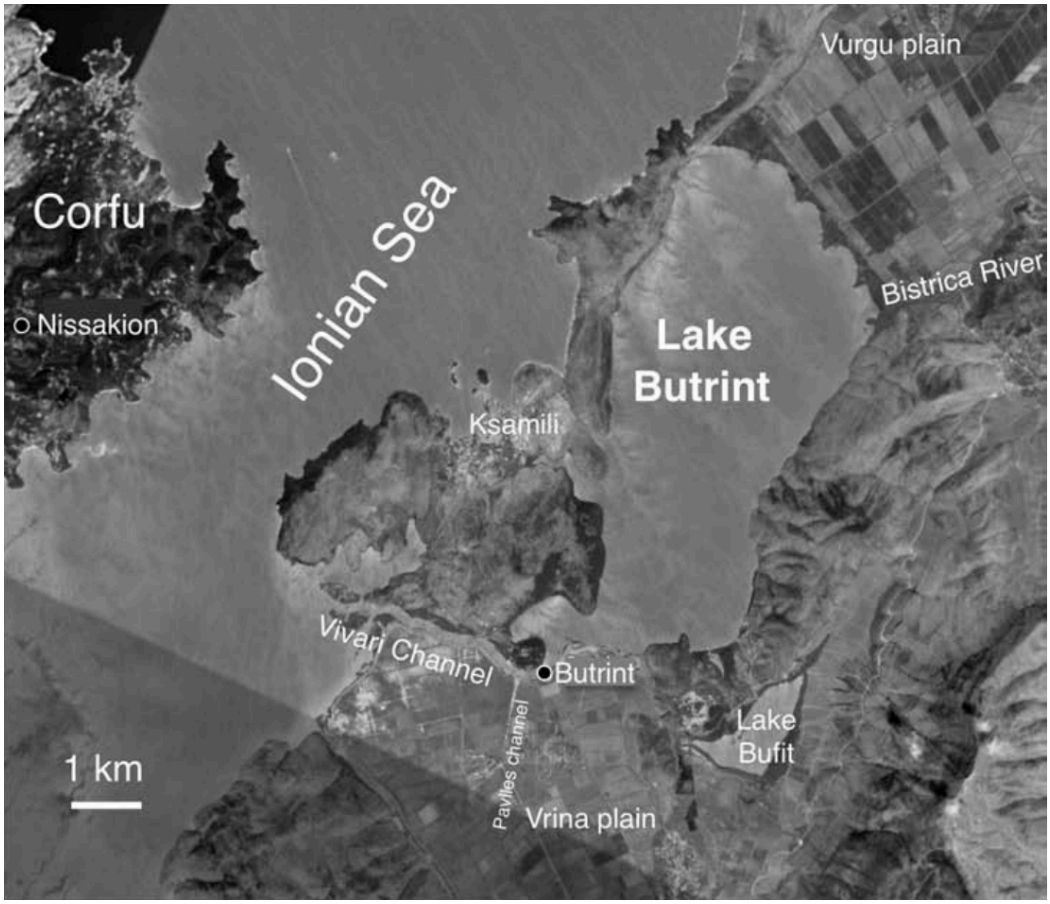

Figure 32. Aerial of Lake Butrint in the present-day (Ariztegui et al 2010, fig. 1)

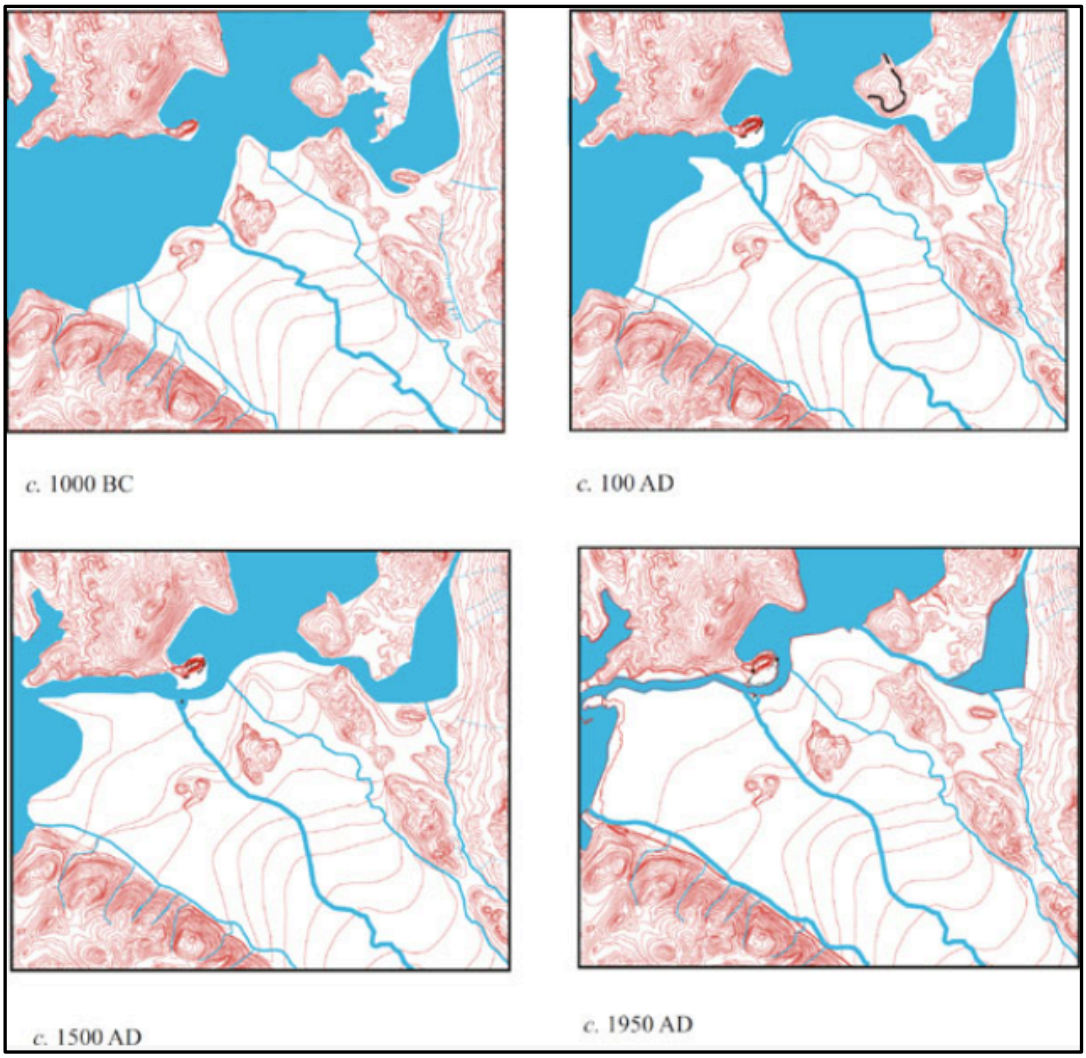

Figure 33. Hypothetical reconstructions based on palaeographic studies of the changing environment and topography surrounding Butrint from 1,000 BCE-1950 CE, showing its development from a coastal to an inland site (Martin 2004, fig. 6.1, from IWA archive)

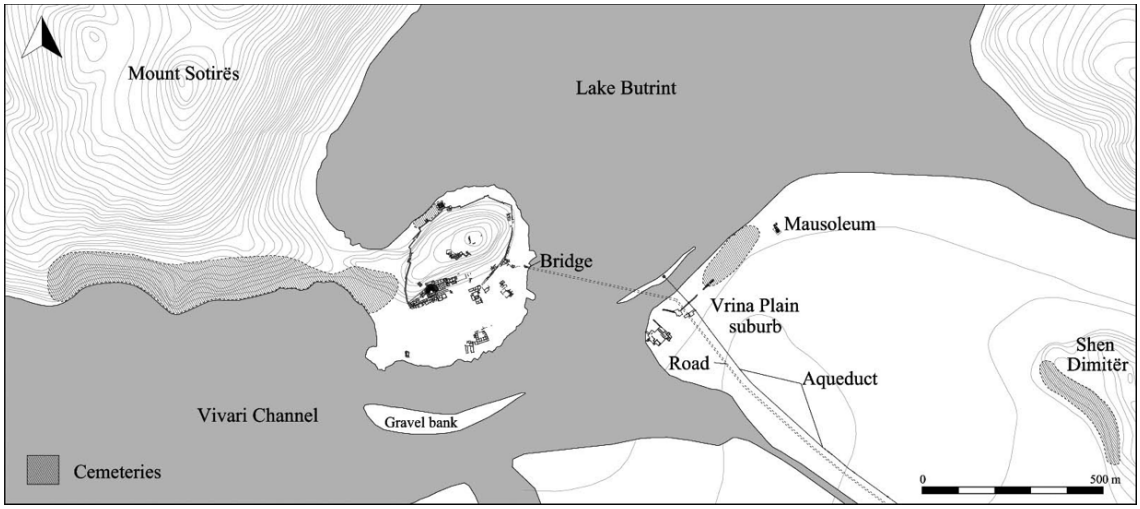

Figure 34. The topography of Butrint in the Roman period (Hodges 2012)

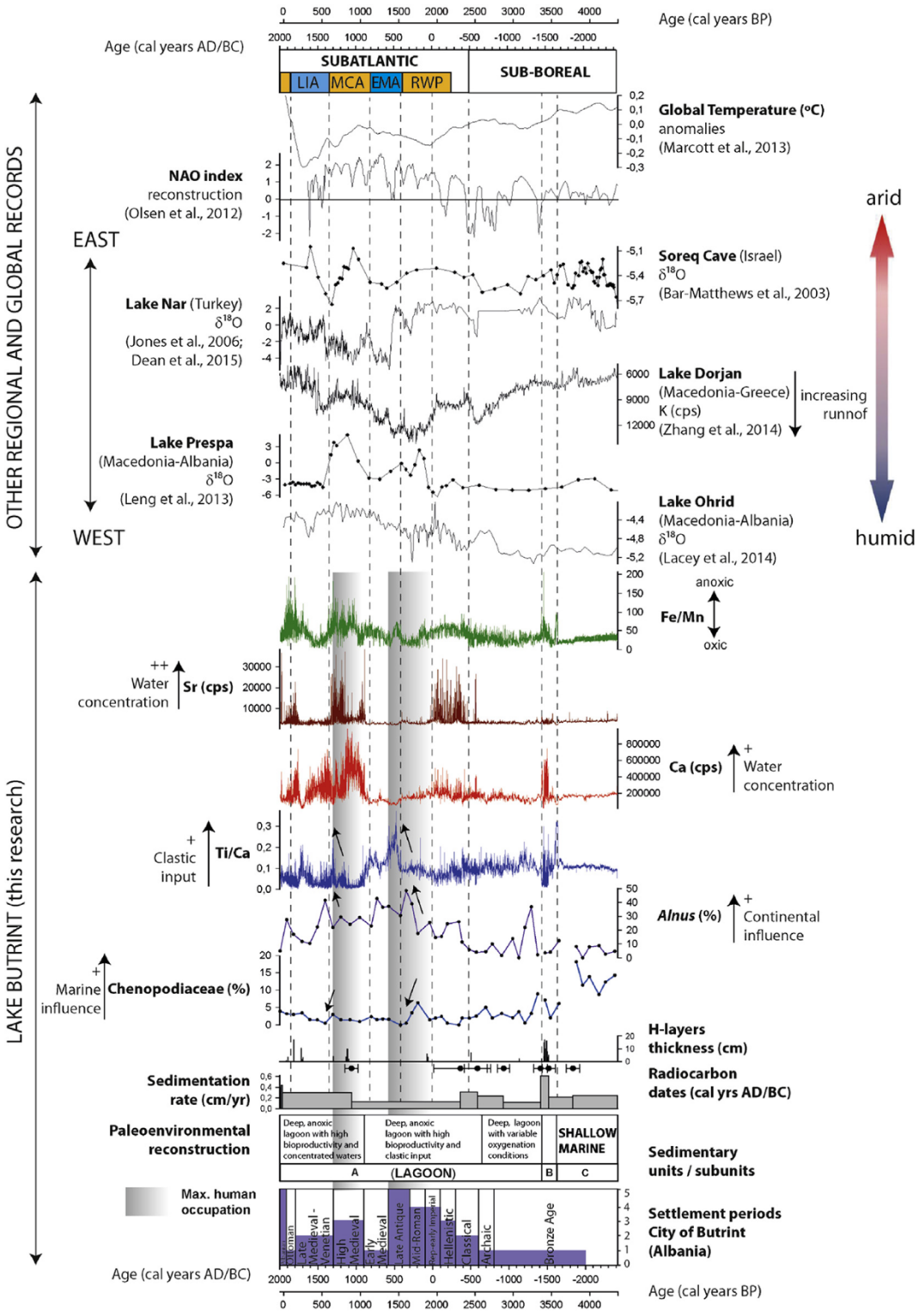

Figure 35. Environmental proxy data analysed in the Lake Butrint sequence (lower part), with other regional and global records (upper part) for the last ~4,000 years (Morellón et al 2016, fig. 8)

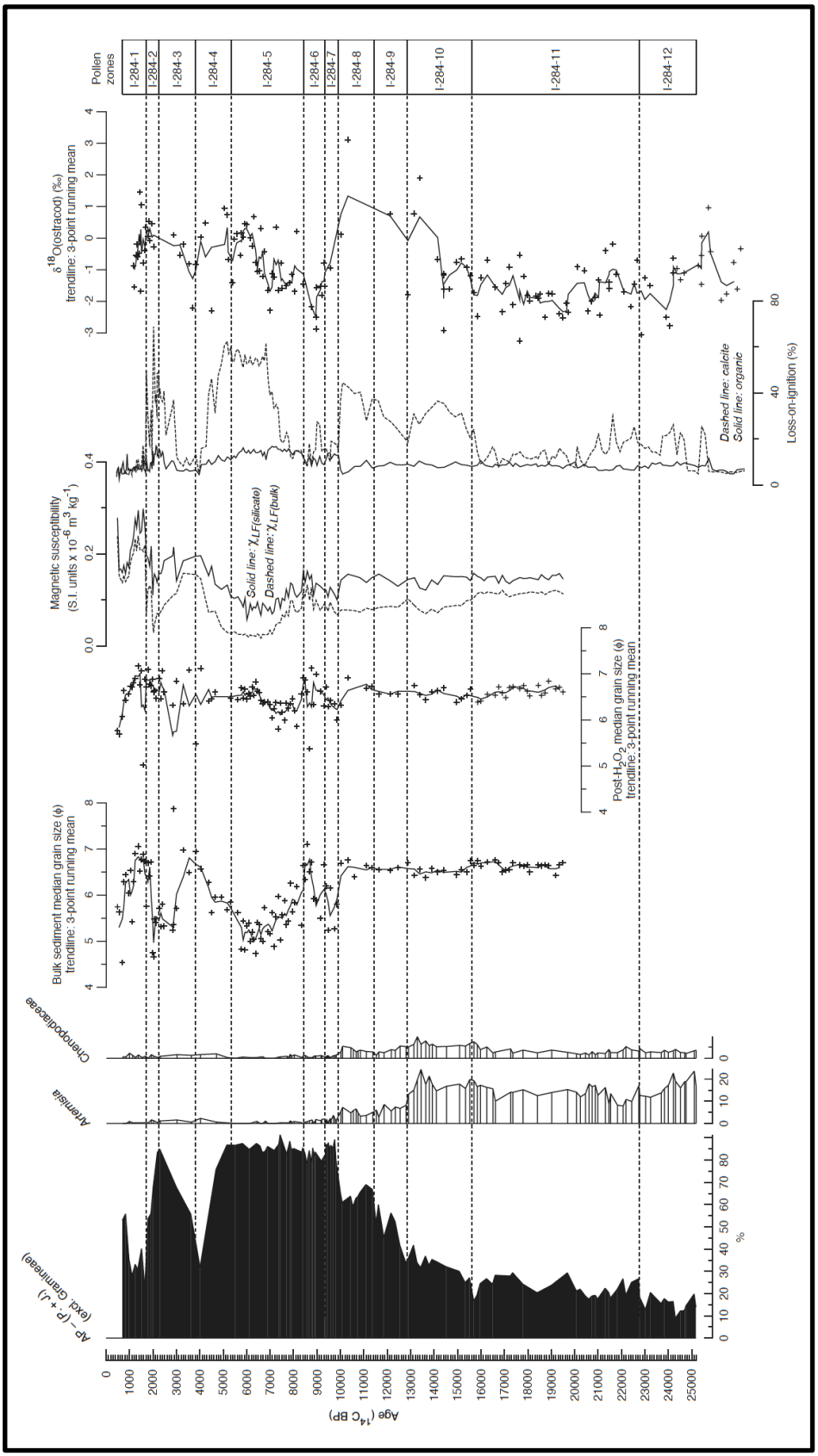

Figure 36. Lake Pamvotis, selected data from core I-284 plotted for the last 25,000 years, the I-284-2 section corresponding to Roman times, showing decreased AP and increasing sedimentation *(Lawson et al. 2008, fig. 8)*

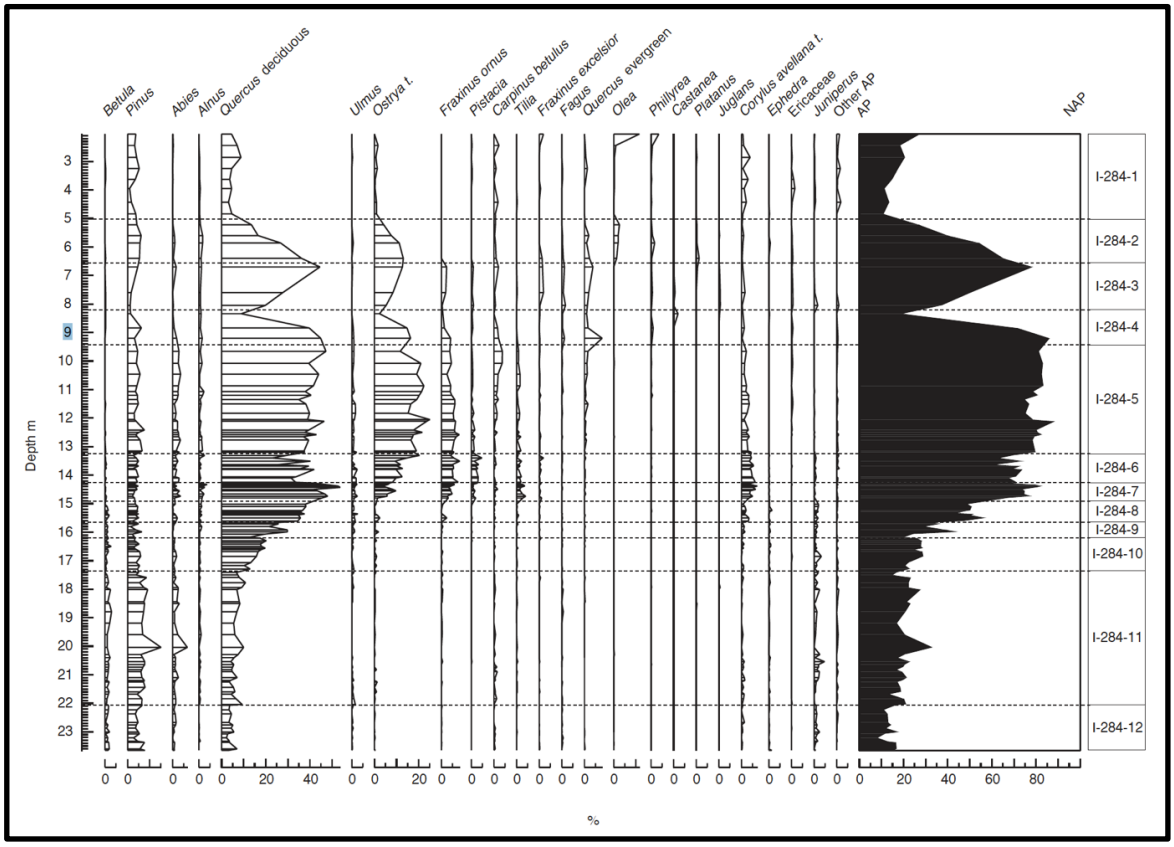

Figure 37. Lake Pamvotis, pollen percentage data from core I-284 plotted for the last 25,000 years (uppermost 23.65 m of the core), the I-284-2 section corresponding to Roman times (ca. 1st-5th centuries CE, *Lawson et al. 2008, fig. 2, the first out of two parts of the figure shown here)*

Figure 38. Cattle grazing in a high-altitude valley near modern-day Metsovo

Figure 39. Transhumance paths (known and supposed) of Vlach shepherds in the 18th and 19th centuries, at the bottom illustrating paths from the western coasts of Epirus to eastern Greece and Macedonia (https://creativecommons.org/licenses/by-sa/4.0/deed.en).

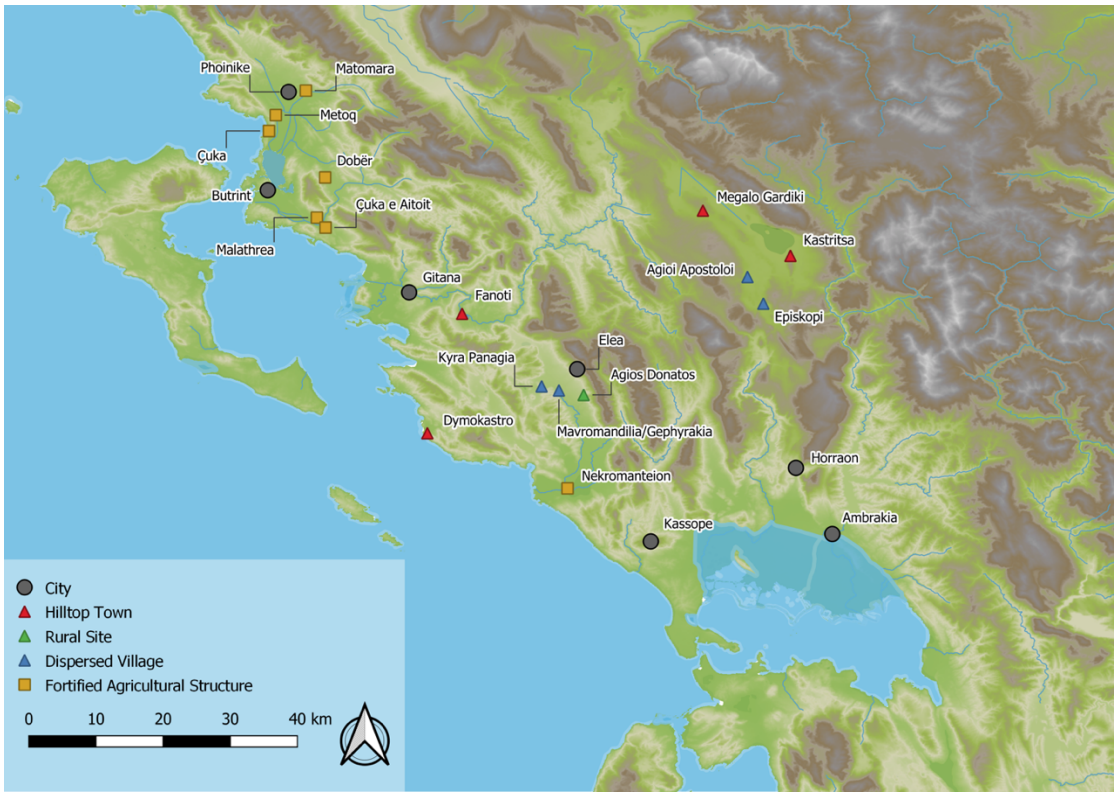

Figure 40. Map of different forms of rural and urban settlement in Epirus after 168/7 BCE, showing sites discussed in chapter 3 (Map made by Hallvard Indgjerd)

Figure 41. View of the Kokytos valley from Agios Donatos

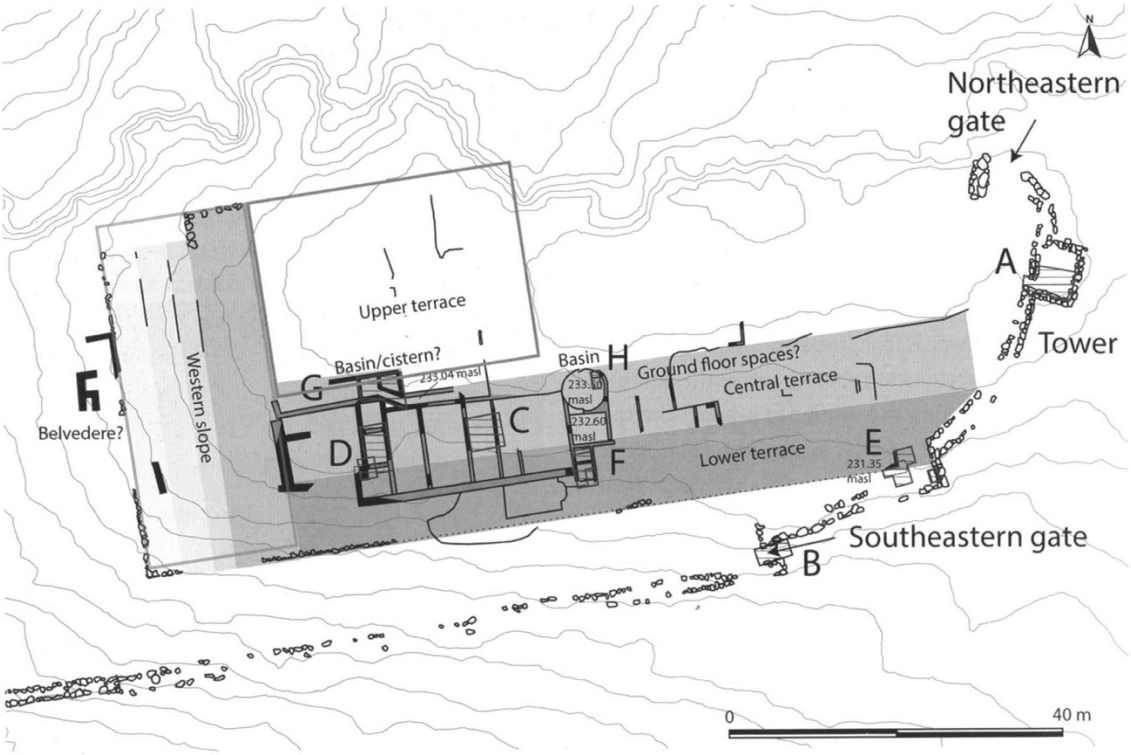

Figure 42. Plan of Agios Donatos, also showing the location of trial trenches (A-G) and delineating excavated or noted remains (Forsén 2019, fig. 2)

Figure 43. Agios Donatos, the small cellar room (Trench F, Forsén and Reynolds 2011, fig. 1)

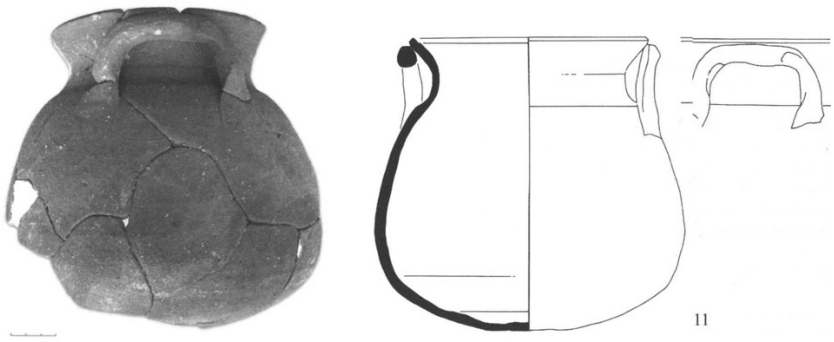

Figure 44. Agios Donatos, photo of cooking pot no. 11 from the early closed deposit (with a 4 cm-scale; Forsén and Reynolds 2011, fig. 6)

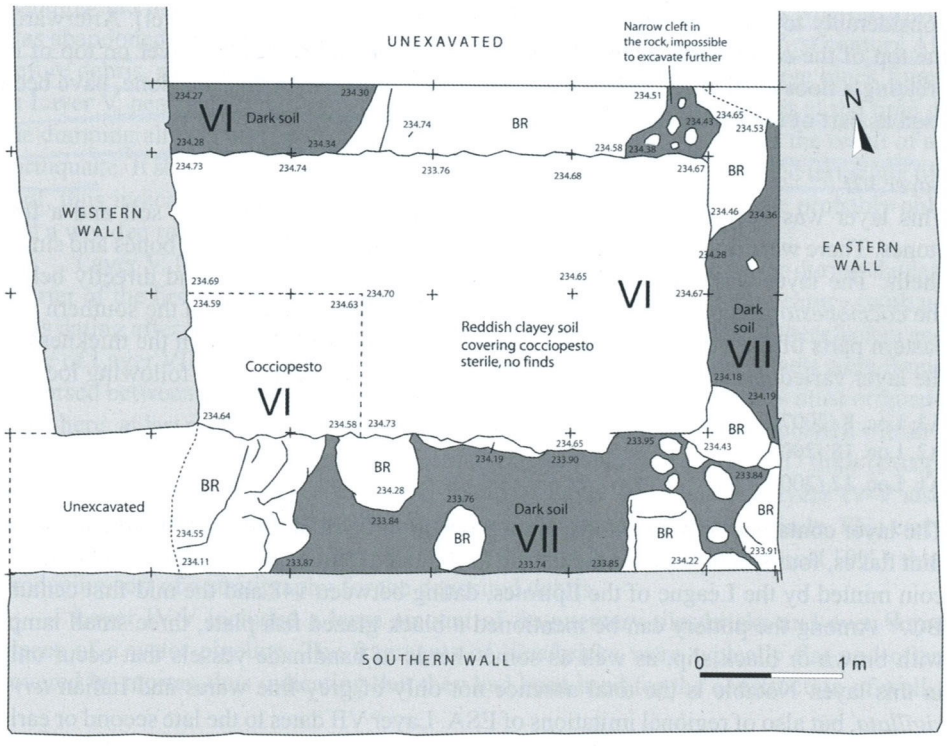

Figure 45. Agios Donatos, excavation in the tower (Trench A), showing the cocciopesto *pavement part of a new tower floor, Layers VII and VI* (*Forsén and Suha 2019, fig. 10*)

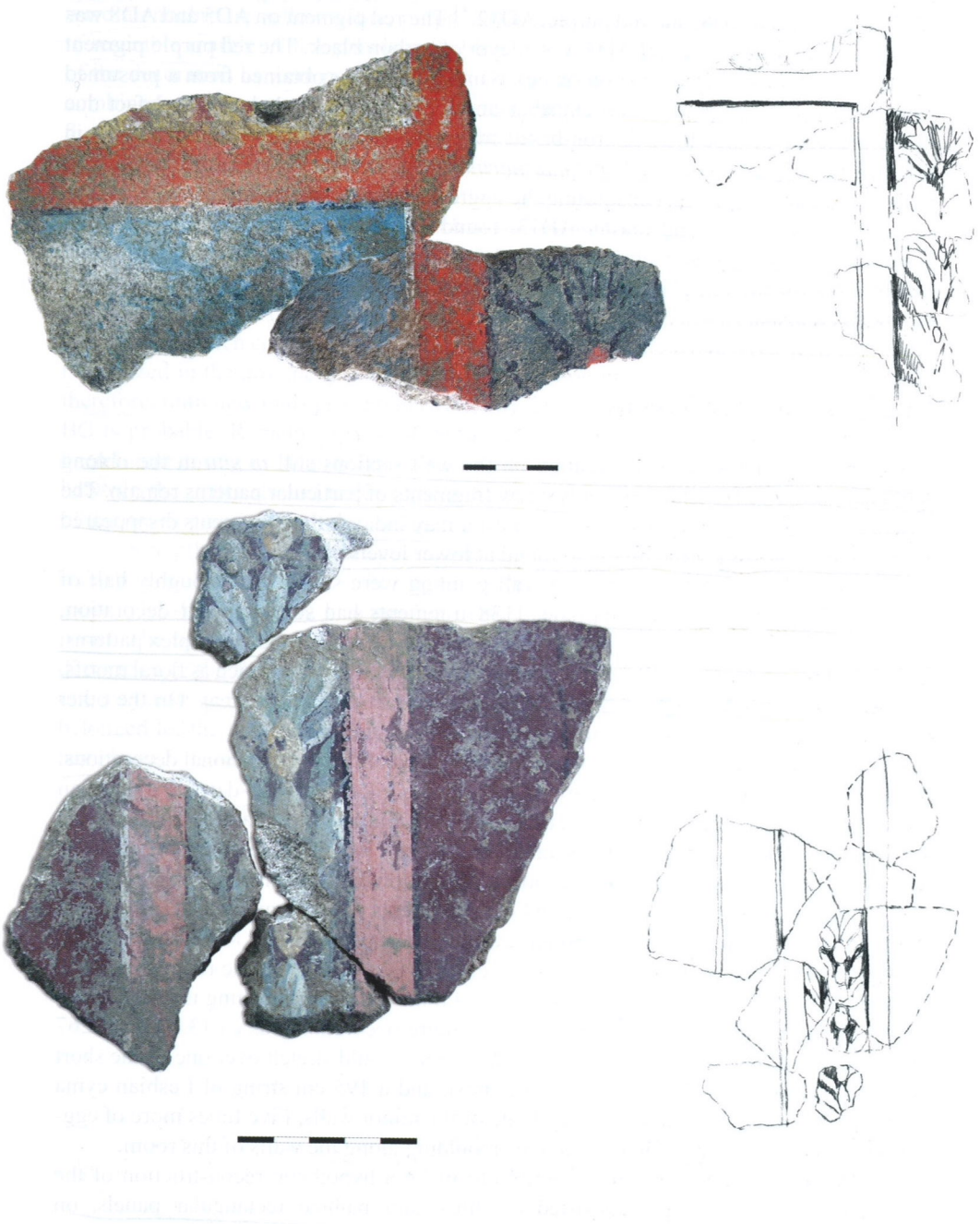

Figure 46. Agios Donatos, fragments from painted panels and drawings of reconstructions, showing above a blue panel with floral decoration, and below purple panels and floral decoration (Freccero 2019, fig. 13)

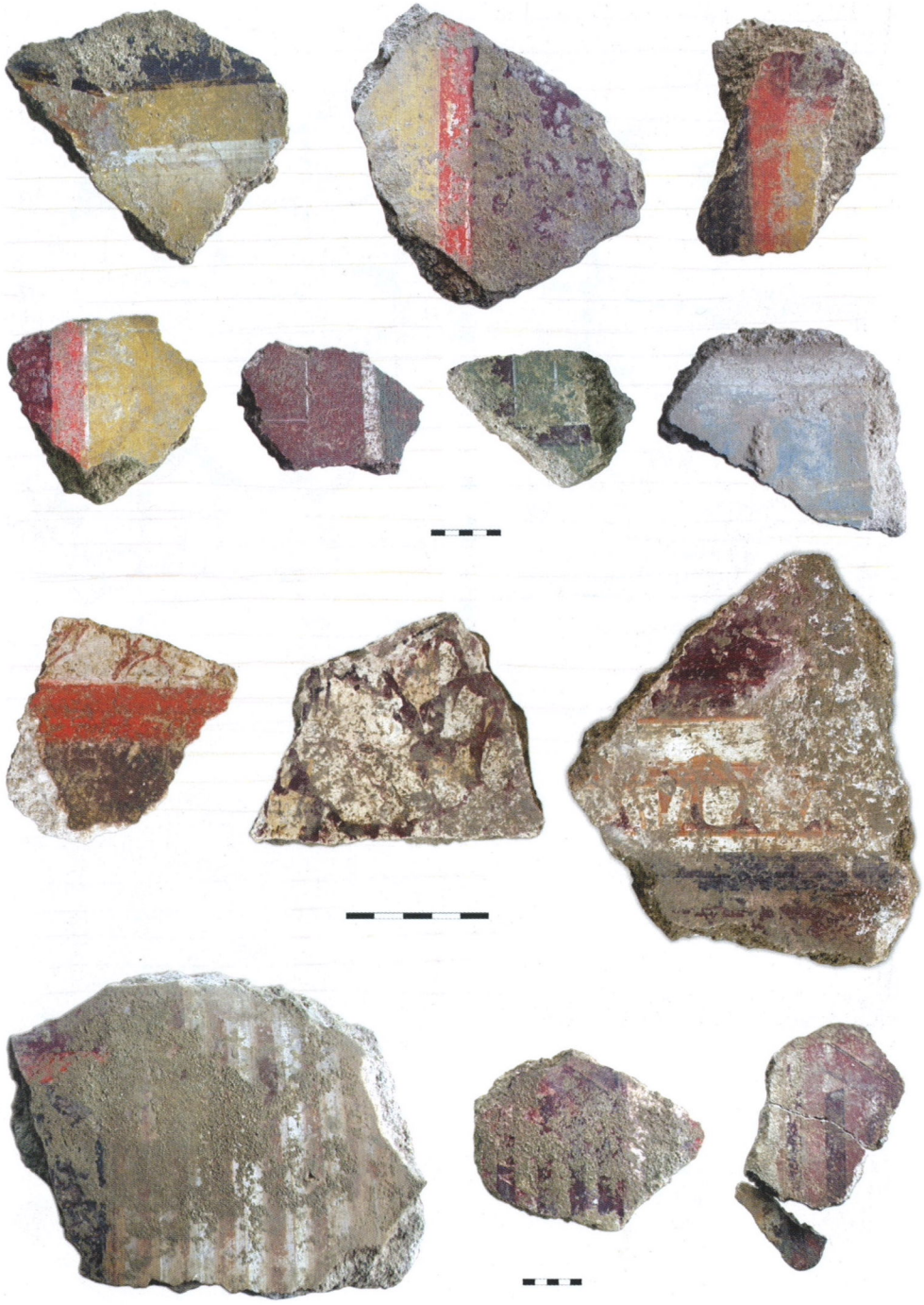

Figure 47. Agios Donatos, fragments from painted panels, in the third and fourth rows showing marble imitation and painted architectural decoration (Freccero 2019, fig. 11)

Figure 48. View from hilltop settlement of Kastritsa to the south-eastern plains of the Ioannina basin, above which the Egnatia Odos is visible exiting the basin in the background

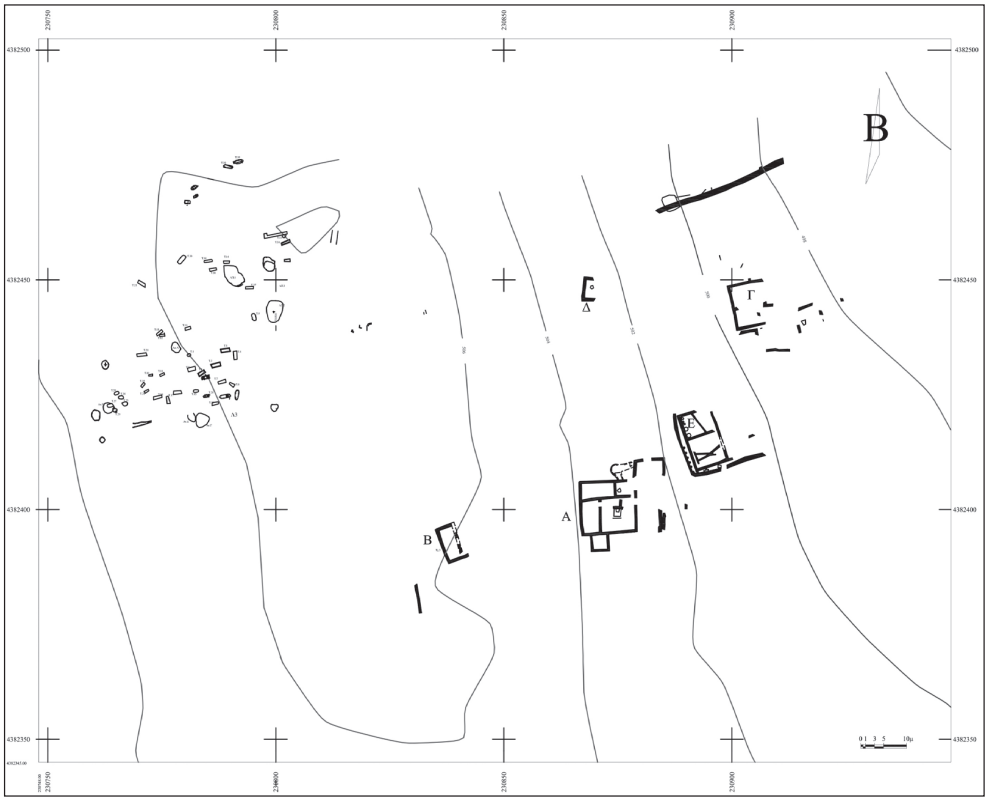

Figure 49. Plan of the dispersed village of Episkopi, consisting of Buildings A, B and E, amongst others (Pliakou 2017, fig. 3)

Figure 50. Plainlands with seasonal lakes near Episkopi, in the southwestern Ioannina basin

Figure 51. Episkopi, Building A, destruction layer (Pliakou 2017, fig. 5)

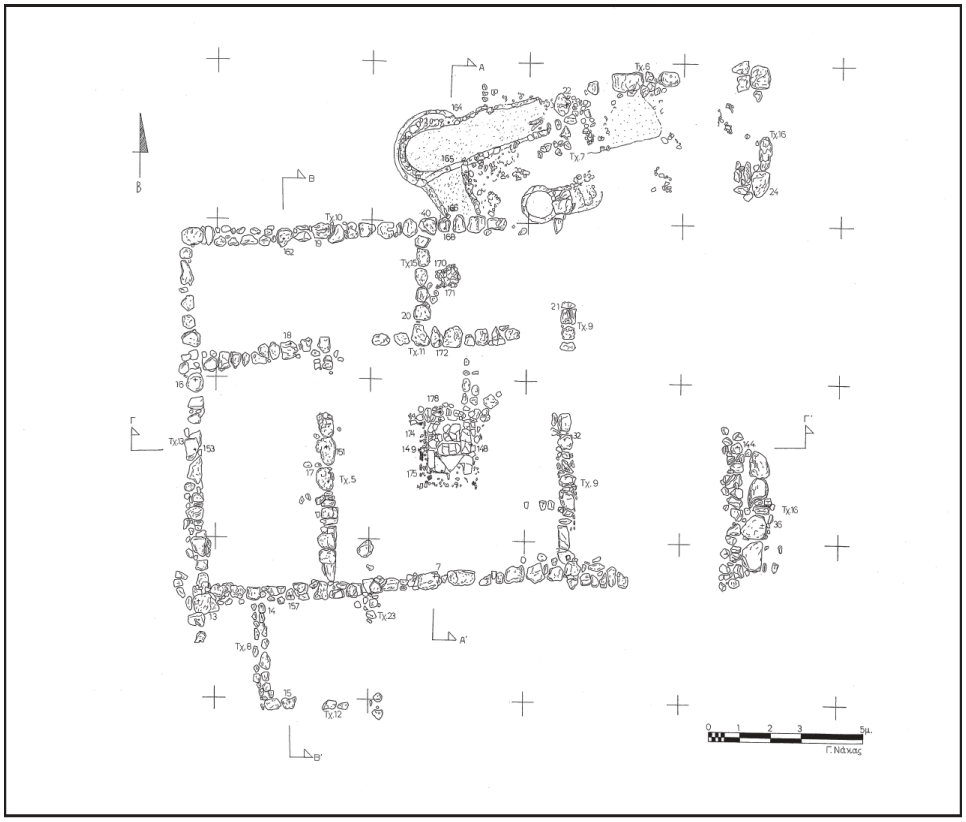

Figure 52. Episkopi, plan of Building A (Pliakou 2017, fig. 4)

Figure 53. Relief skyphos, decorated with "Macedonian star" (rim diameter 13 cm, Pliakou 2016b, fig. 6)

Figure 54. Cooking pot with stepped shoulder to short collar and everted rim, late 2nd-early 1st centuries BCE (max. width 14 cm, Pliakou 2016a, no. 1)

Figure 55. Episkopi, "Hellenistic" lamp (length: 7.5 cm, Pliakou 2016a, no. 3)

Figure 56. Episkopi, Phoenician amphoriskos (height: 33 cm, Pliakou 2016c, no. 4)

Figure 57. Episkopi, plate (rim diameter: 26.5 cm), possibly red regional terra sigilata *(Pliakou 2016c, no. 3)*

Figure 58. Episkopi, amphorae *from the destruction layer, "Aci-1" (left) and Lamboglia 2 (right) (Pliakou 2017, fig. 6)*

Figure 59. Episkopi, fragments from clay vessel for grinding cereals (left) and pick-axe blades (right, Pliakou 2017, fig. 7)

Figure 60. Megalo Gardiki, blade from plough, from layers dating to the 2nd-1st centuries BCE (Pliakou 2008, 69)

Figure 61. Episkopi, spindle-whorls (diameter 2 cm, Pliakou 2016a, no. 20)

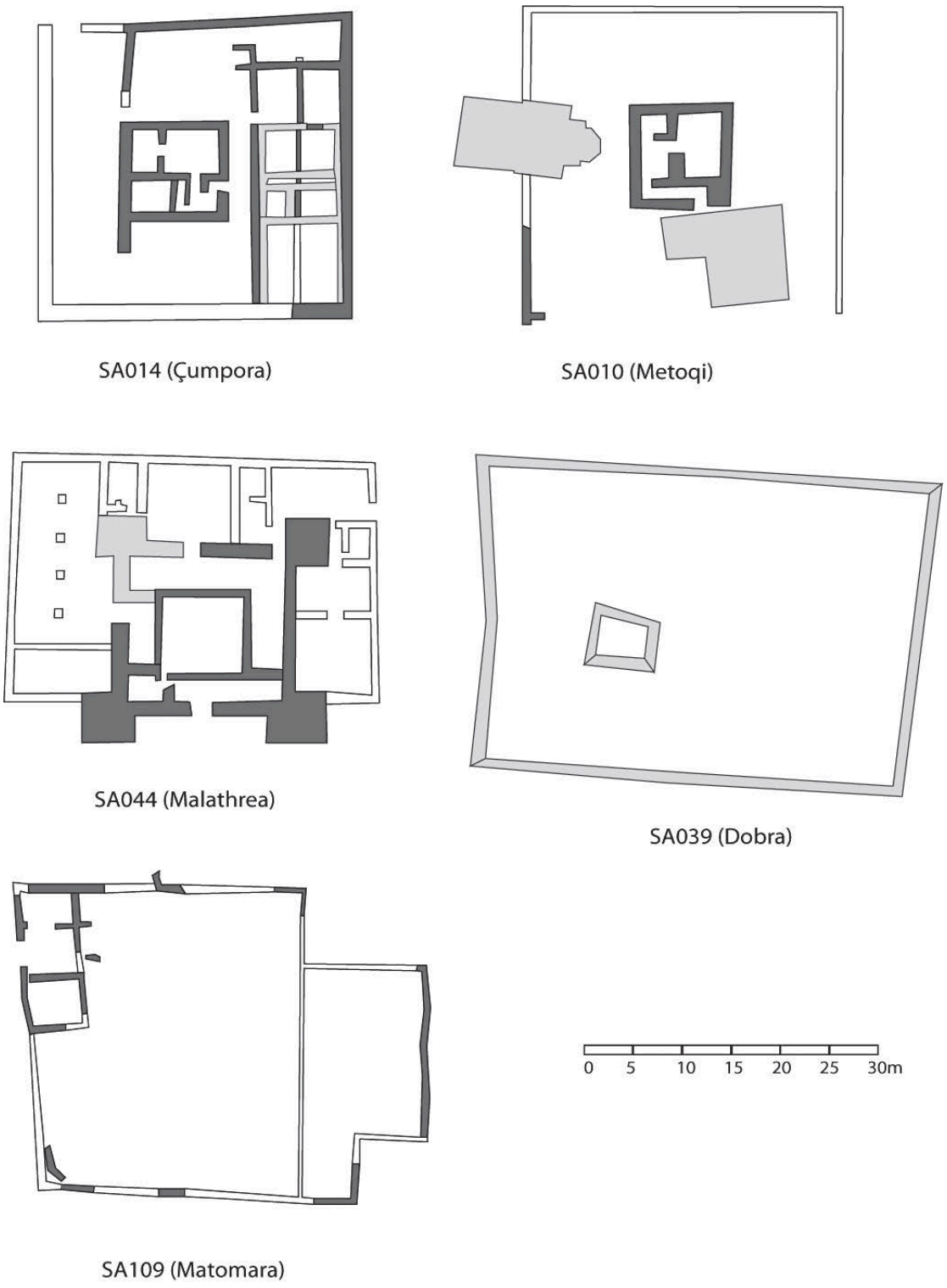

Figure 62. Schematic plans of five of the six excavated fortified rural structures (Çumpora refers to Çuka; Bogdani 2012, fig. 4).

Figure 63. Çuka, remains of the fortified structure, with the tower in the foreground (Çondi 2017, 166)

Figure 64. Çuka, ashlar masonry of the tower entrance

Figure 65. Çuka, ashlar masonry in room C of the tower

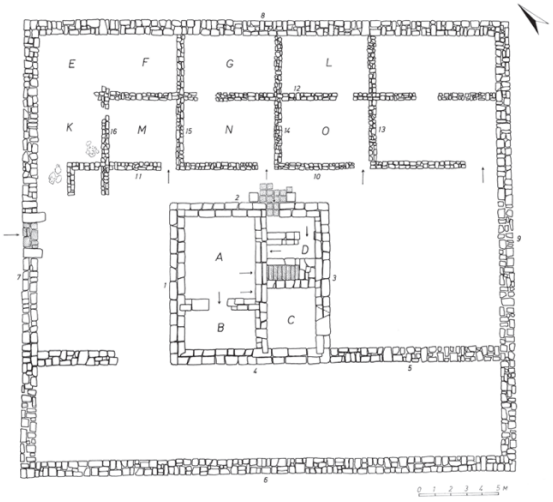

Figure 66. Plan of Çuka (with 5 m-scale; Çondi 2017, 166)

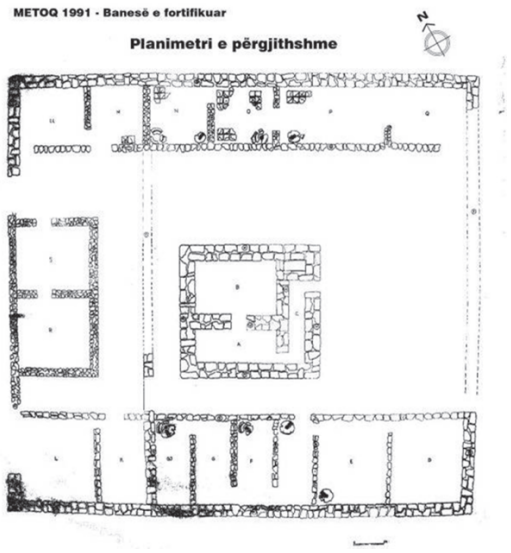

Figure 67. Plan of Metoq (with 10 m-scale; Çondi 2017, 176)

Figure 68. Çuka/Çumpora, photo from inside the tower, showing the staircase

Figure 69. Malathrea, south-eastern tower (Çondi 1984, fig. 4)

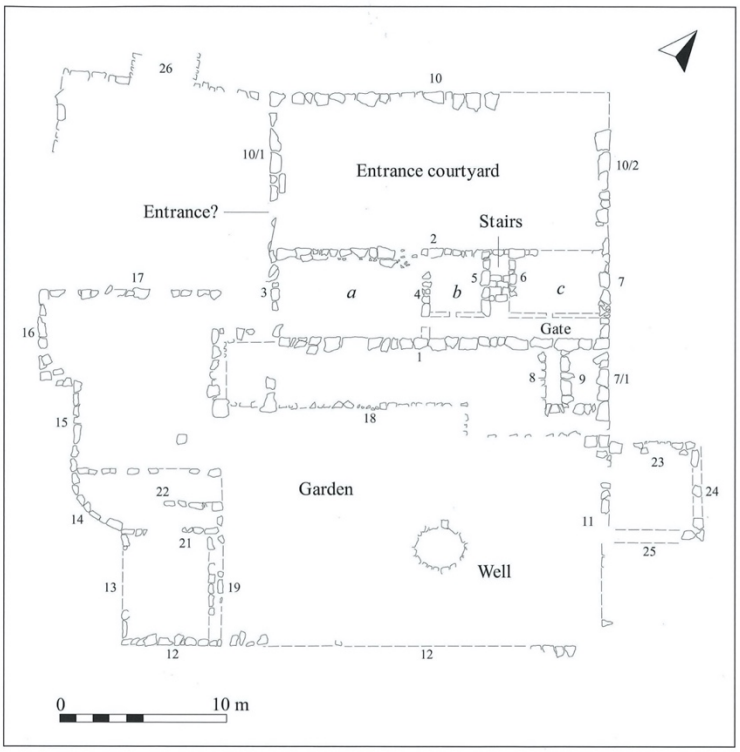

Figure 70. Plan of Building 1 at Çuka e Aitoit (Islami 2020, fig. 11.18, drawn by Nevila Molla)

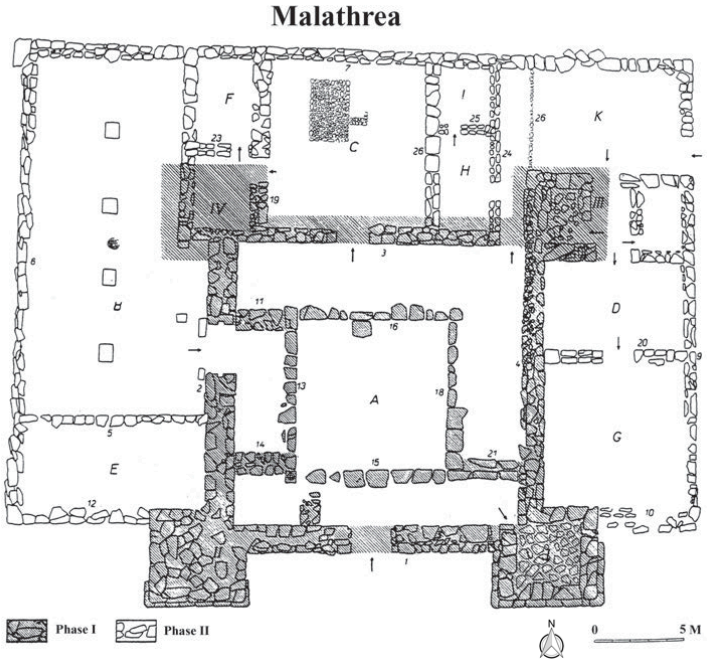

Figure 71. Plan of Malathrea, showing the two architectural phases proposed by Çondi (Bogdani 2012, fig. 3 after Çondi 1984, fig. 2)

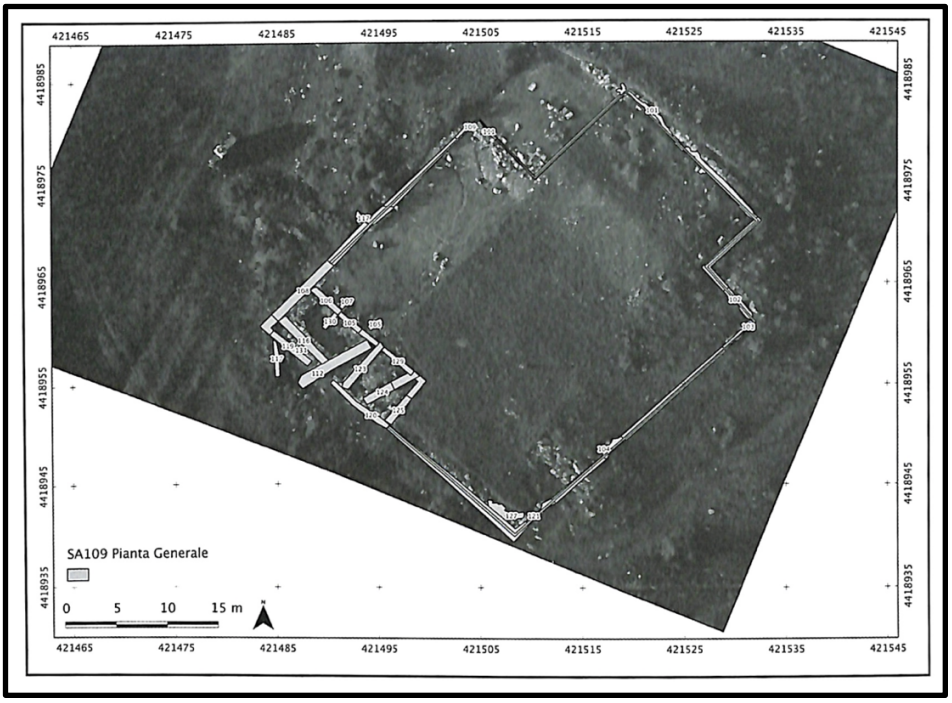

Figure 72. Matomara, general plan (Bogdani 2012a, fig. 6)

Figure 73. Approach to Malathrea

Figure 74. Malathrea, looking out over the Vrina plain from the Hellenistic-period entrance

Figure 75. View from the tower at Çuka over the Vurgu plain, with Phoinike visible in the background

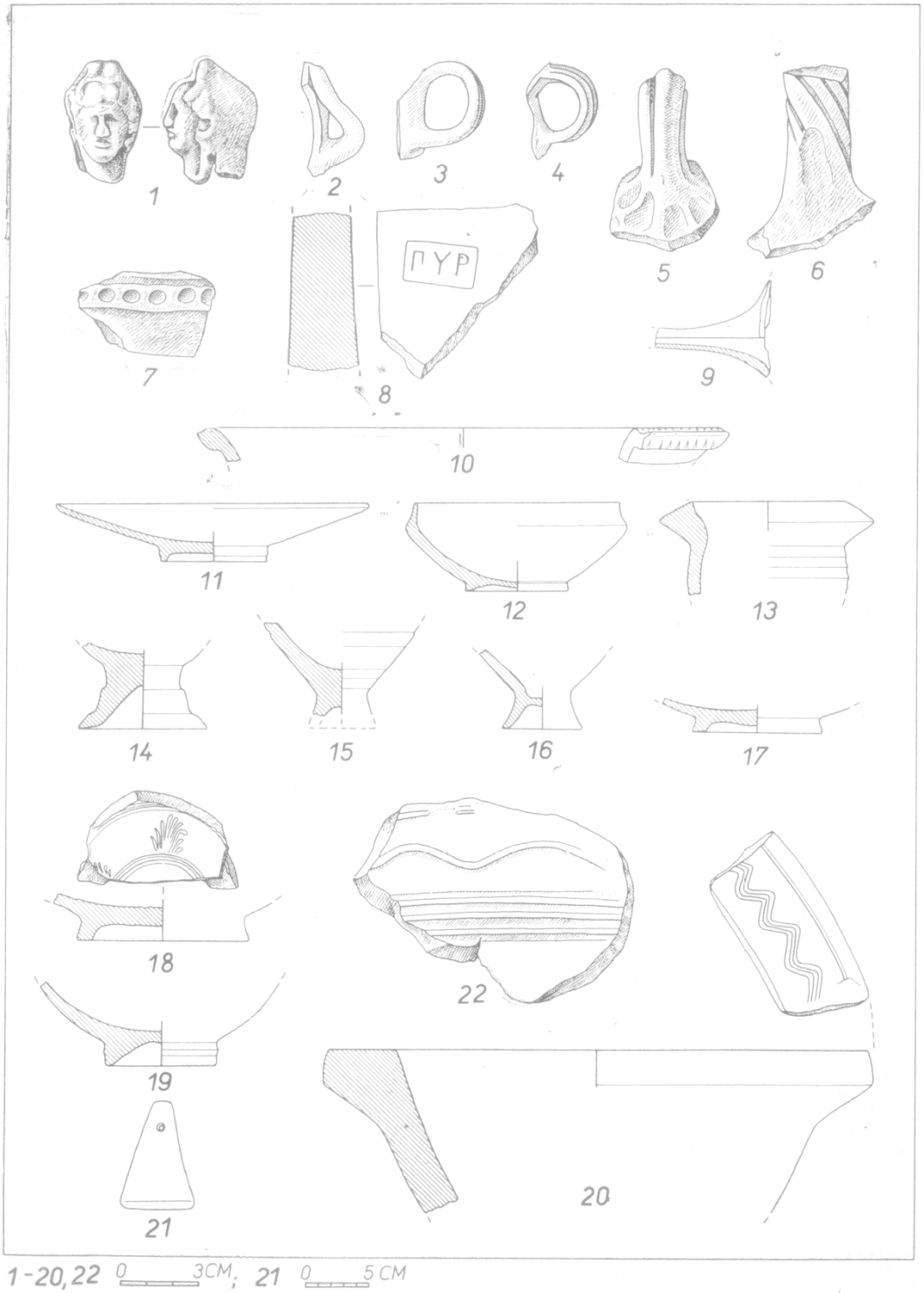

Figure 76. Malathrea, finds mainly associated with the so-called Hellenistic phase. Note nos. 11-18, depicting plates, dishes and cups, nos. 5-6 amphora *handles and no. 13 an* amphora *rim, as well as no. 22, a* pithos *sherd (Çondi 1984a, pl. I, 149)*

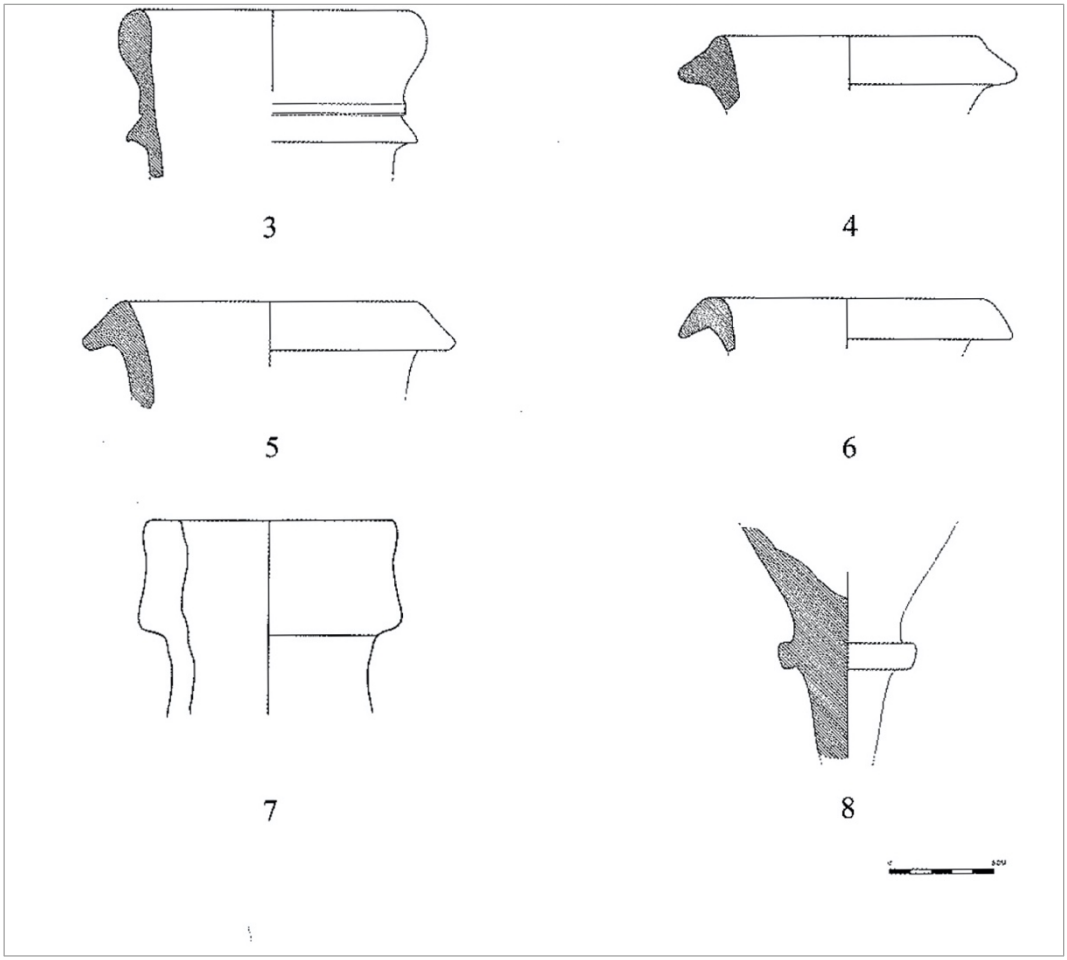

Figure 77. Matomara, imported amphorae*, mainly Adriatic, no. 5 (late Greco-Italic) and no. 7 (Dressel 1B, of which 8 examples were found; adapted from Aleotti 2012, fig. 2, who originally interpreted no. 7 as a Lamboglia 2)*

Figure 78. Malathrea, storage rooms D and G, view from the south-eastern tower (Photo: Rory MacLean)

Figure 79. Malathrea, storage rooms D and G, view from the west

Figure 80. Nekromanteion, one of the storerooms in the ground floor of the tower

Figure 81. Nekromanteion, underground chamber

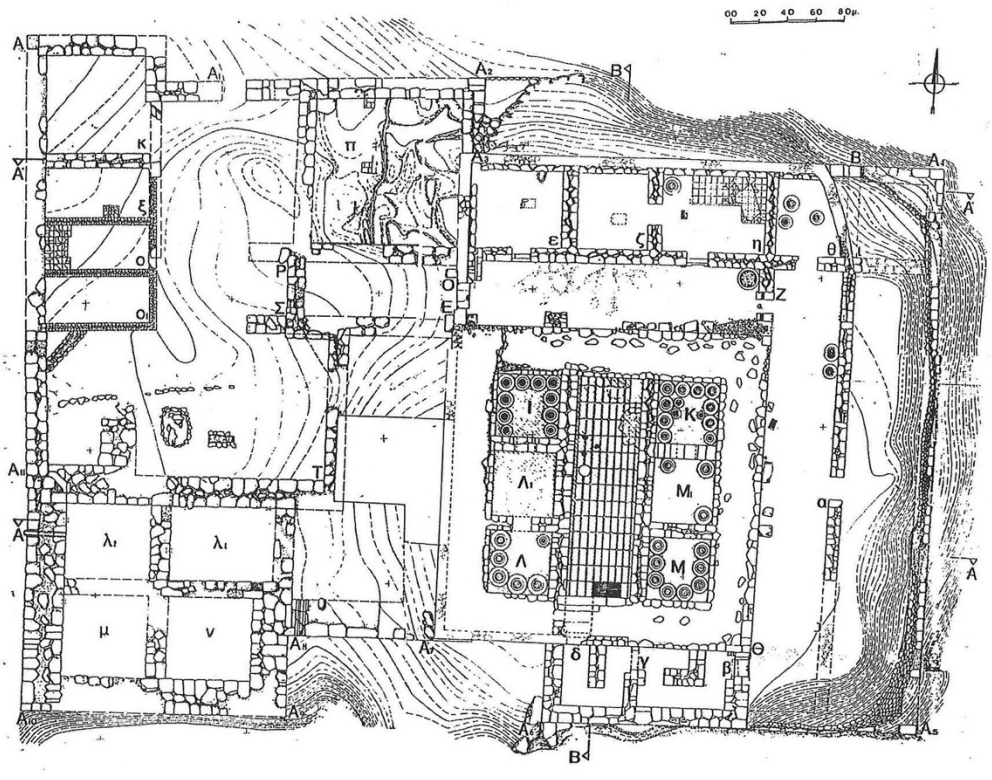

Figure 82. Nekromanteion, phased plan (Gravani and Katsikoudis 2019, fig. 3)

Figure 83. Nekromanteion, hopper-rubber mills

Figure 84. Fragments of segmented mills (possibly animal-powered)

Figure 85. Fragments segmented mills (possibly animal-powered)

Figure 86. Nekromanteion, amphorae *sealed with clay*

Figure 87. Nekromanteion, amphora *sealed with clay, and significantly burnt in the foreground*

Figure 88: Phoinike, the theatre and view over the Vurgu plain

Figure 89. Kastritsa, Building Complex E, aerial photograph (Yiouni et al. *2015, 59)*

Figure 90. Kastritsa, Building Complex E, mosaic (Kyrkou 2020, fig. 165)

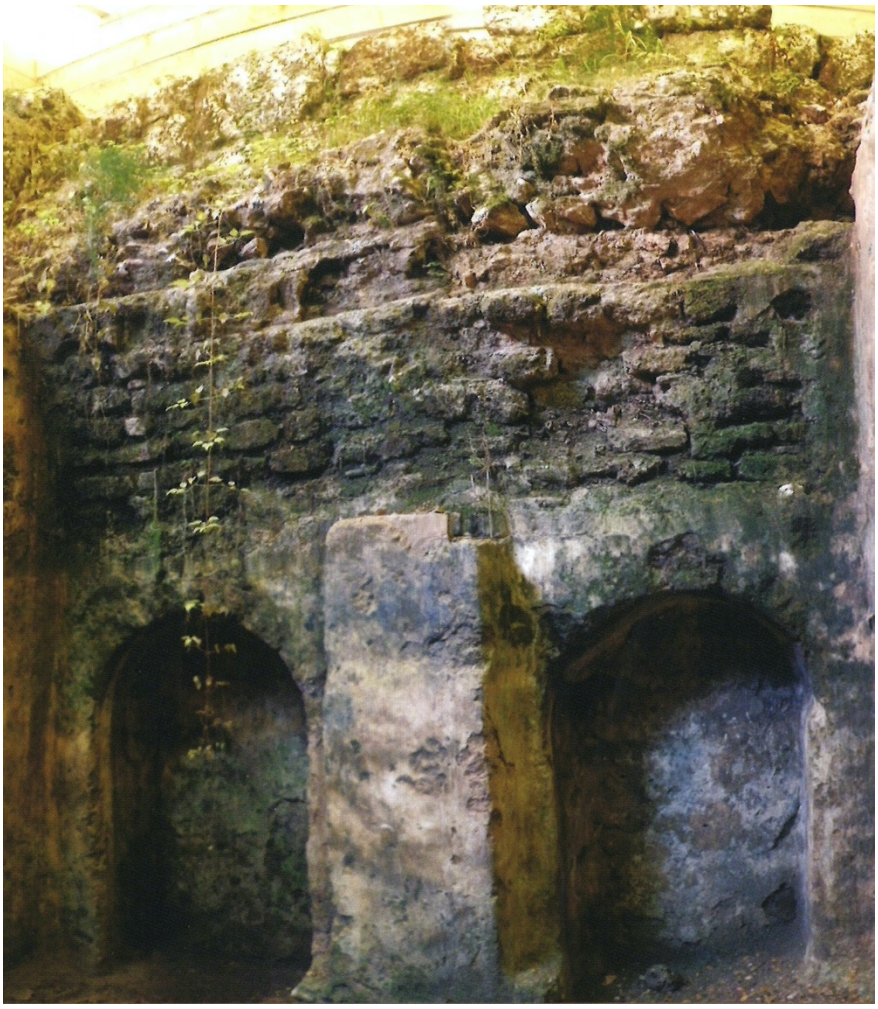

Figure 91. Kastritsa, cistern with Roman refurbishments (Yiouni et al. *2015, 65)*

Ορράον. Σπίτι 1, τομή με αποκατεστημένα τα ανατολικά δωμάτια. Κάτοψη και όψη από τα δυτικά. Κλίμακα 1:200.

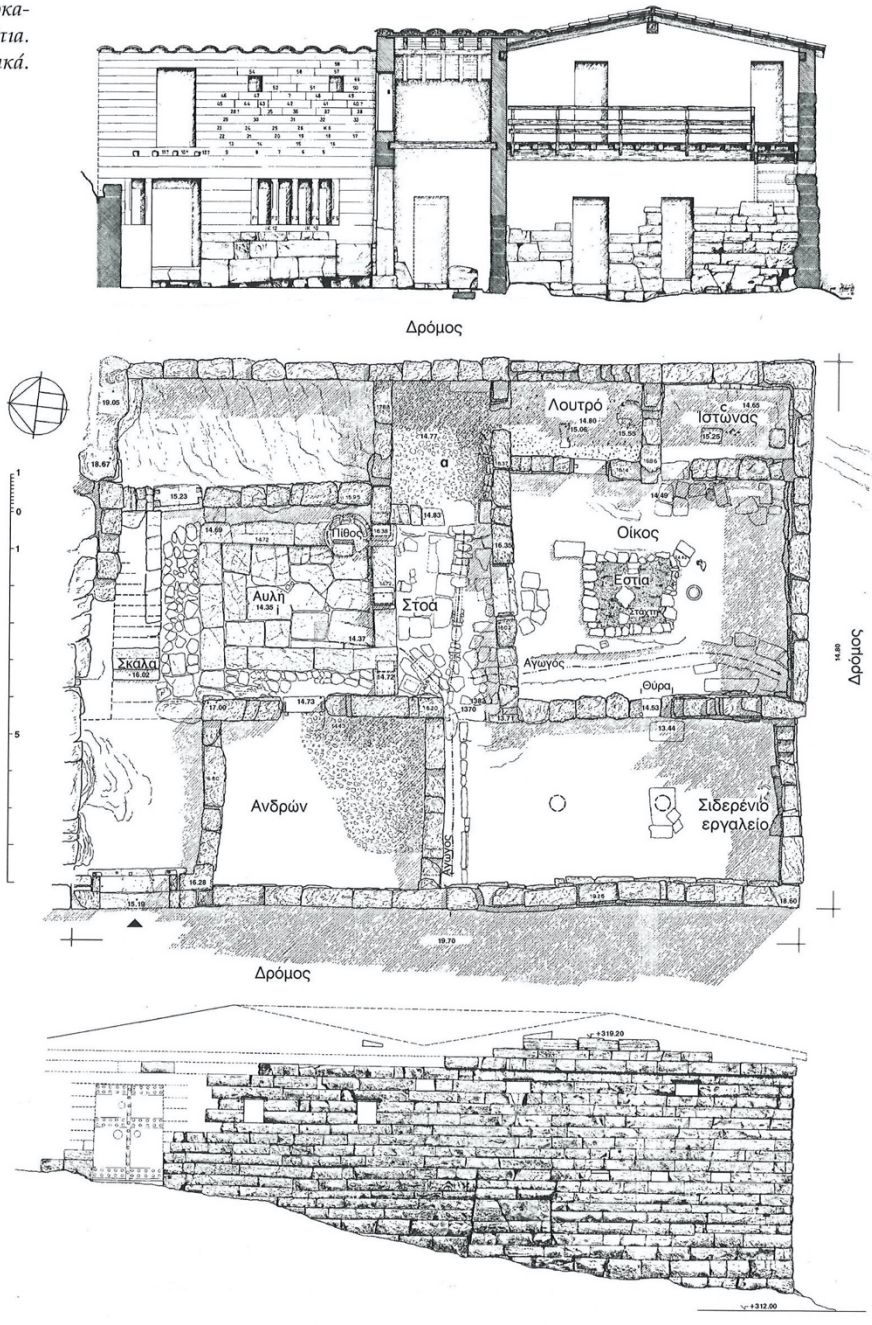

Figure 92. Plan of House 1 at Horraon (Hoepfner et al. 2005b, 415)

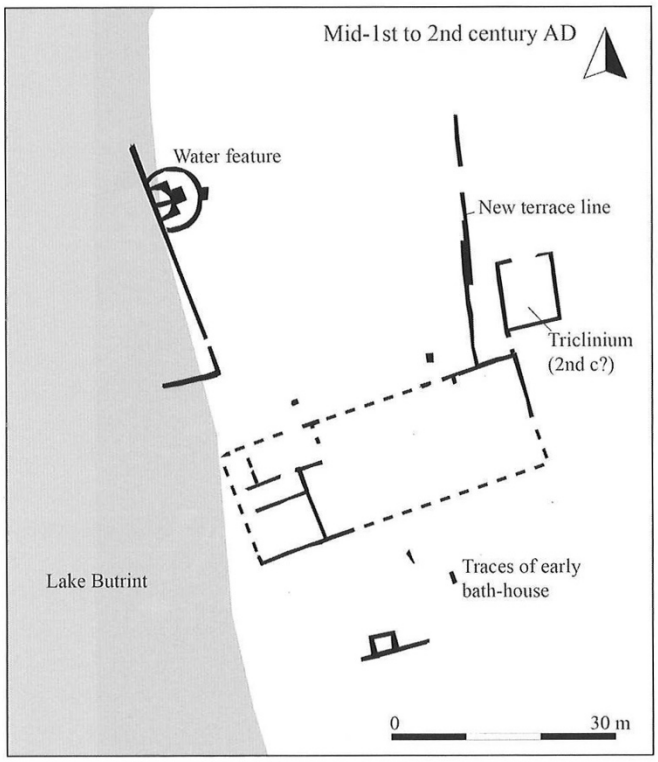

Figure 93. Plan of Diaporit, ca. *mid-1st to 2nd century CE (Bowden and Perzhita 2020, fig. 19.8, drawn by Will Bowden/BF archive)*

Figure 94. View of the possible fountain at Diaporit (Bowden and Perzhita 2020, fig. 19.8, photo by Will Bowden)

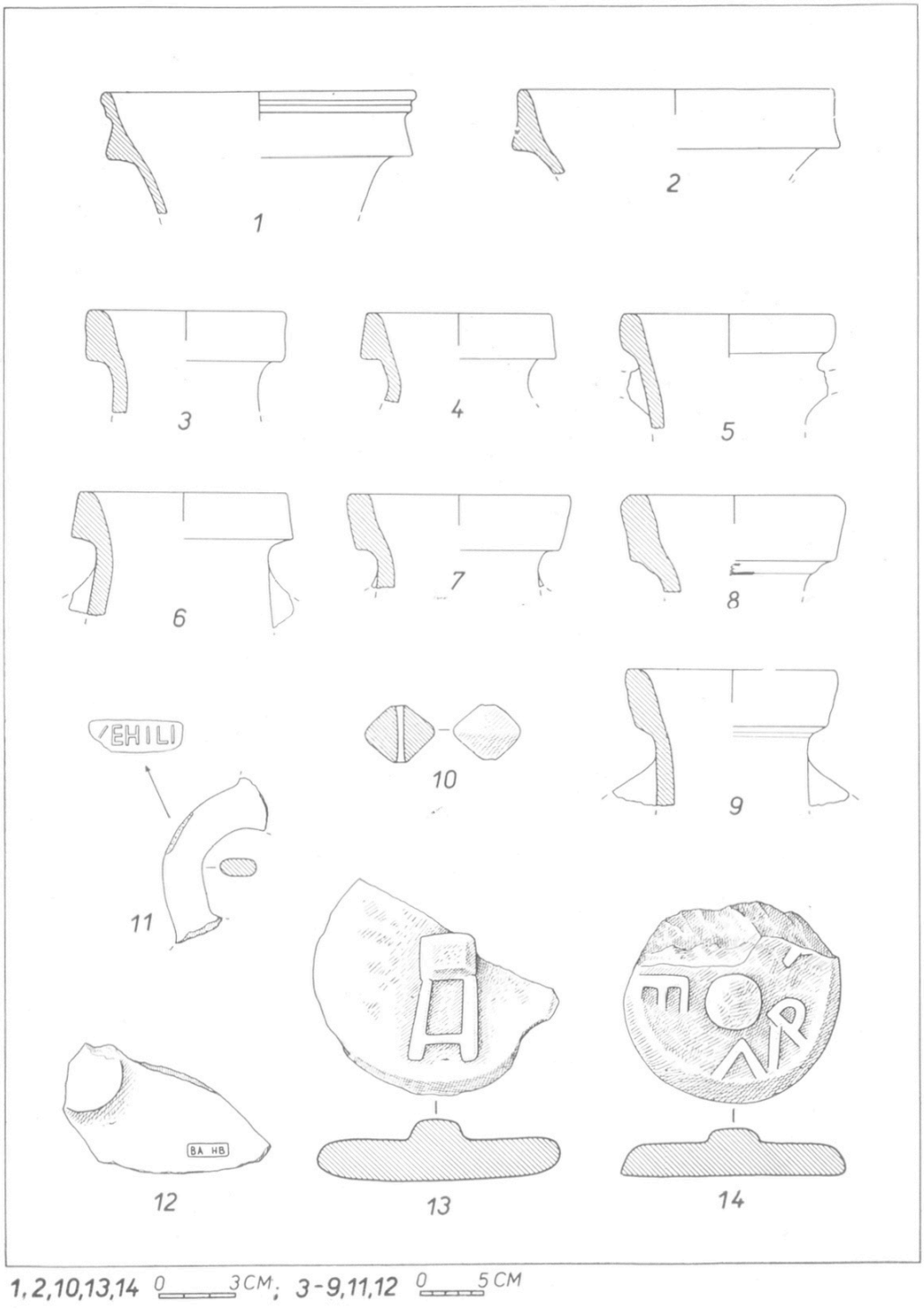

Figure 95. Malathrea, finds, mainly amphorae, apparently deriving from Roman layers (Çondi 1984a, pl. I, 150)

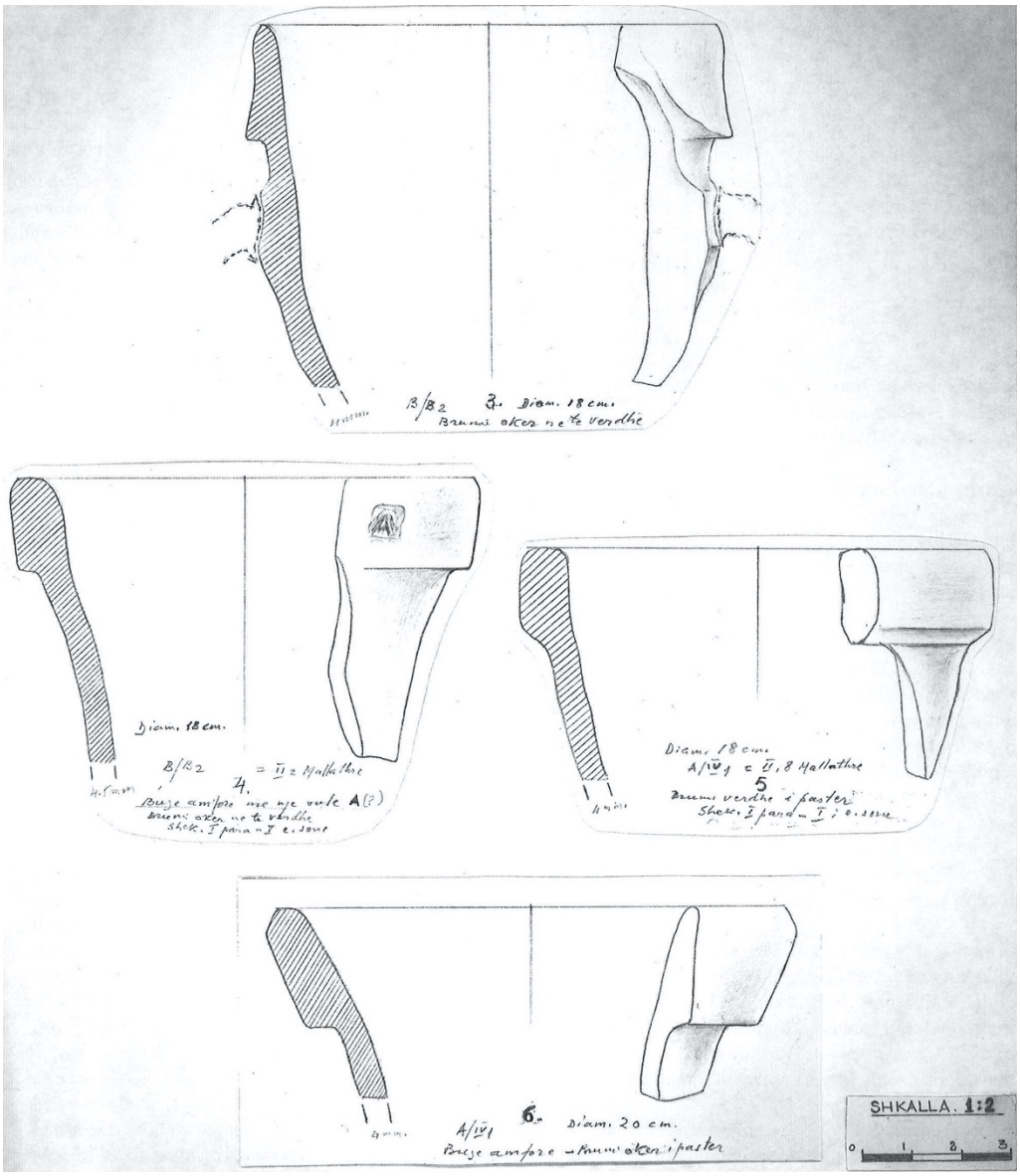

Figure 96. Çuka e Aitoit, amphorae (Islami 2020, fig. 11.35)

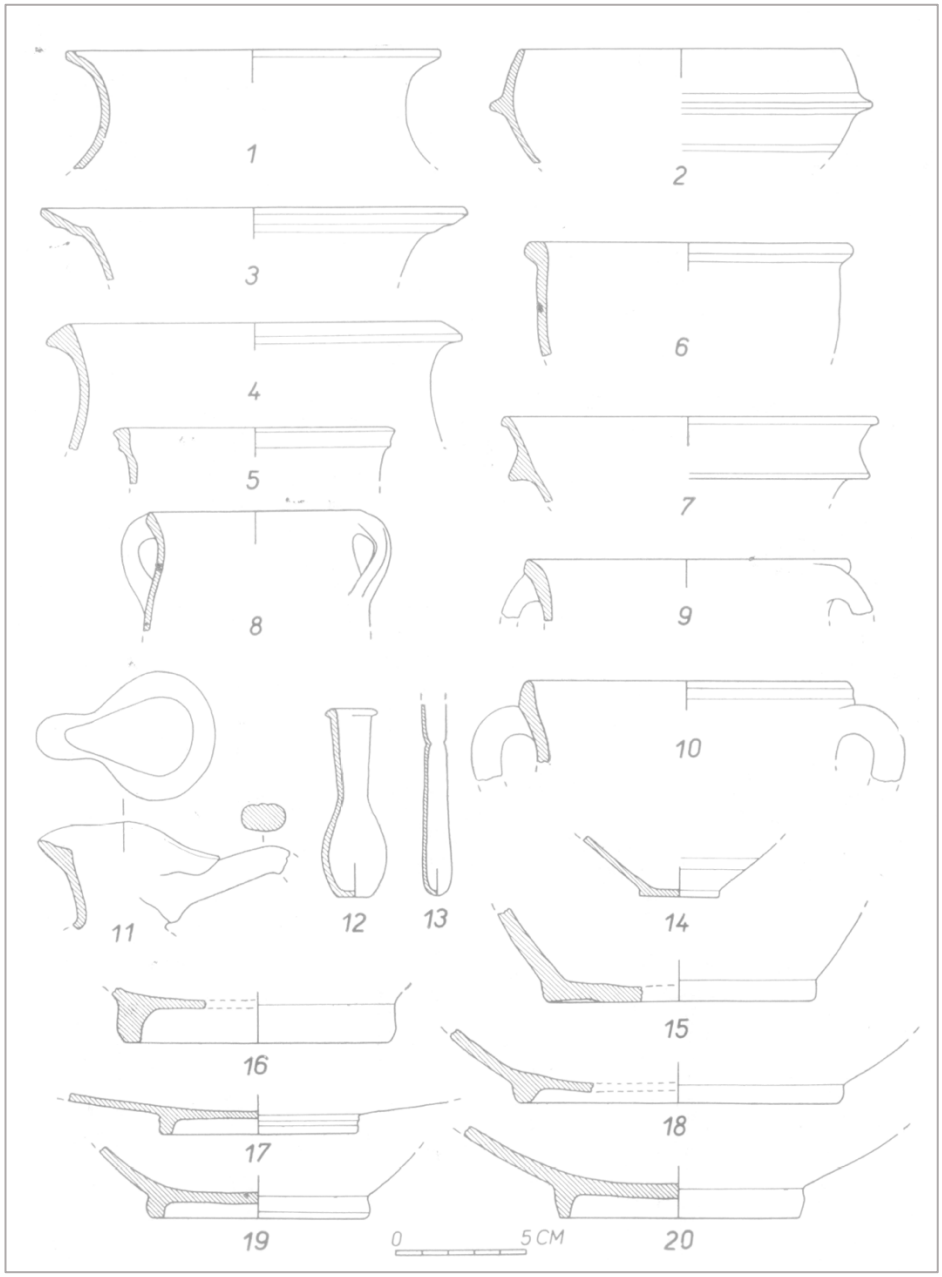

Figure 97. Malathrea, finds mainly deriving from Roman layers, specifically the tableware (nos. 14-20), cookware (nos. 4-10), and unguentria (nos. 12-13; Çondi 1984a, pl. II, 151)

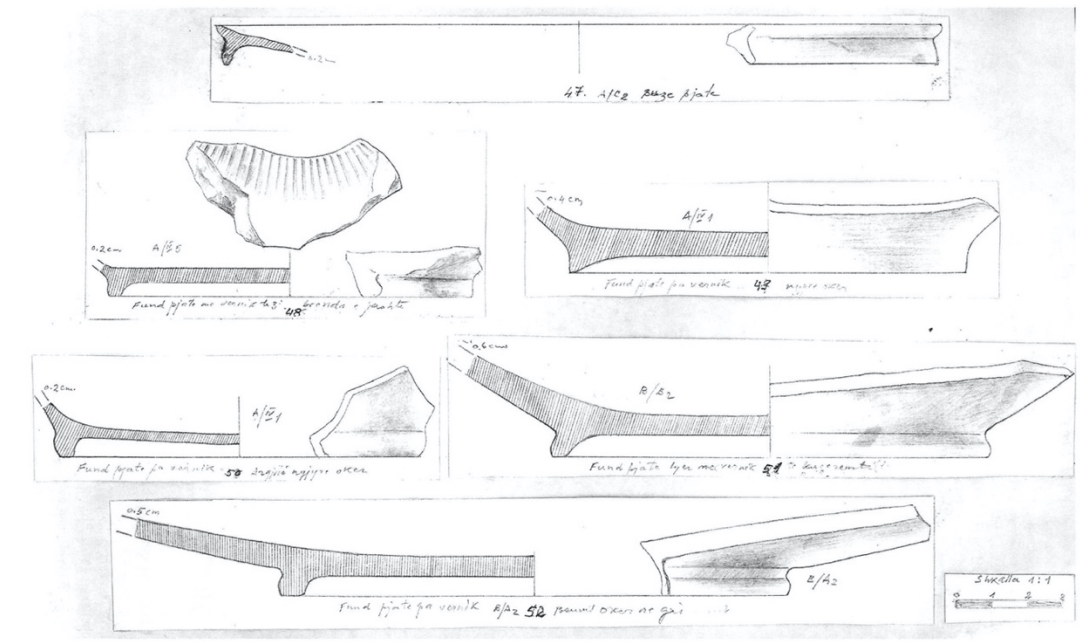

Figure 98. Çuka e Aitoit, drawings of rims and bases of dishes, some with black slip, one with a grooved band on the exterior, and another with red slip like terra sigillata, dated probably to the 1st century CE (Islami 2020, fig. 11.42)

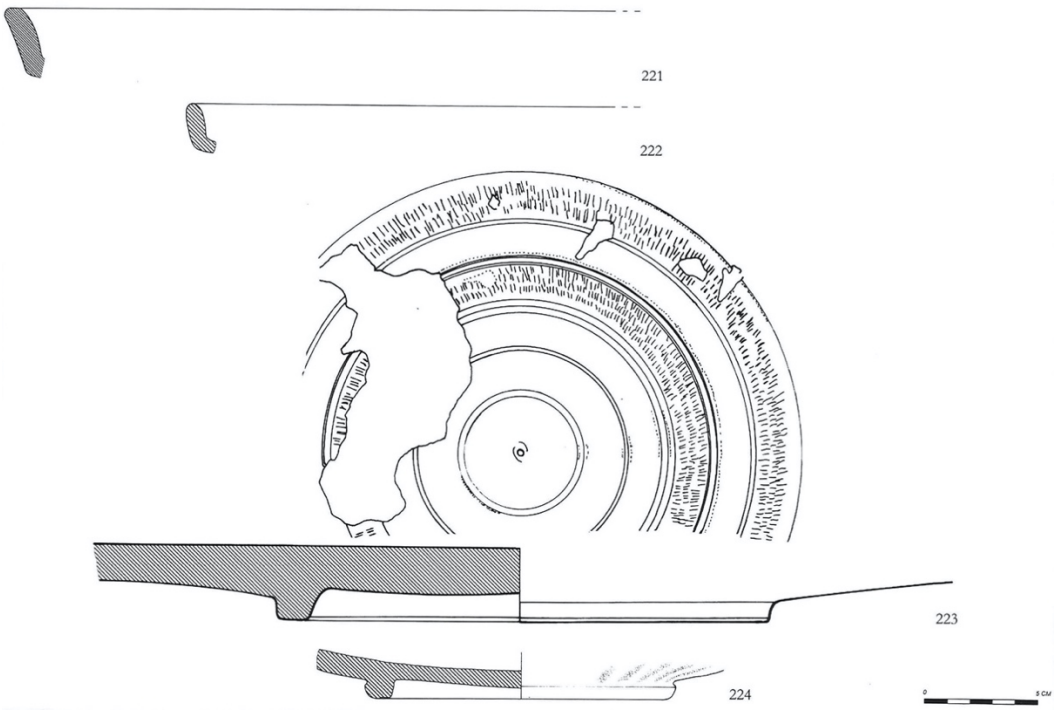

Figure 99. Phoinike "vassoi carenati", similar to Ephesian "Graue Platten", 1st century BCE-firsts decades of the 1st century CE, with nos. 221-222, 224 dated to the Augustan period (Gamberini 2016, pl. 26)

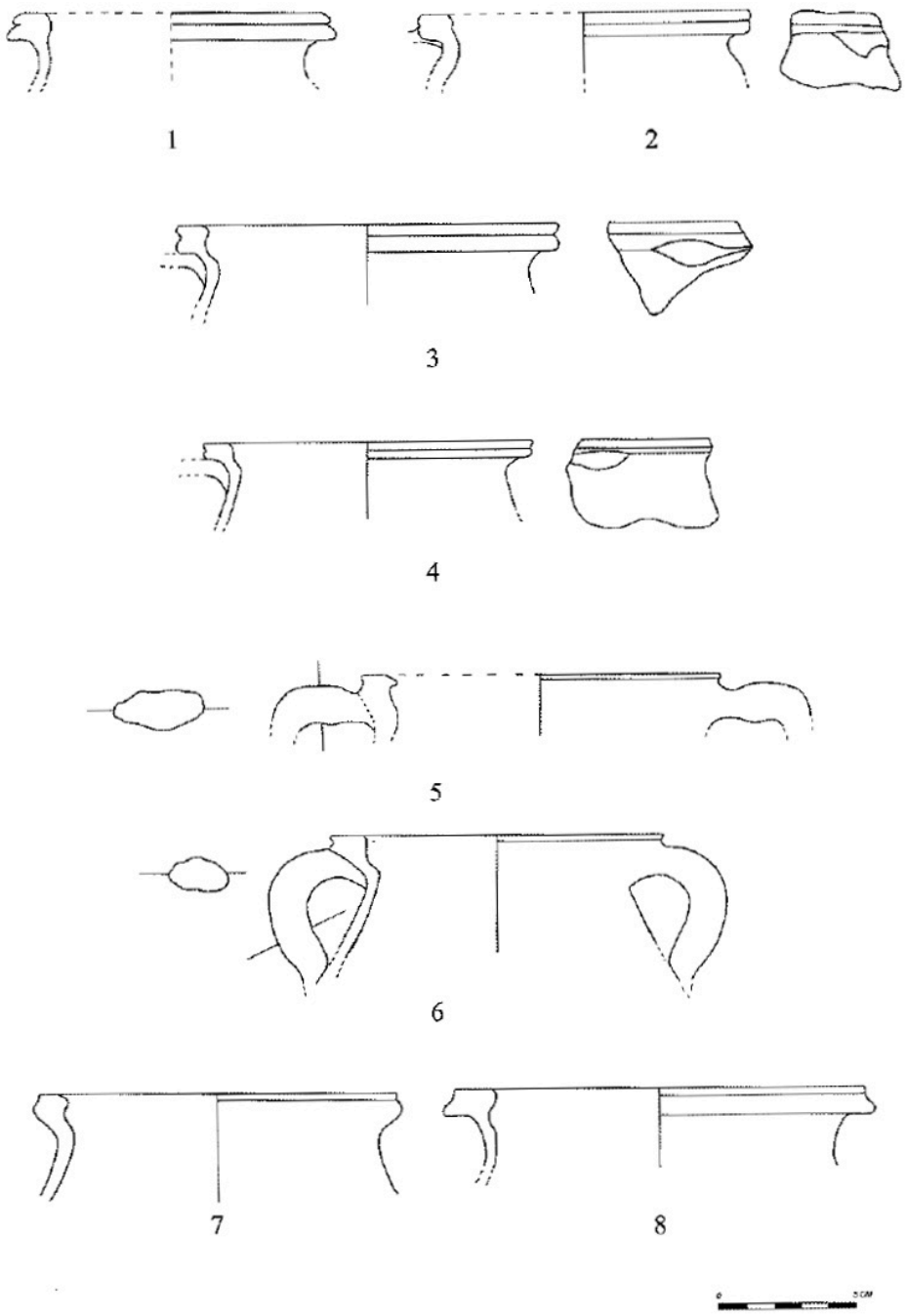

Figure 100. Matomara, Roman-period cooking pots, nos. 1-4 and 6 as Reynolds' "Epirote Grooved Rim Cooking Pot"/ERCP 3 (with a 5 cm-scale; Aleotti 2012, fig. 4)

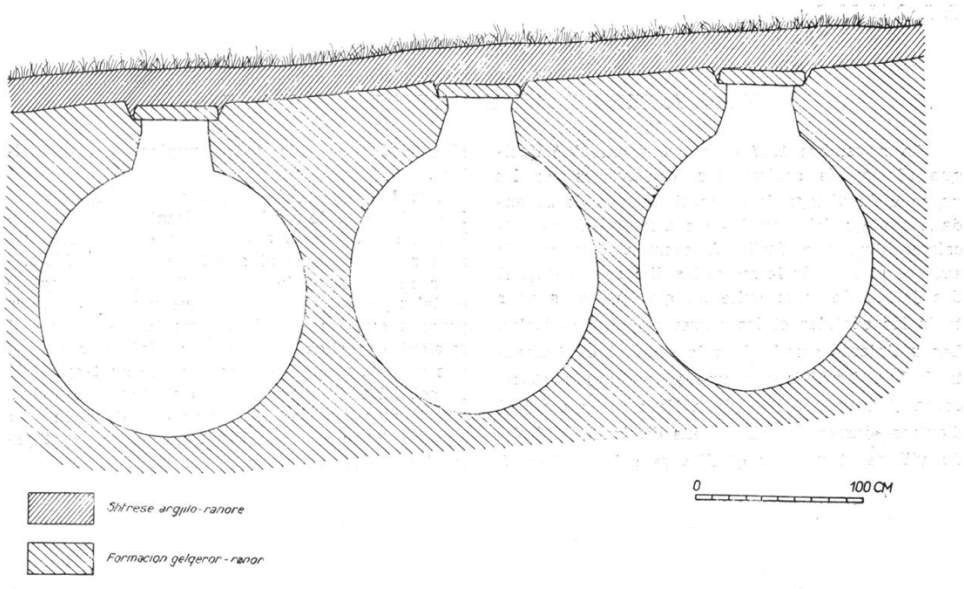

Figure 101. Qesarat, pithos-shaped, rock-cut pits (Zheku 1983, fig. 1)

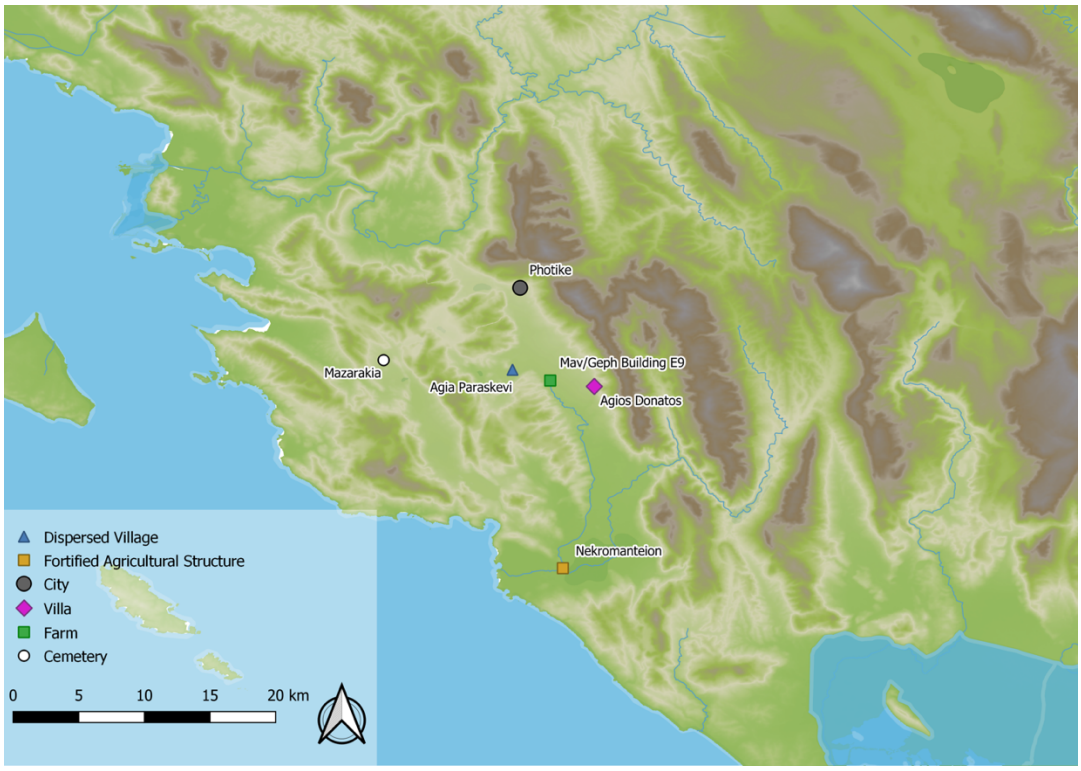

Figure 102. Early Roman rural sites in the Kokytos valley and its environs discussed in this thesis, additionally showing the proposed location of Photike (Map made by Hallvard Indgjerd)

Figure 103. Mazarakia cemetery, the podium of the altar-shaped grave monument (Pali et al *2019, fig. 2)*

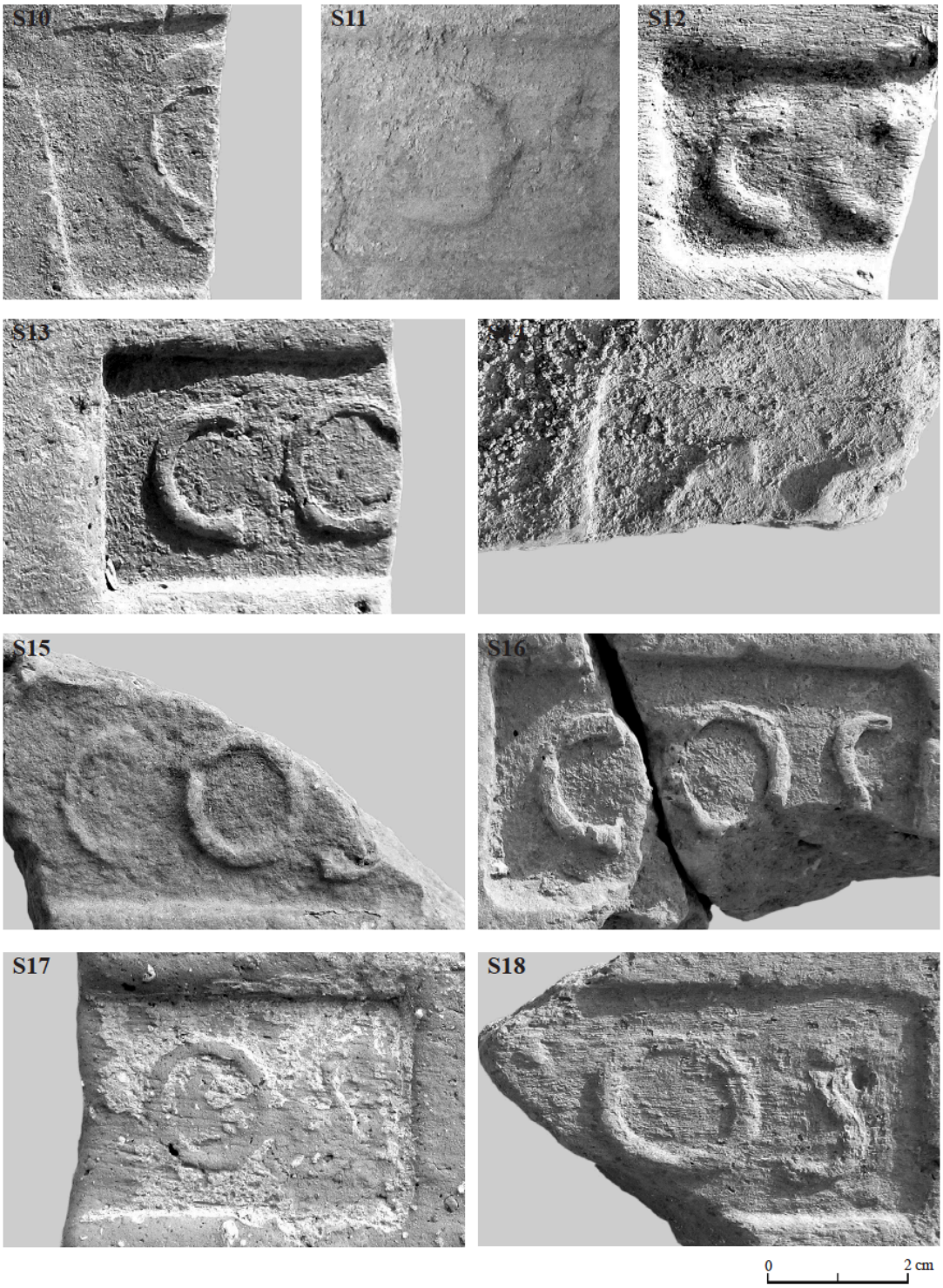

Figure 104. Agios Donatos, bricks bearing the COS stamps (the latter in ligature, Forsén et al 2019, fig. 2)

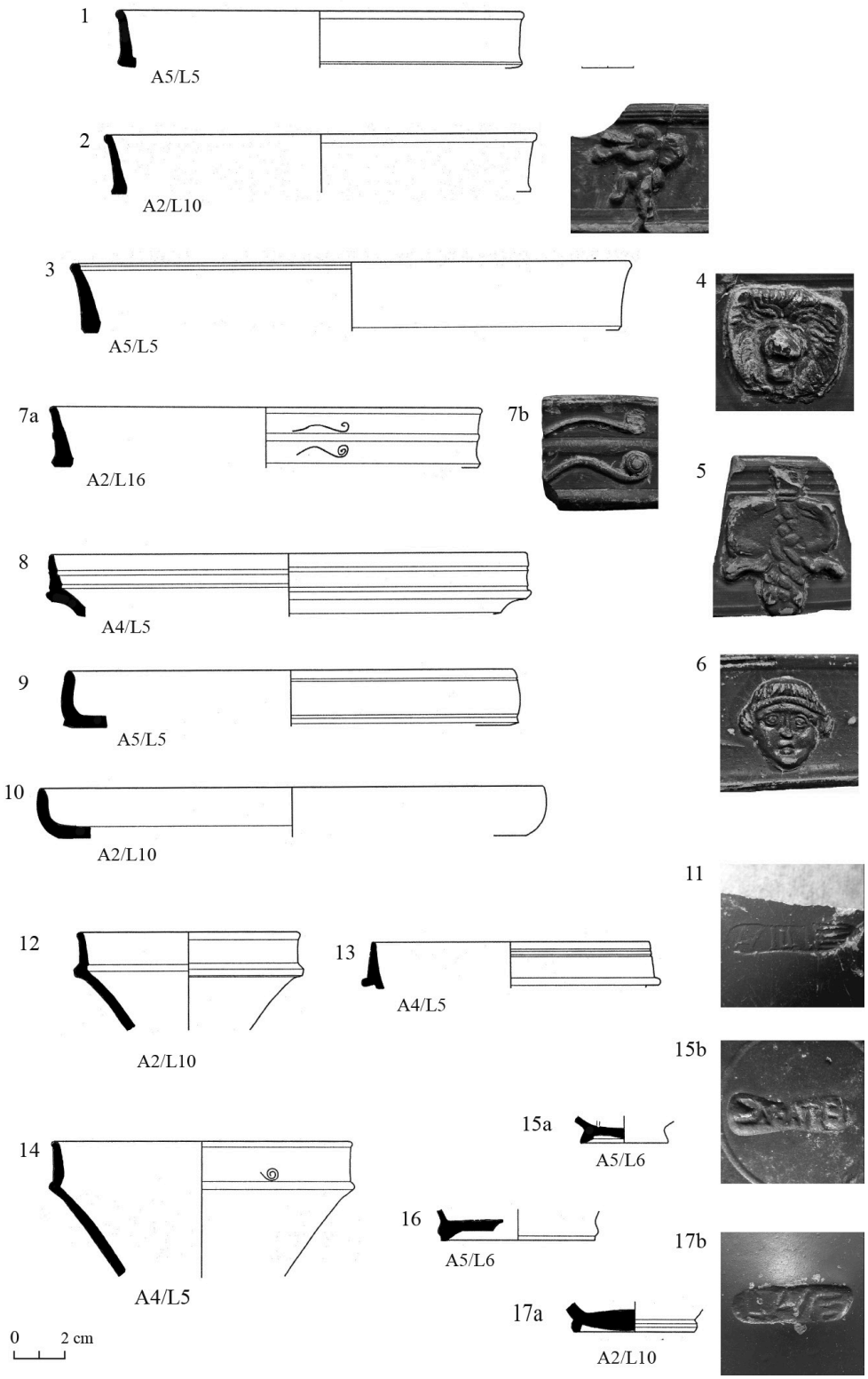

Figure 105. Agios Donatos, drawings of ITS tableware forms from Layer V (Reynolds and Ikäheimo 2019, fig.13)

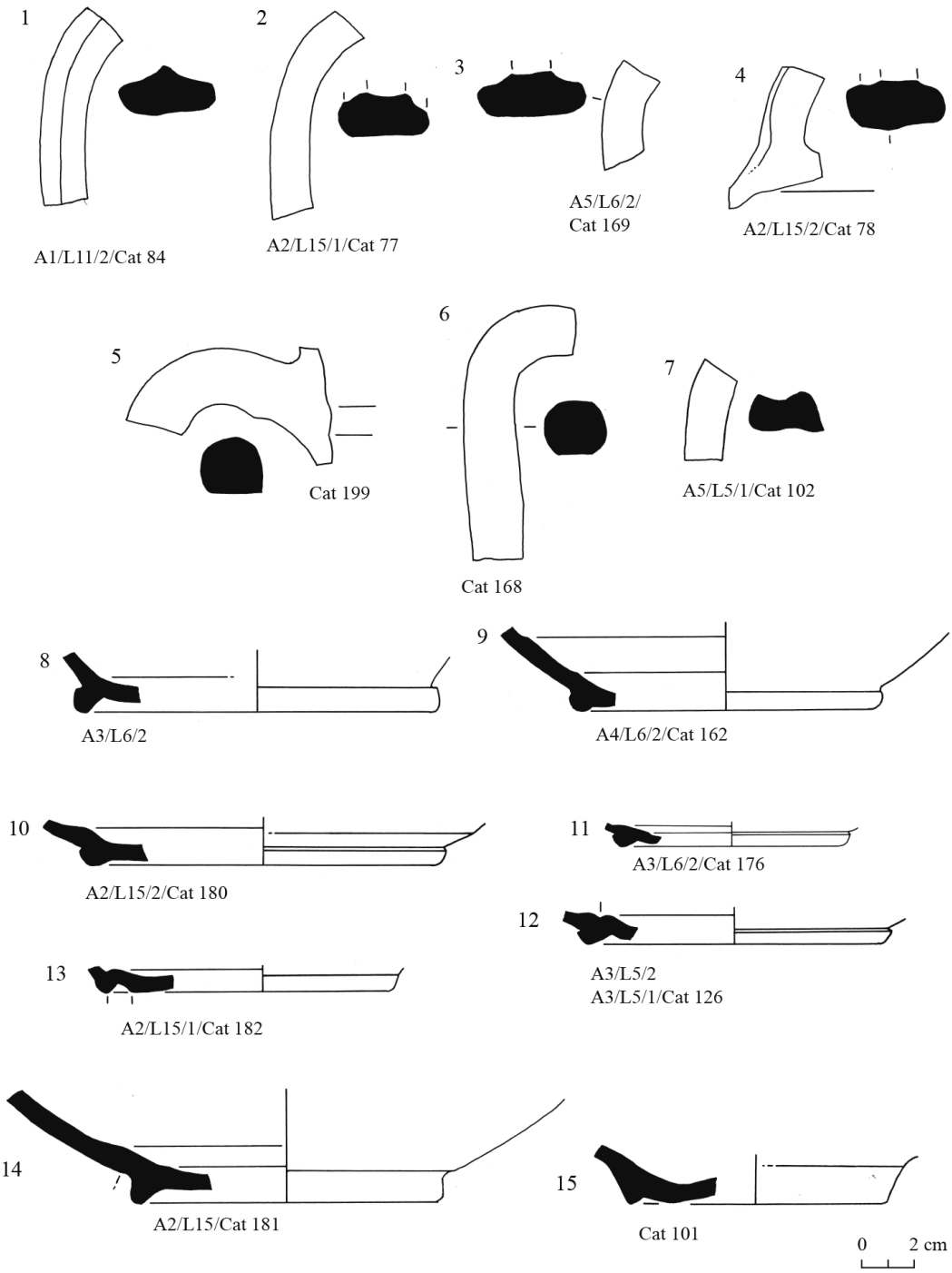

Figure 106. Agios Donatos, amphorae *from Layer V, including examples of the bases of free-standing* amphorae *(Reynolds and Ikäheimo 2019, fig.19)*

Figure 107. Mavromandilia, farm building E 9, with wall foundations of limestone blocks (foreground) and walls built with medium-sized and small stones (background). To the left can be seen the top surface of the vat (Forsén et al. *2011, fig. 22)*

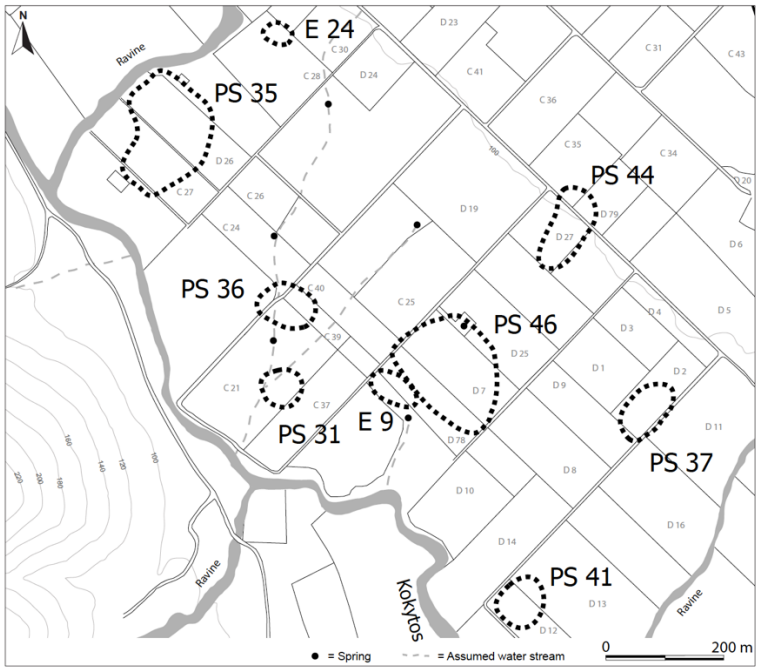

Figure 108. Plan of the dispersed village at Mavromandilia/Gephyrakia, showing sites with finds from the EIA through the ER period (Forsén et al *2011, fig. 21)*

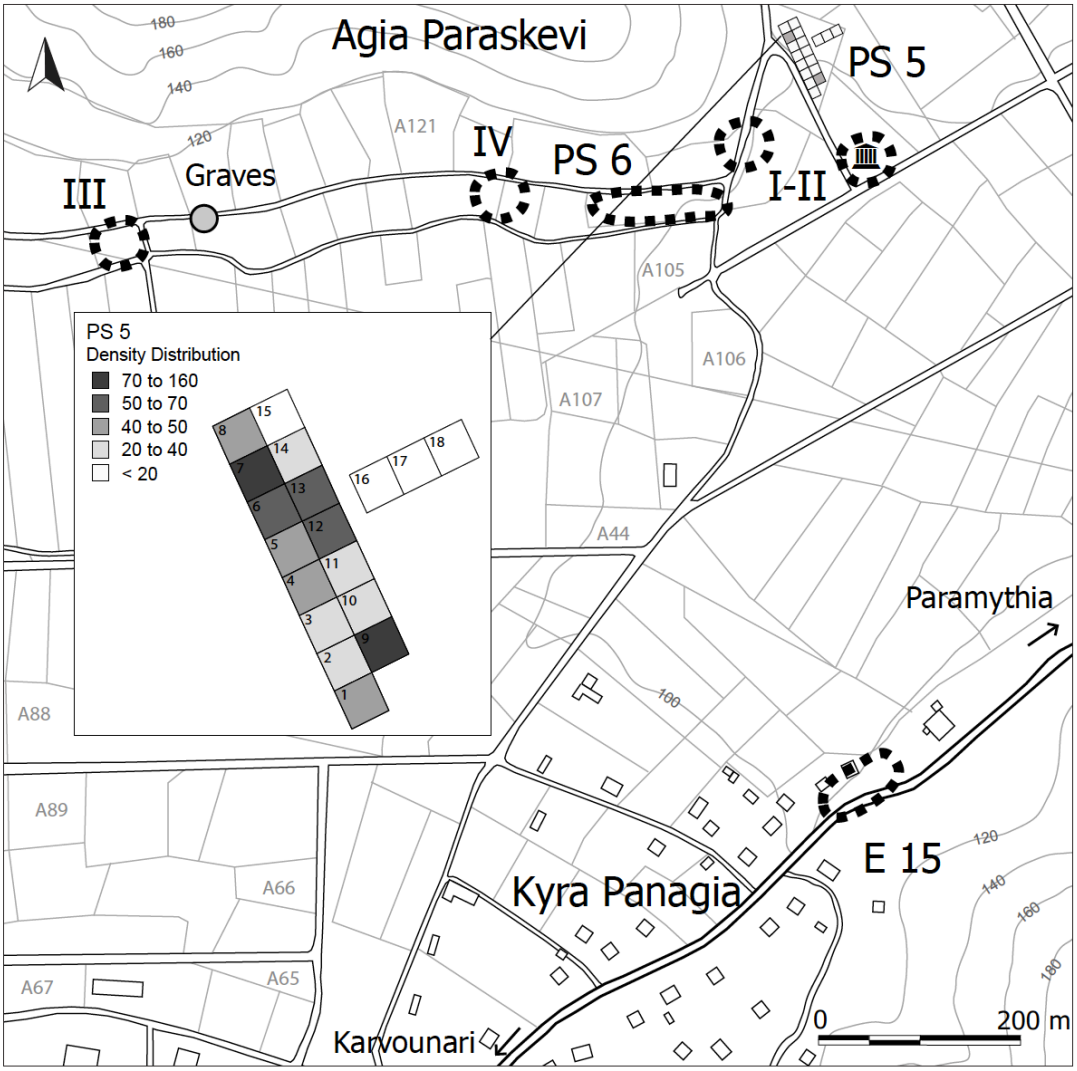

Figure 109. Plan of the cluster of rural sites near Kyra Panagia, to the north the village of Agia Paraskevi and to the south E 15 belonging to another hamlet (Forsén et al *2011, fig. 8)*

Map 7

NICOPOLIS

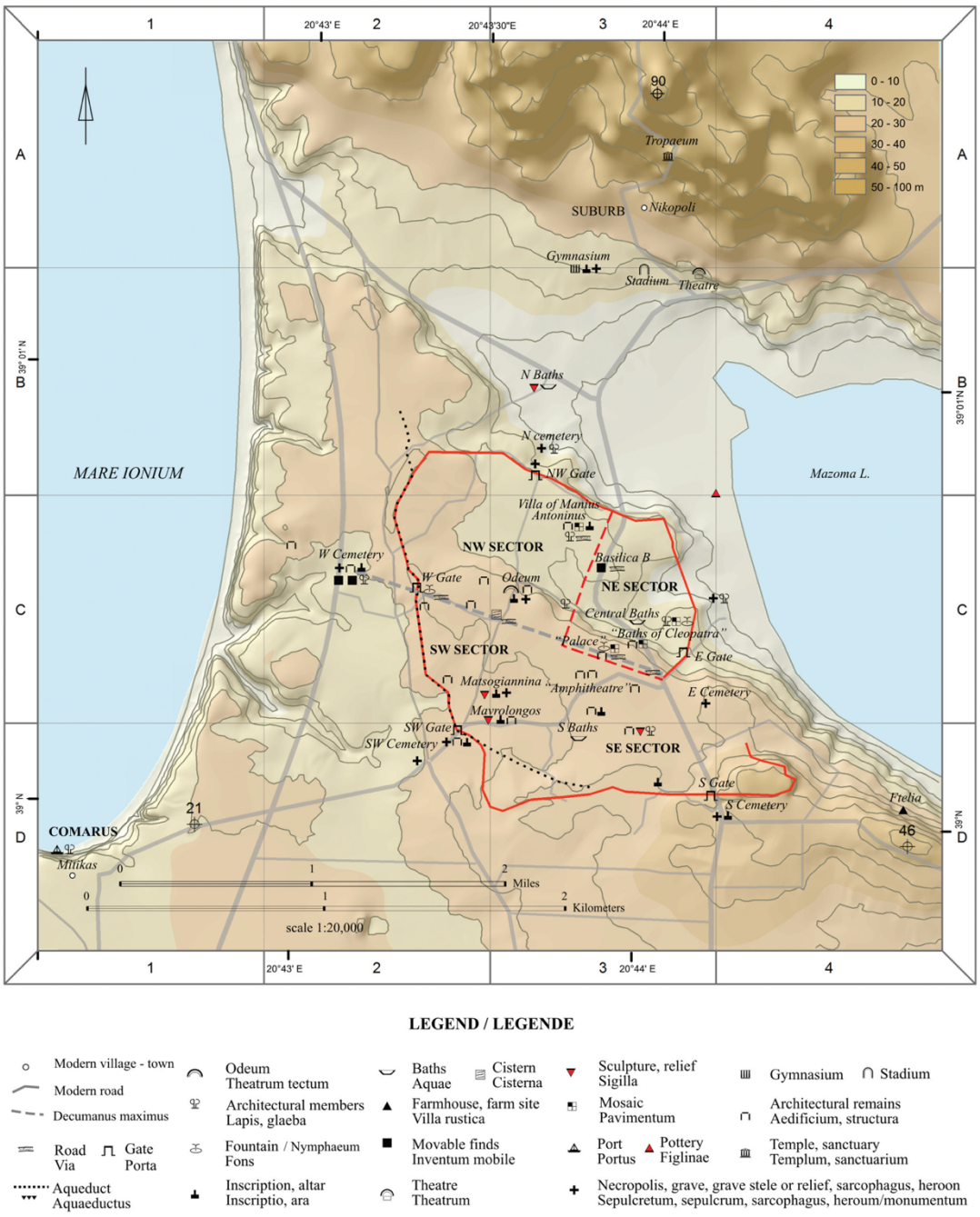

LEGEND / LEGENDE

- Modern village - town
- Modern road
- Decumanus maximus
- Road Via / Gate Porta
- Aqueduct Aquaeductus
- Odeum Theatrum tectum
- Architectural members Lapis, glaeba
- Fountain / Nymphaeum Fons
- Inscription, altar Inscriptio, ara
- Baths Aquae / Cistern Cisterna
- Farmhouse, farm site Villa rustica
- Movable finds Inventum mobile
- Theatre Theatrum
- Sculpture, relief Sigilla
- Mosaic Pavimentum
- Port Portus / Pottery Figlinae
- Necropolis, grave, grave stele or relief, sarcophagus, heroon Sepulcretum, sepulcrum, sarcophagus, heroum/monumentum
- Gymnasium / Stadium
- Architectural remains Aedificium, structura
- Temple, sanctuary Templum, sanctuarium

Figure 110. Topographic map of Nikopolis and the suburb to the north where the extramural sanctuary was located, with different ancient remains indicated (Antoniadis 2016, map 7)

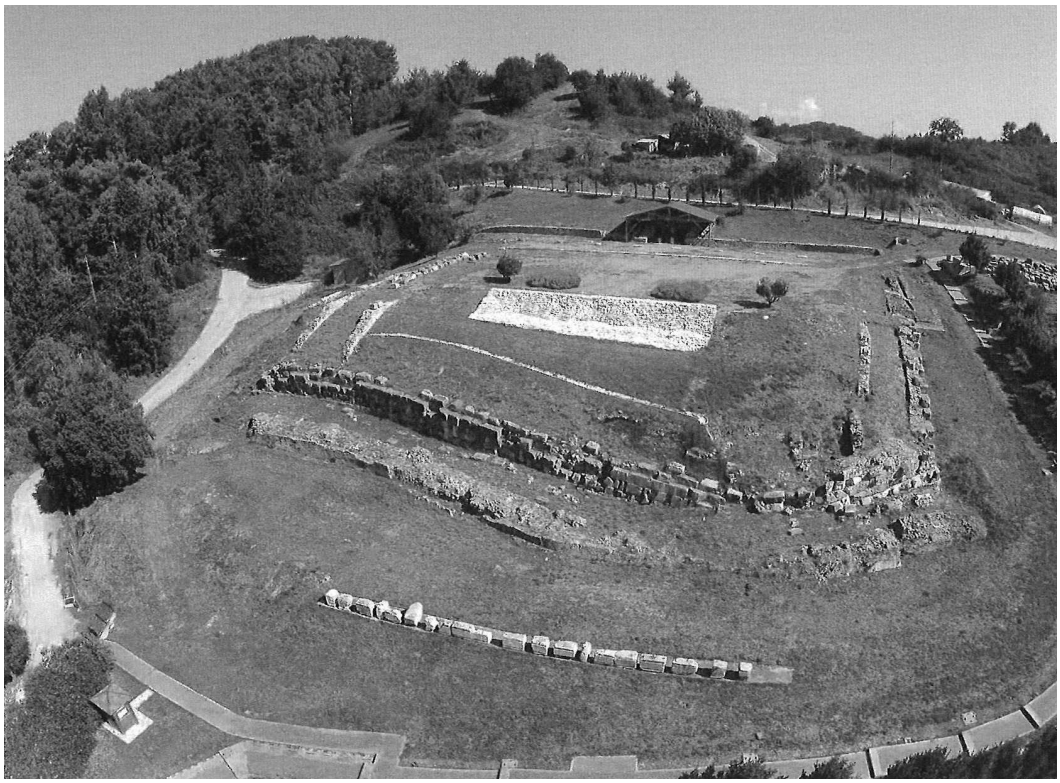

Figure 111. Actium Victory Monument, Nikopolis (Zachos et al. *2018, fig. 1)*

Figure 112. Preveza peninsula, western part, adapted aerial photograph (1/16,000) of the region south of Nikopolis with visible traces of the centuriation demarcated (after Cladas 1975, fig. 1)

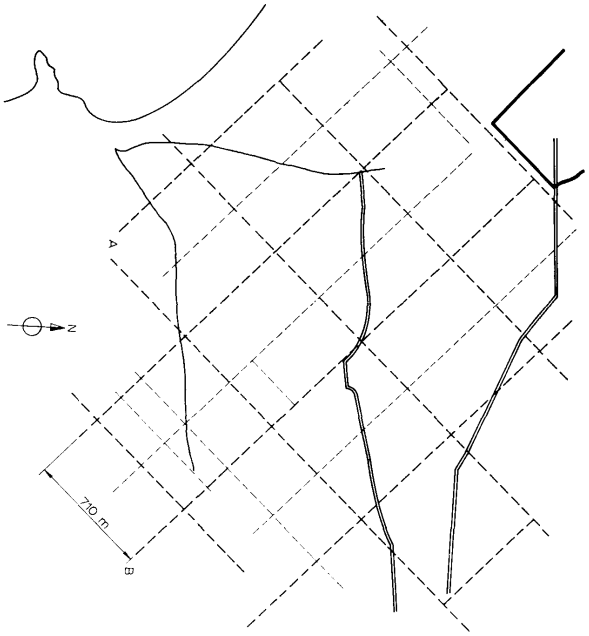

Figure 113. Application of the centuriation system on a plan of the region to the south of Nikopolis (Cladas 1975, fig. 3)

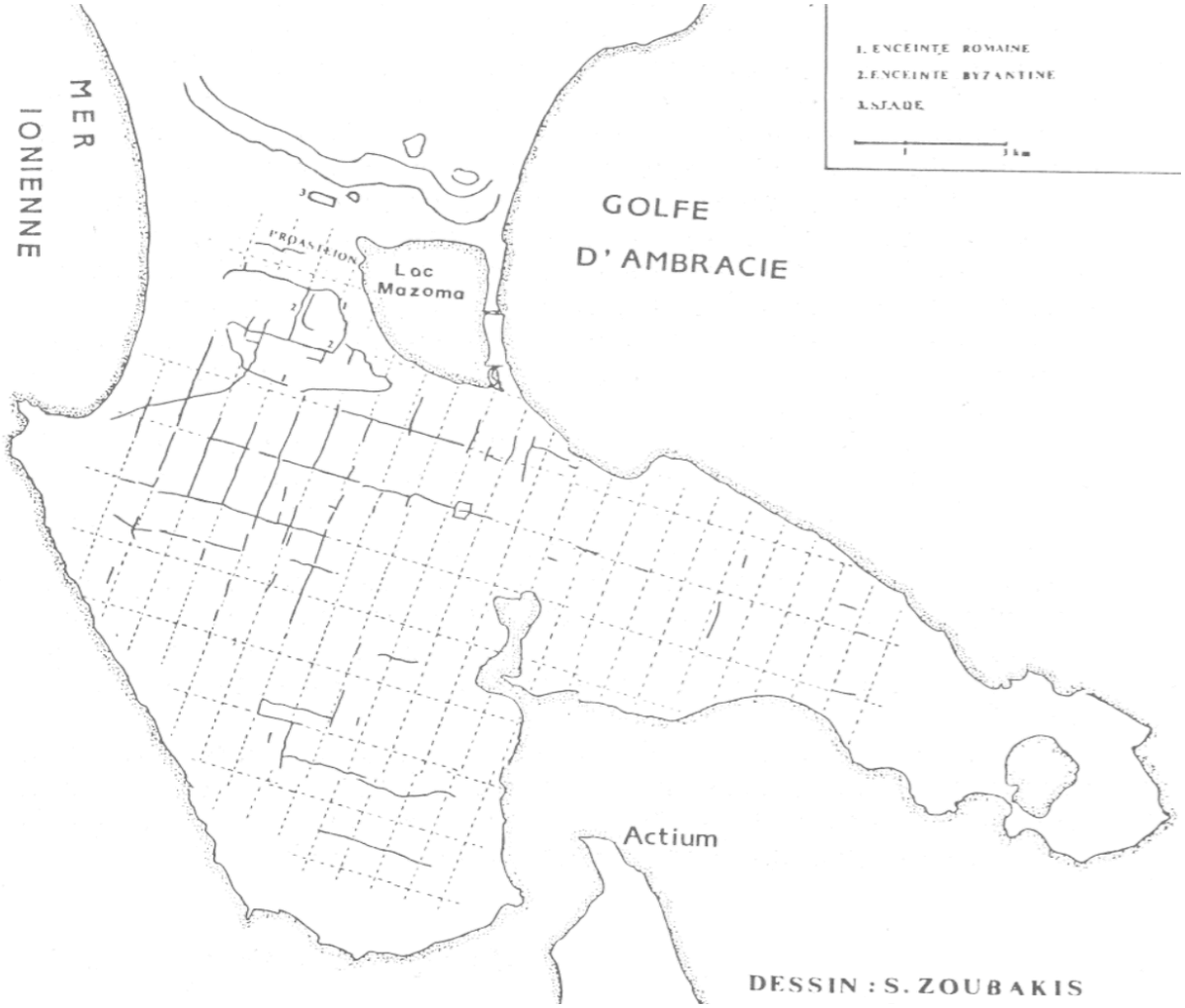

Figure 114. Map of the traces of the centuriation at Actia Nikopolis identified by Doukellis, drawn by S. Zoumbaki; map oriented north with scale of 3 km displayed in the top right-hand corner (Doukellis 1988, 163)

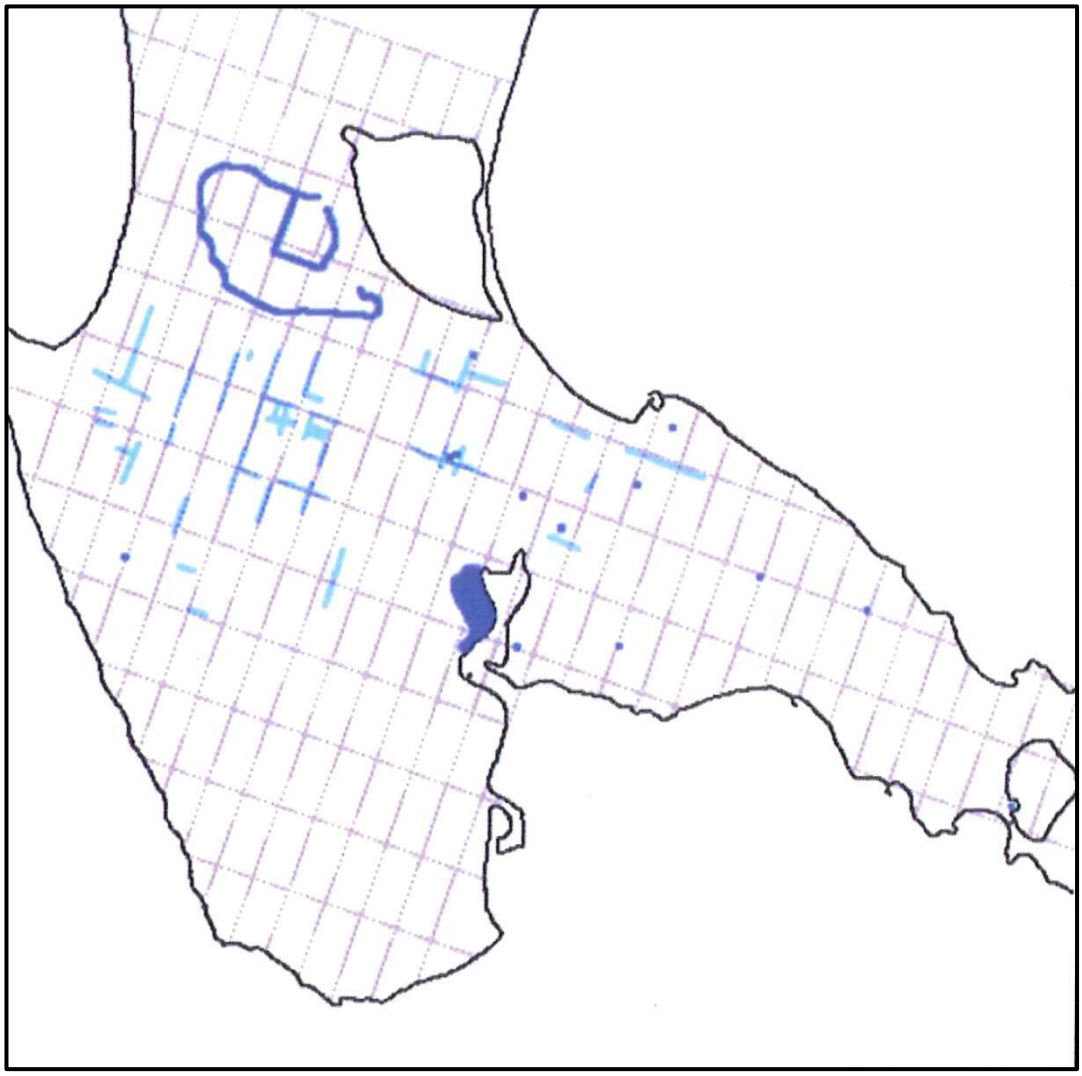

Figure 115. Actia Nikopolis, map oriented north showing the centuriation grid, with the projected limites of the cadastre *identified by Doukellis (dotted lines) and with further traces of landworks identified by Stein (light blue lines); rural sites discovered by the Nikopolis Project survey are also pinpointed (dark blue circles, Stein 2001, fig. 7)*

Figure 116. Actia Nikopolis, map of Riginos and Sakkas (oriented north), pinpointing the location of excavated sites on the blueprint of the centuriation: (1) Analipsis A, (2) Analipsis B, (3) Tarana A, (4) Tarana B, (5) Archaeological Museum of Nicopolis, (6) Vaggeli plot (2018, fig. 1)

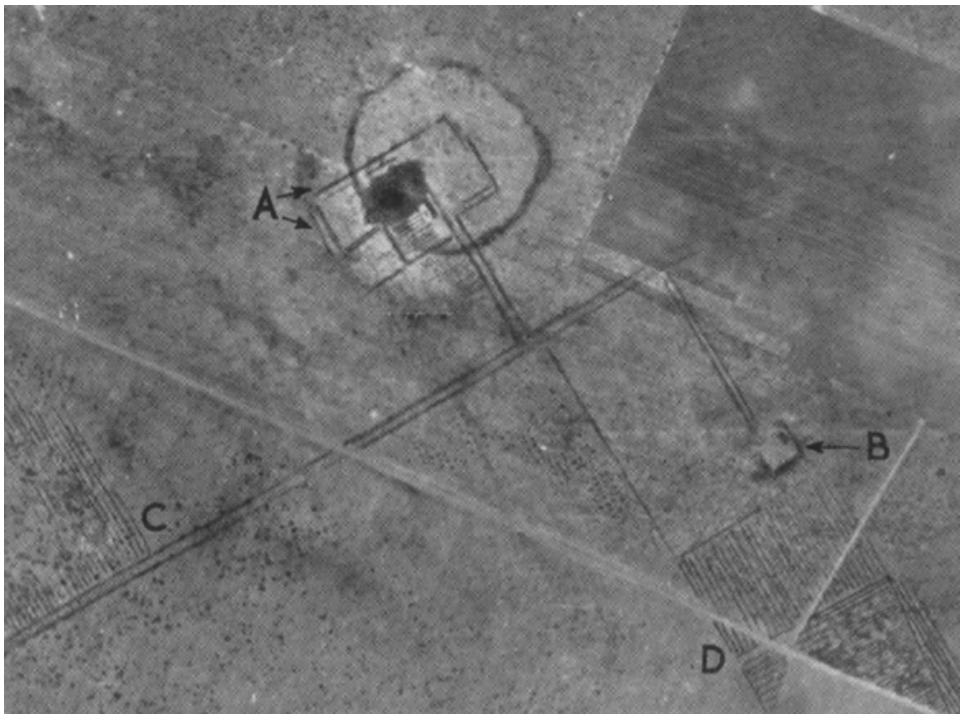

Figure 117. Luceria, aerial photograph showing visible traces of the centuriation and of an ancient farmstead at localita Villano *(Kim 2021, fig. 9)*

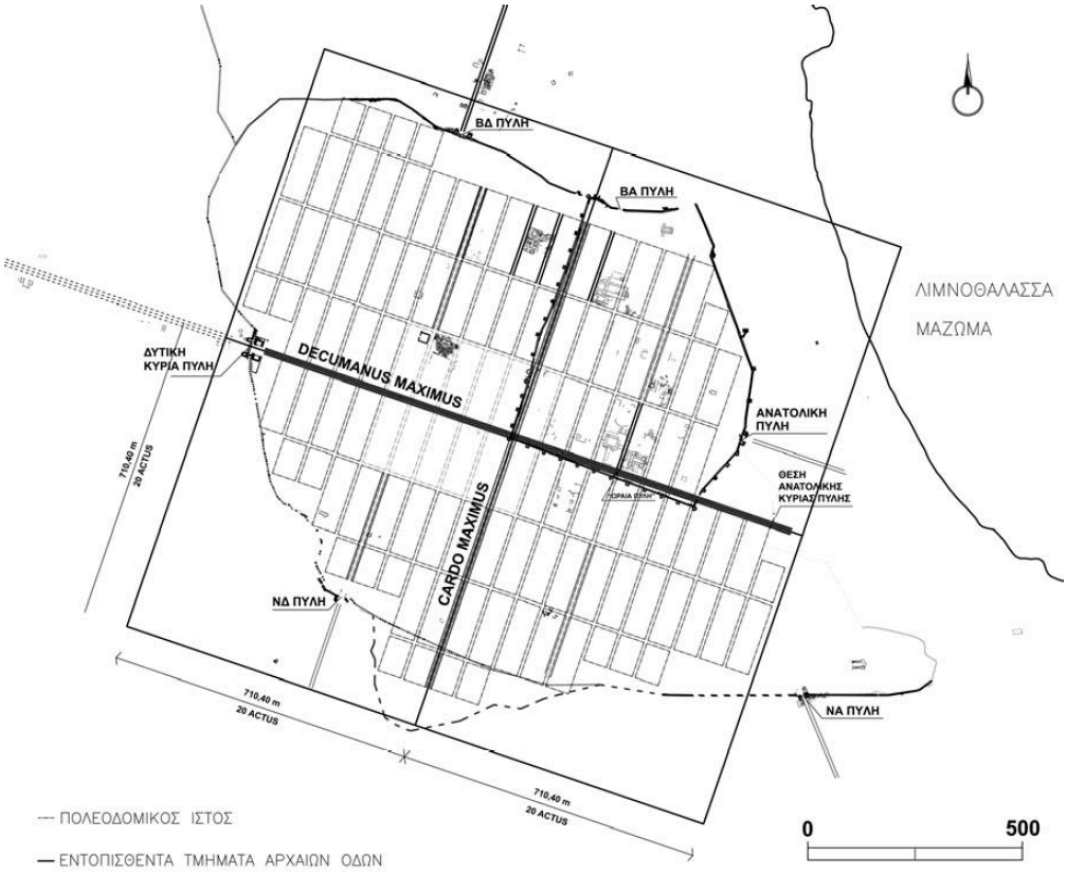

Figure 118. Plan of Nikopolis proposed by Zachos, showing the projected urban grid (light grey lines) and highlighting streets parts of which have been excavated (dark lines, Zachos 2007, fig. 9)

Figure 119. Map of the Nikopolis peninsula showing the centuriation divisions and the city grid enclosed by the wall-circuit (map oriented north; Zachos 2007, fig. 160 after Stein 2001).

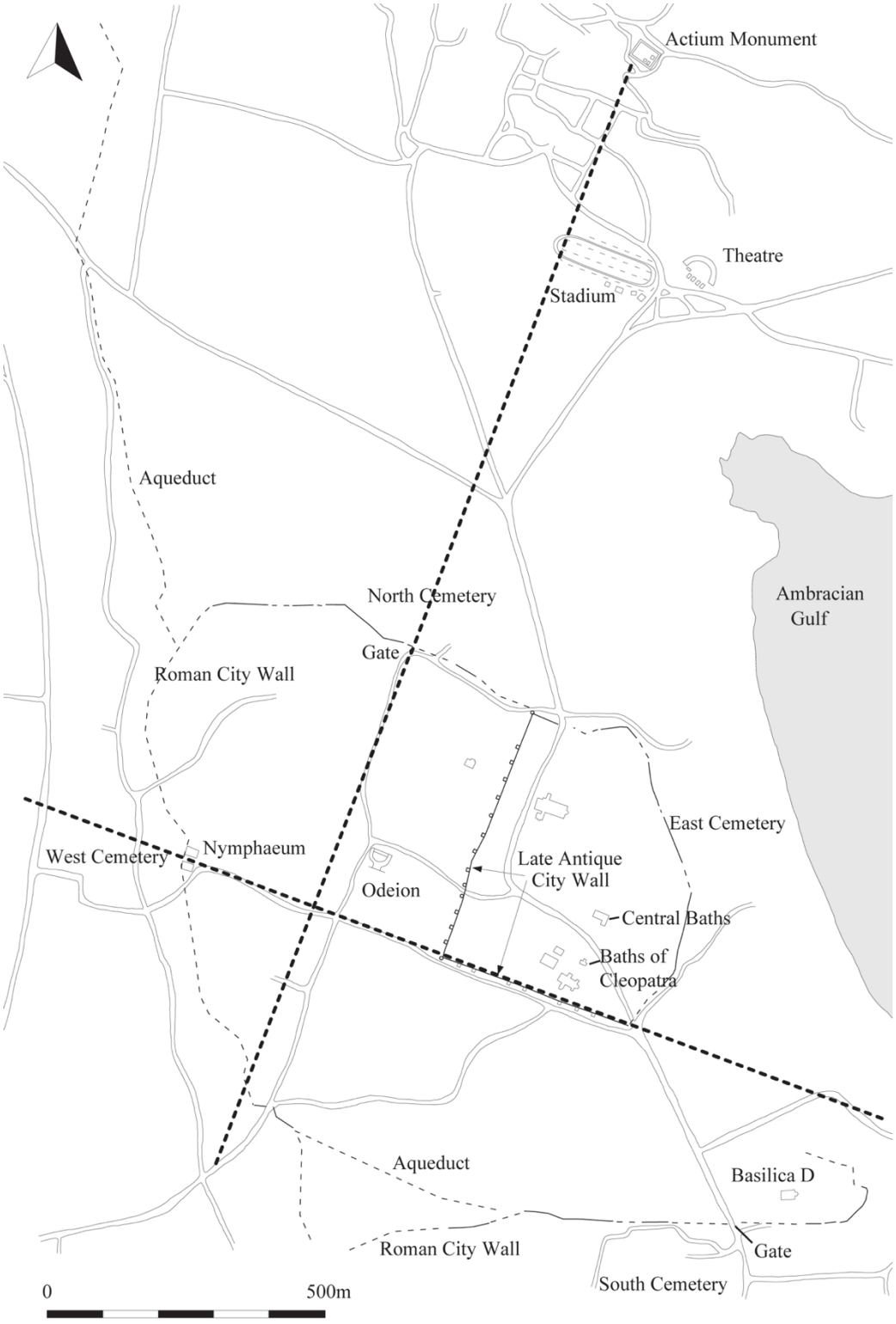

Figure 120. Plan of Nikopolis indicating using dashed lines the cardo maximus *proposed by Bowden and* the decumanus maximus *(Bowden 2011, fig. 7.4, mainly after the topographic map by Pierrepont White 1986-97)*

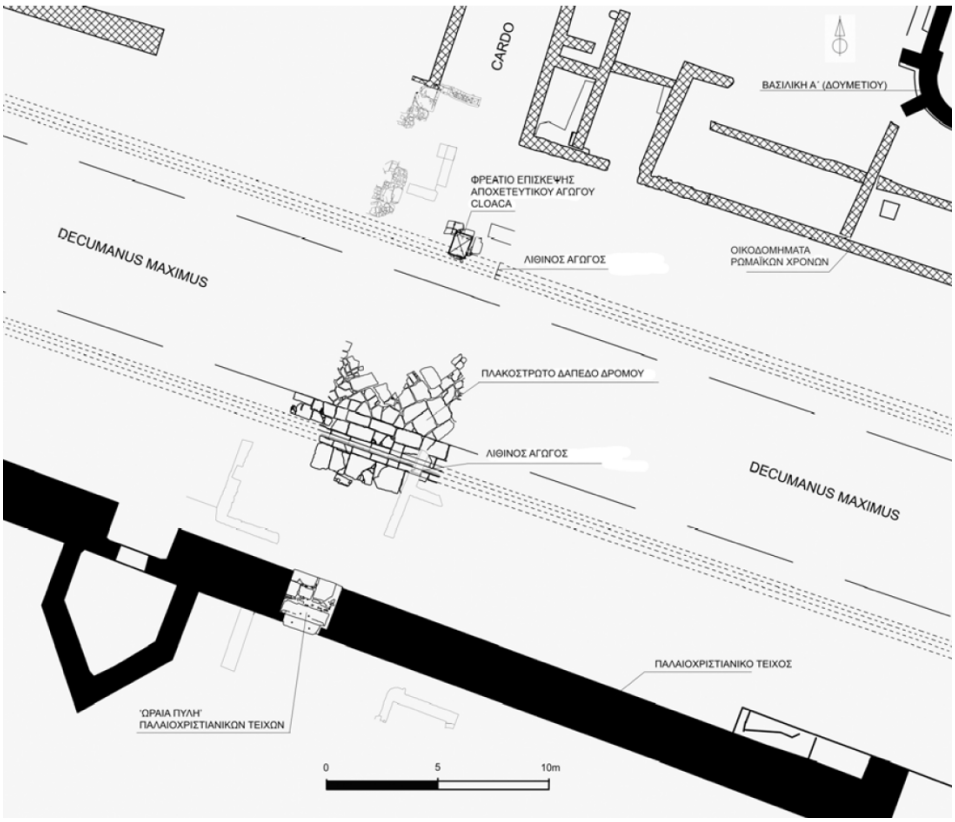

Figure 121. Nikopolis, drawing of the short segment excavated of the decumanus maximus*, next to a small gate ('Ωραία Πύλη') of the southwestern course of the Late Roman wall-circuit (Zachos 2007, fig. 7)*

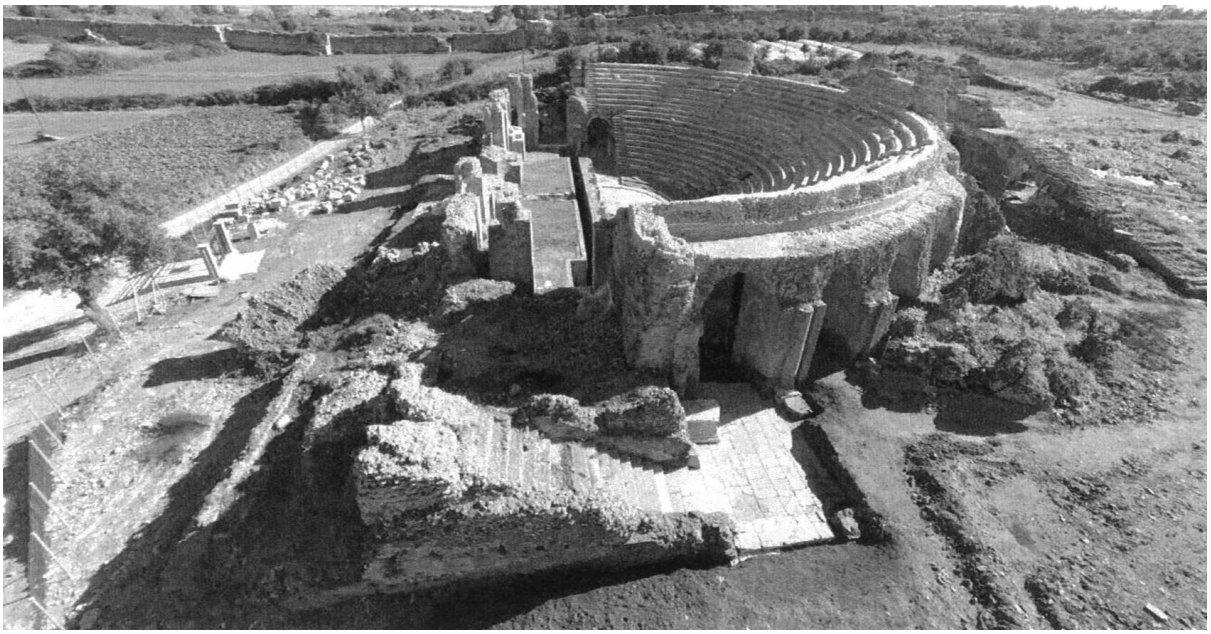

Figure 122. Nikopolos, the odeion *(Zachos* et al. *2018, fig. 3)*

Figure 123. Analipsis B, vat 1, rim fragments of ITS cup, Conspectus 23 (Copyright owned by the Ephorate of Antiquities of Preveza)

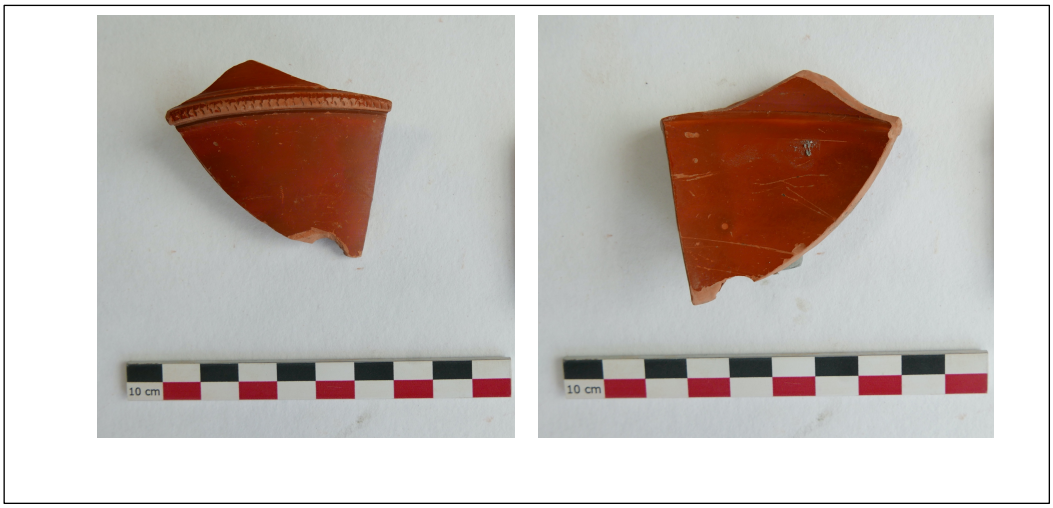

Figure 124. Tarana A, fragment of rim, shoulder and body of ITS cup, Conspectus 22.5 (Copyright owned by the Ephorate of Antiquities of Preveza)

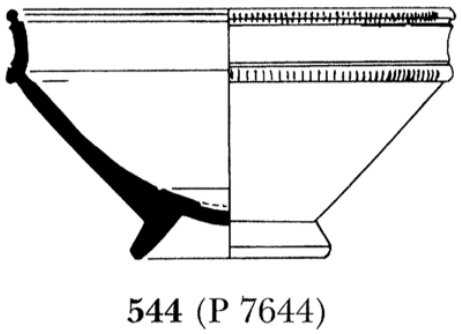

Figure 125. Athenian Agora, drawing of ITS cup, Conspectus 22.5, from a context dating between 20-40/50 CE (Hayes 2008 544)

Figure 126. Tarana tomb 15, lamp Loeschke type III / Bailey type D, subgroup v 5 (Copyright owned by the Ephorate of Antiquities of Preveza)

Figure 127. Tarana tomb 15, lamp, detail of triangular handle 5 (Copyright owned by the Ephorate of Antiquities of Preveza)

Figure 128.Triangular lamp handle, Claudian-early Trajanic(Bailey 1980, pl. 36, Q 1048)

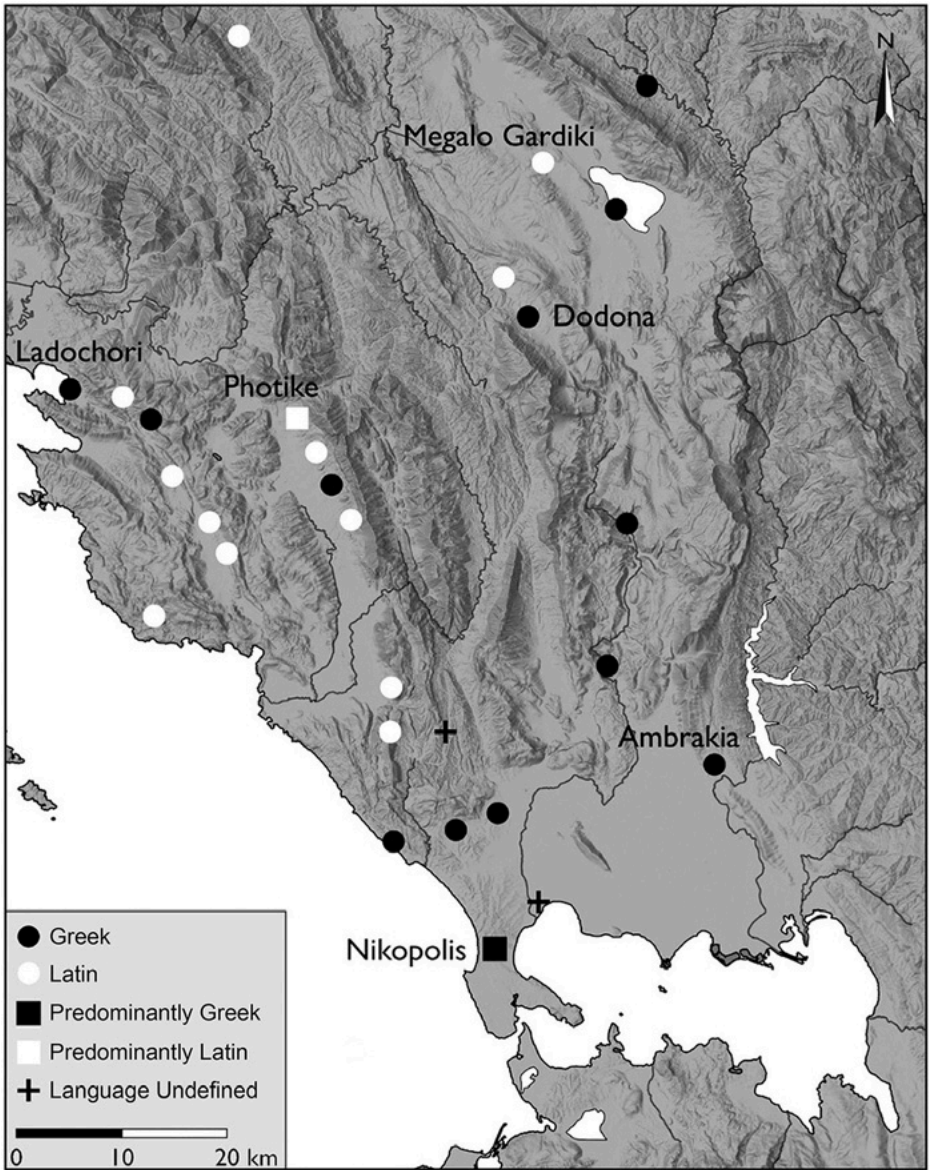

Figure 129. Distribution of inscriptions by their use of the Greek or Latin language in southern Epirus (Forsén 2021, fig. 10.6)

Figure 130. Map of definite villas in Roman Epirus (Map made by Hallvard Indgjerd)

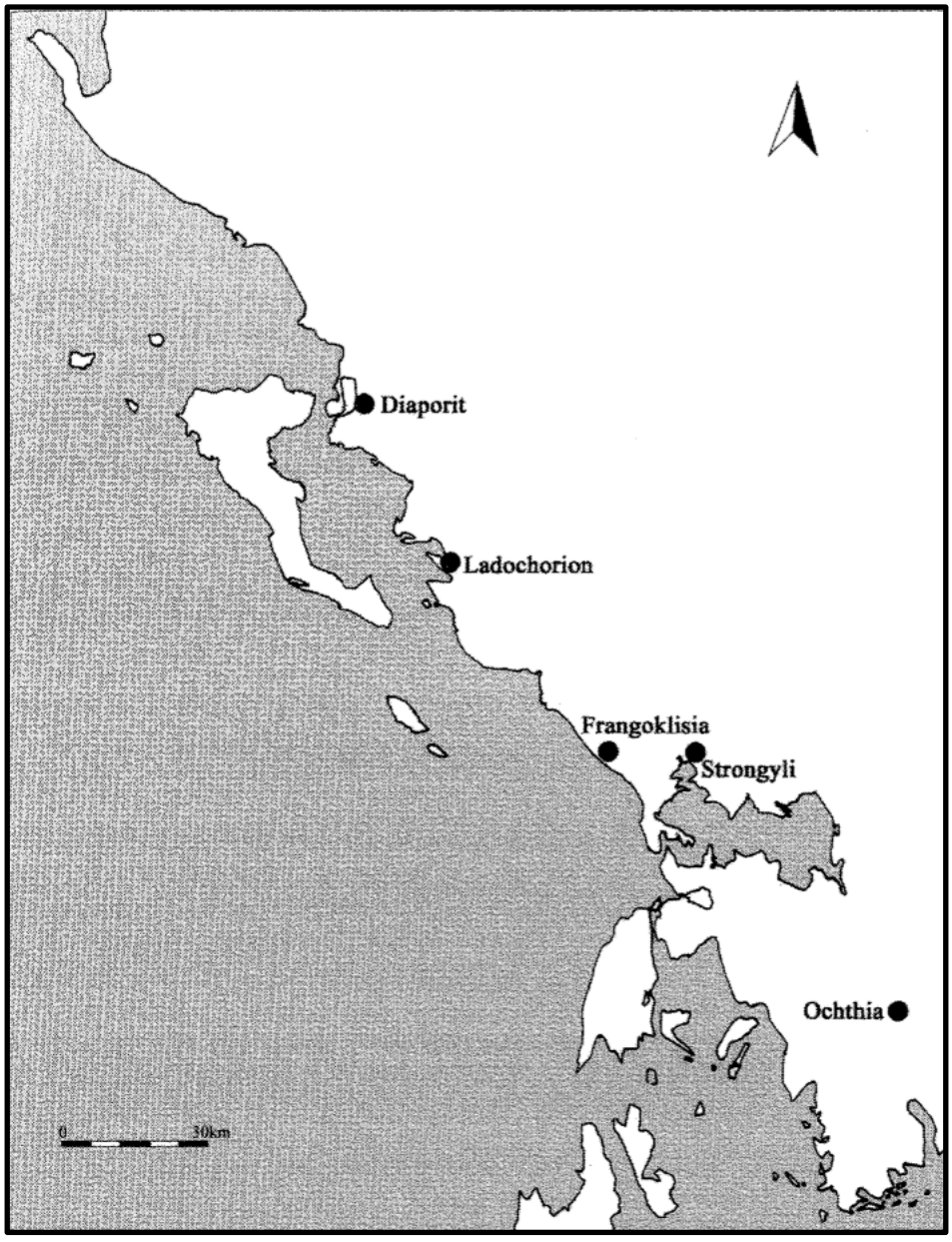

Figure 131. Map of villa sites with Late Antique occupation in Epirus Vetus (Bowden 2003, fig. 4)

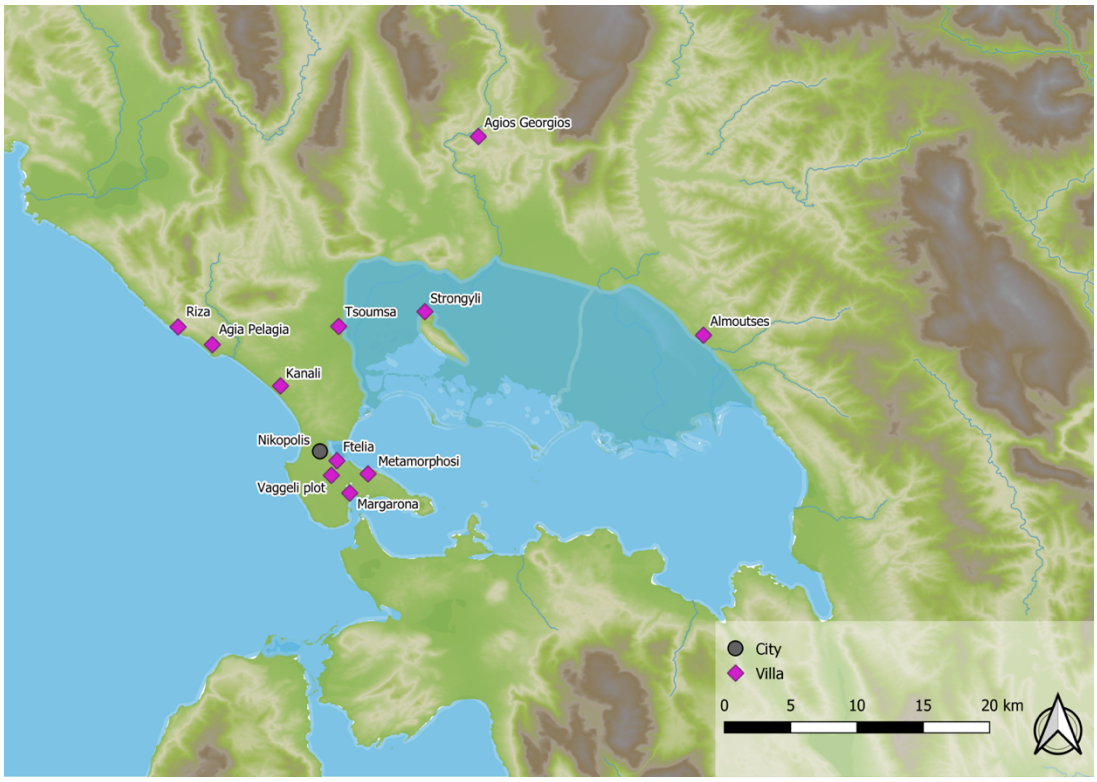

Figure 132. Map of villas in the area of the Ambracian Gulf discussed in chapter 6 (Map made by Hallvard Indgjerd)

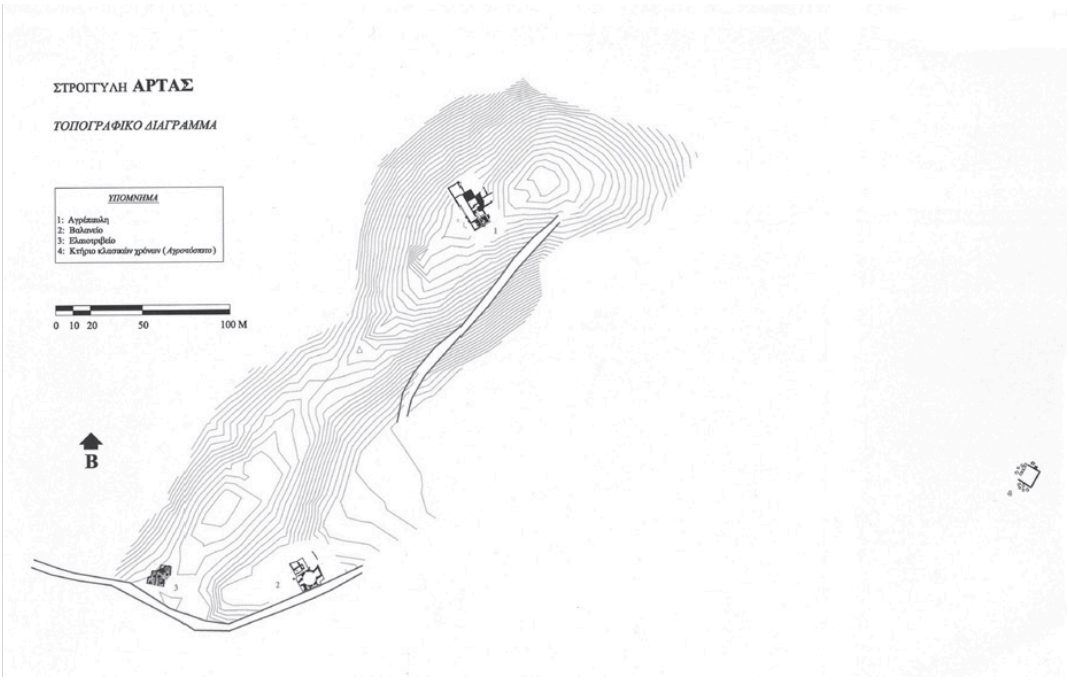

Figure 133. Topographic map of Strongyli, with the villa residence atop the hill, the octagonal bath complex to south and the production installation to the southwest (Giannaki 2017, fig. 2)

Figure 134. View from the top of the Podarouli hillockto Mt Zalongo,across the northern plains of the modern-day Ambracian Gulf area, which would have been mostly underwater in antiquity

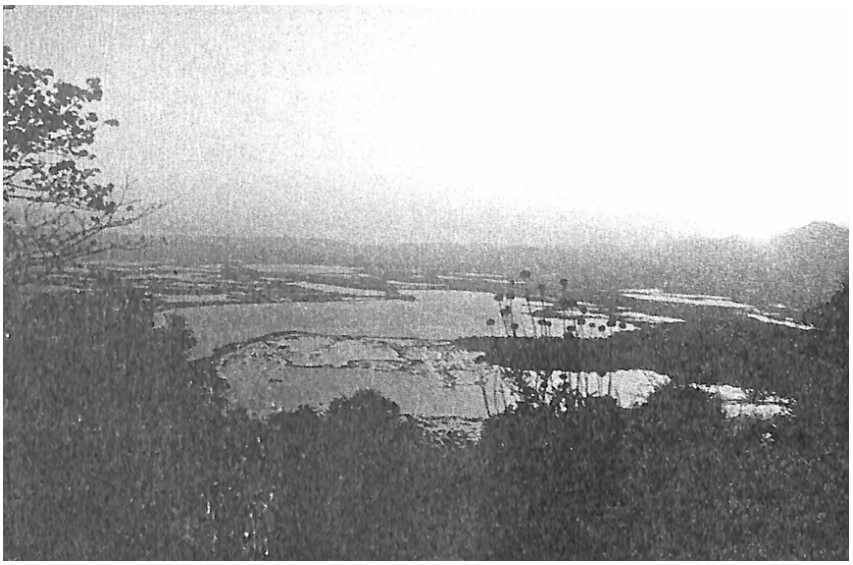

Figure 135. The northern modern-day marshes of the gulf (after Ntouzougli 2003, fig. 1)

Figure 136. Strongyli, mosaic 13 details, showing one of the goblets (top, badly preserved) and a kantharos *(bottom) (Ntouzougli 2003, figs. 3 and 10; 1993 fig. 5)*

Figure 137. Strongyli, mosaic 13, detail of one of the goblets (Ntouzougli 2003, fig. 13)

Figure 138. Strongyli, mosaic 12 (Ntouzougli 1998, fig. 8)

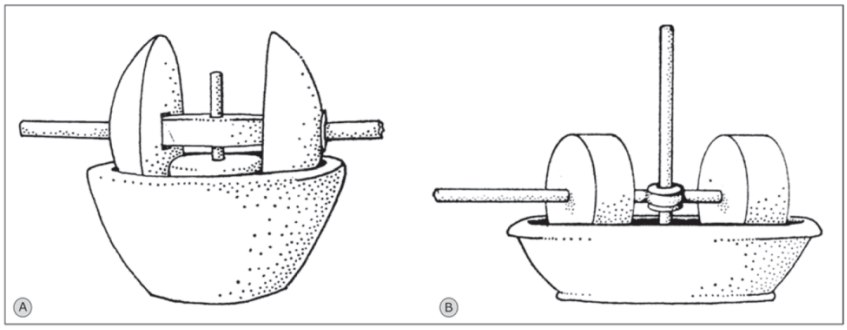

Figure 139. Trapetum (A) and mola olearia (B) grinding mill types (Van Limbergen 2019, fig. 3, after White 1975, figs. 56 and 58)

Figure 140. Strongyli press bed 1, prior to the start of the excavation (Copyright owned by the Ephorate of Antiquities of Arta, Photocard reference: ΕΛΑΙΟΤΡΙΒΕΙΟ ΡΩΜ. ΑΓΡΕΠΑΥΛΗΣ, film F/3853, shot 16).

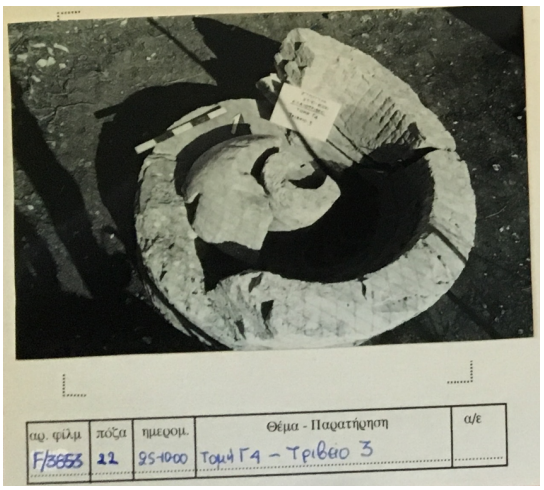

Figure 141. Strongyli mill 3, with half of an orbis within (Copyright owned by the Ephorate of Antiquities of Arta, Photocard reference: ΕΛΑΙΟΤΡΙΒΕΙΟ ΡΩΜ. ΑΓΡΕΠΑΥΛΗΣ, film F/3853, shot 22)

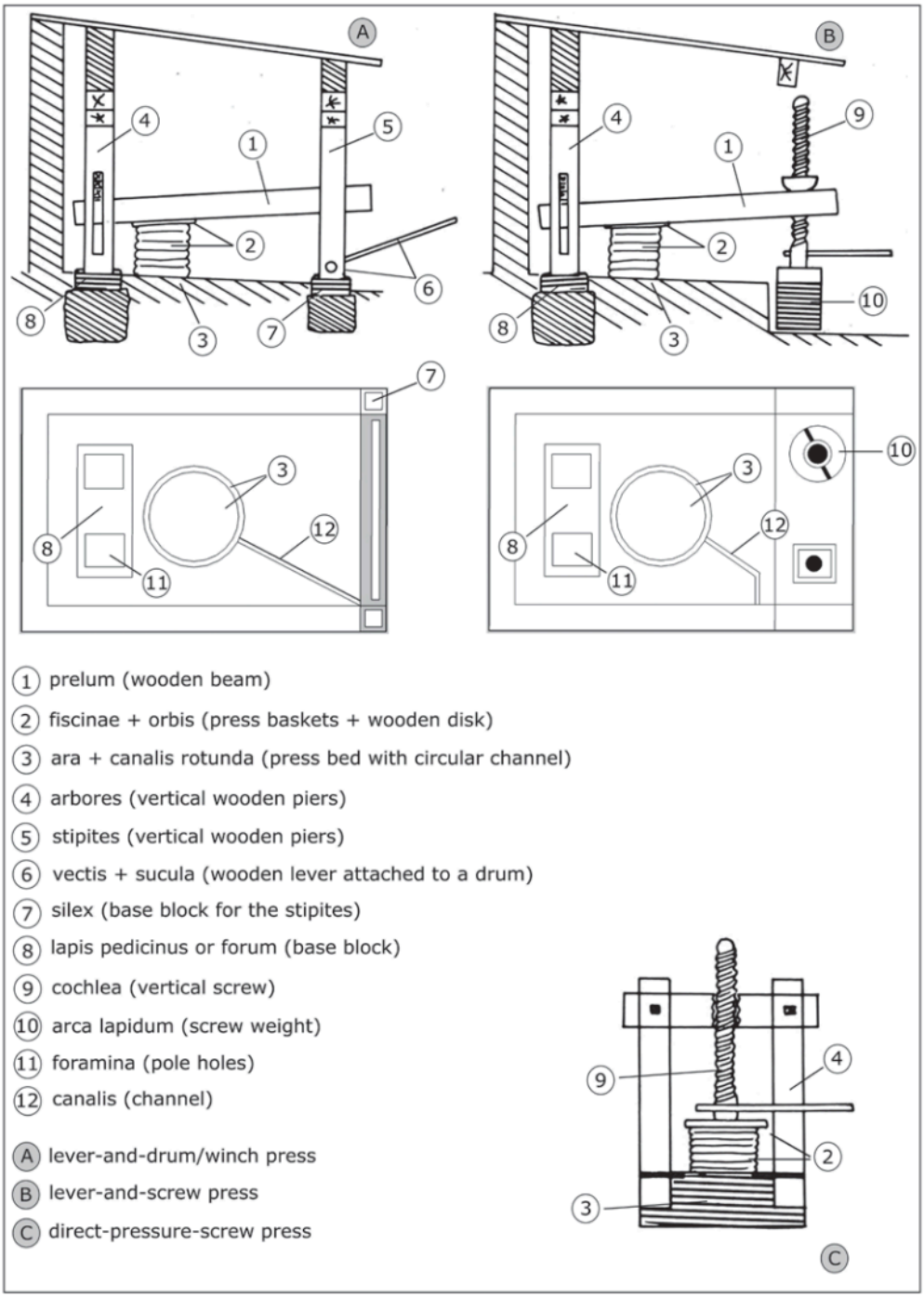

Figure 142. Schematic reconstructions of ancient press types (Van Limbergen 2019, fig. 4, A-B after Brun 1987, 86, fig. 28; C after Brun 1987, 125, fig. 61)

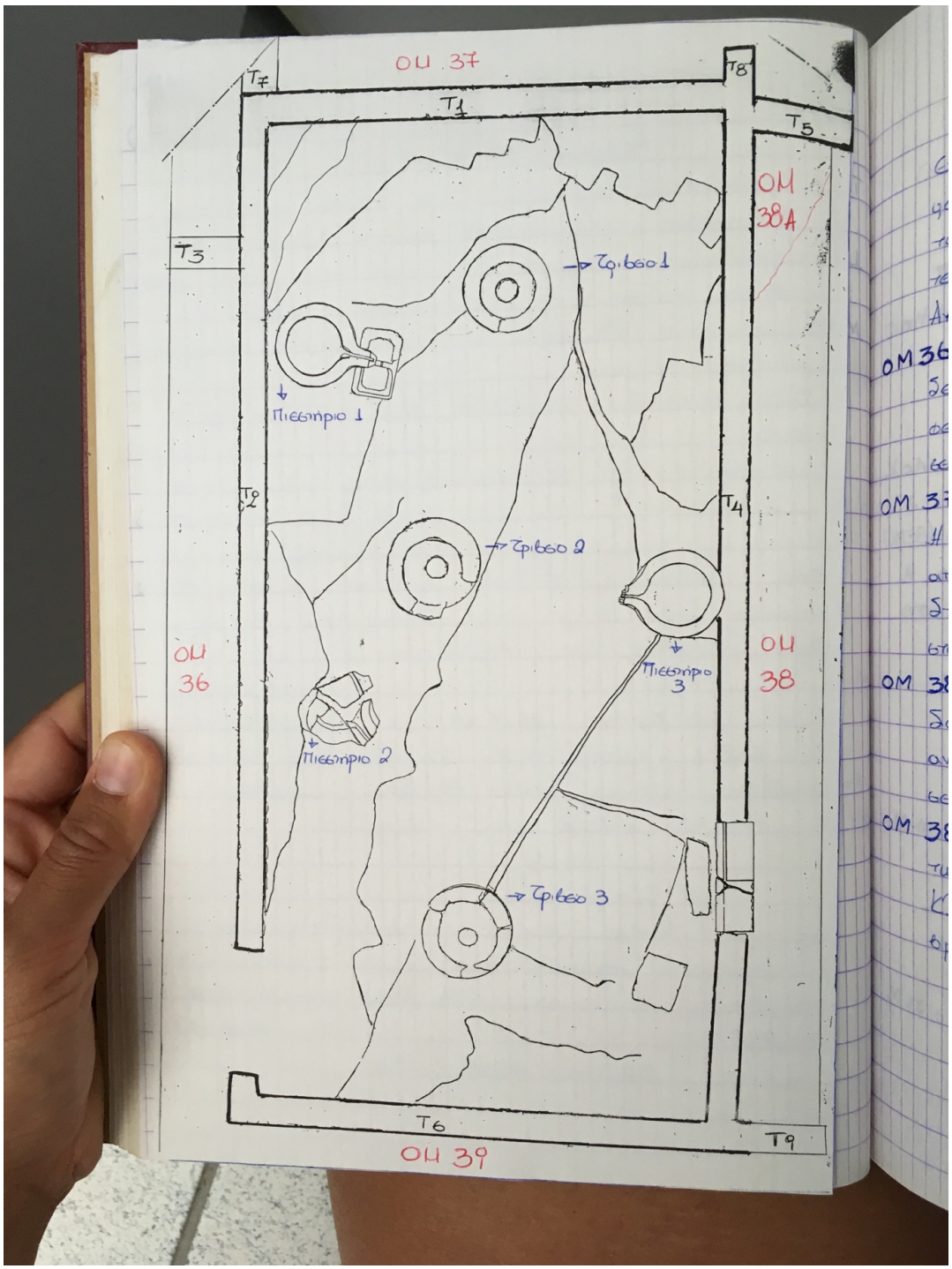

Figure 143. Plan drawing of the Strongyli production installation (Copyright owned by the sEphorate of Antiquities of Arta, Giannaki, EJ 4 (2000-2001), 114).

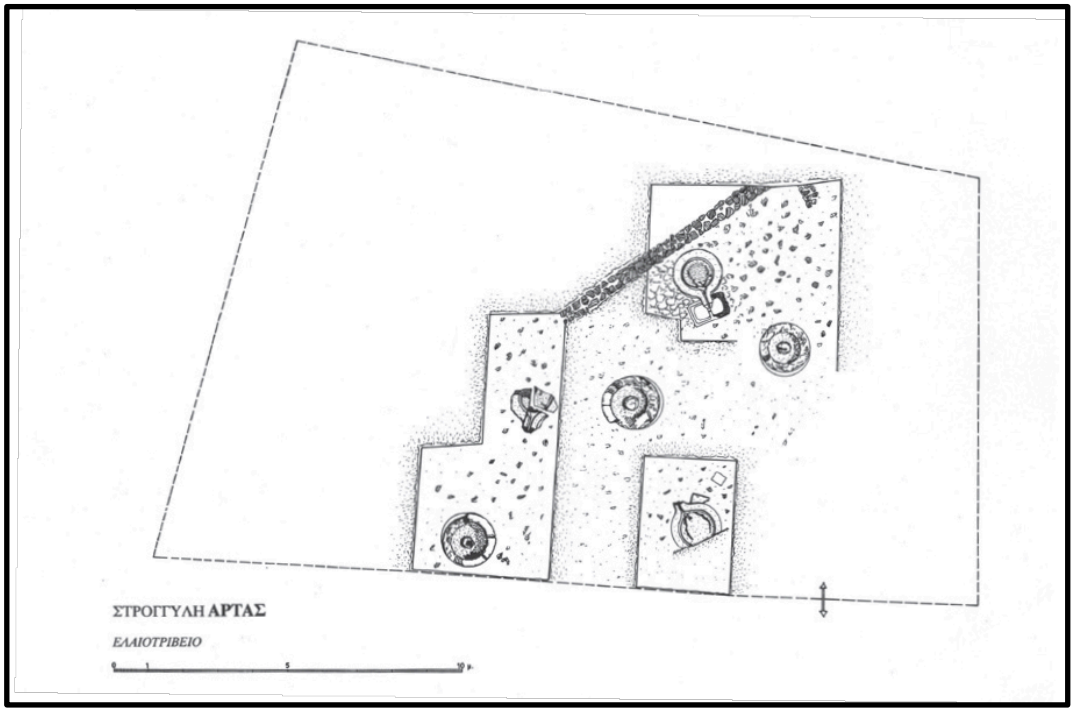

Figure 144. Plan of the Strongyli production installation (before the end of excavation; Giannaki 2017, fig. 3)

Figure 145. The octagonal room of the Strongyli bath suite (Ntouzougli, ADelt 49 (1994), pl. 127b)

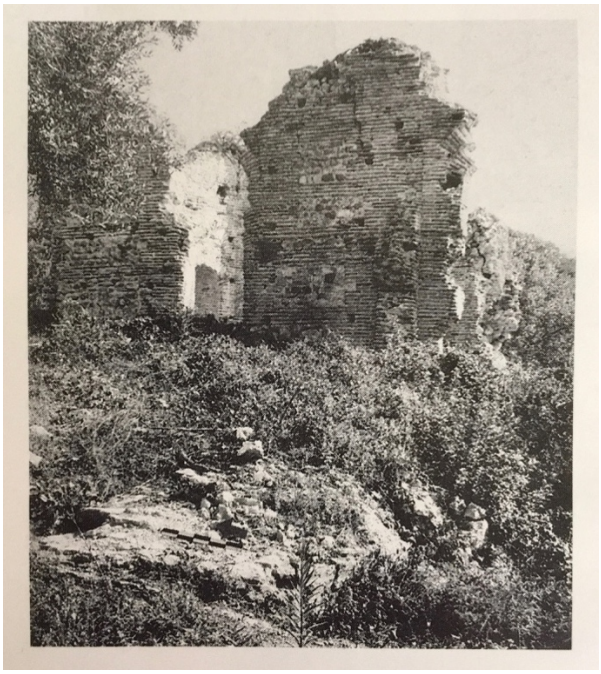

Figure 146. Riza, remains of the decagonal structure (Zachos 1993, pl. 53γ)

Figure 147. Riza, remains of the decagonal structure

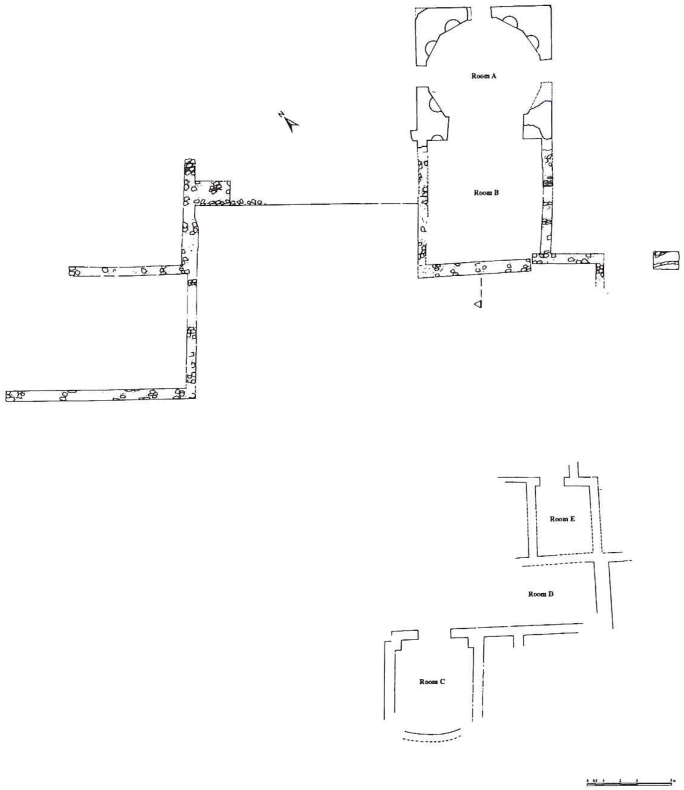

Figure 148. Plan of the decagonal building at Riza (scale: 5 m; Chrysostomou 1982, fig. 2)

Figure 149. Photo of the oilery post excavation and during anastylosis *(Giannaki 2017, fig. 5)*

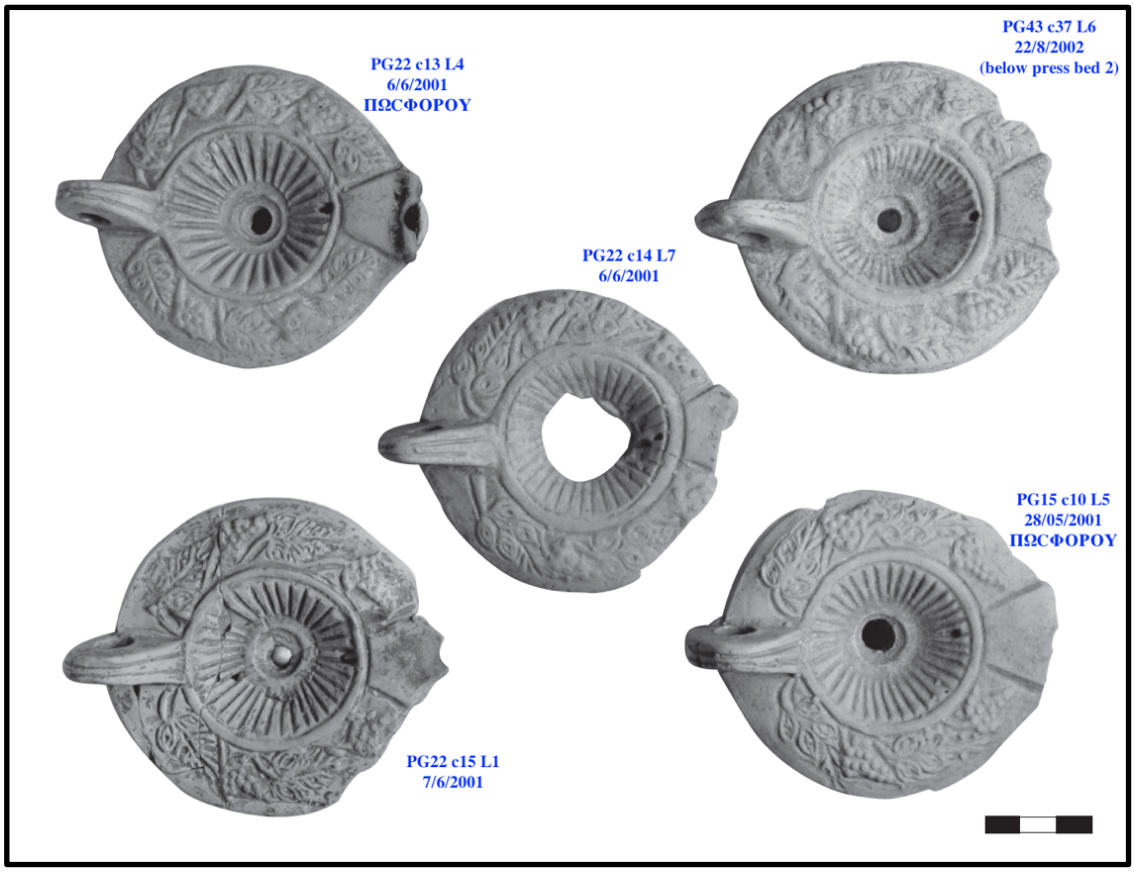

Figure 150. Lamps from the oilery and the pottery groups they derive from (after Giannaki 2017, fig. 15)

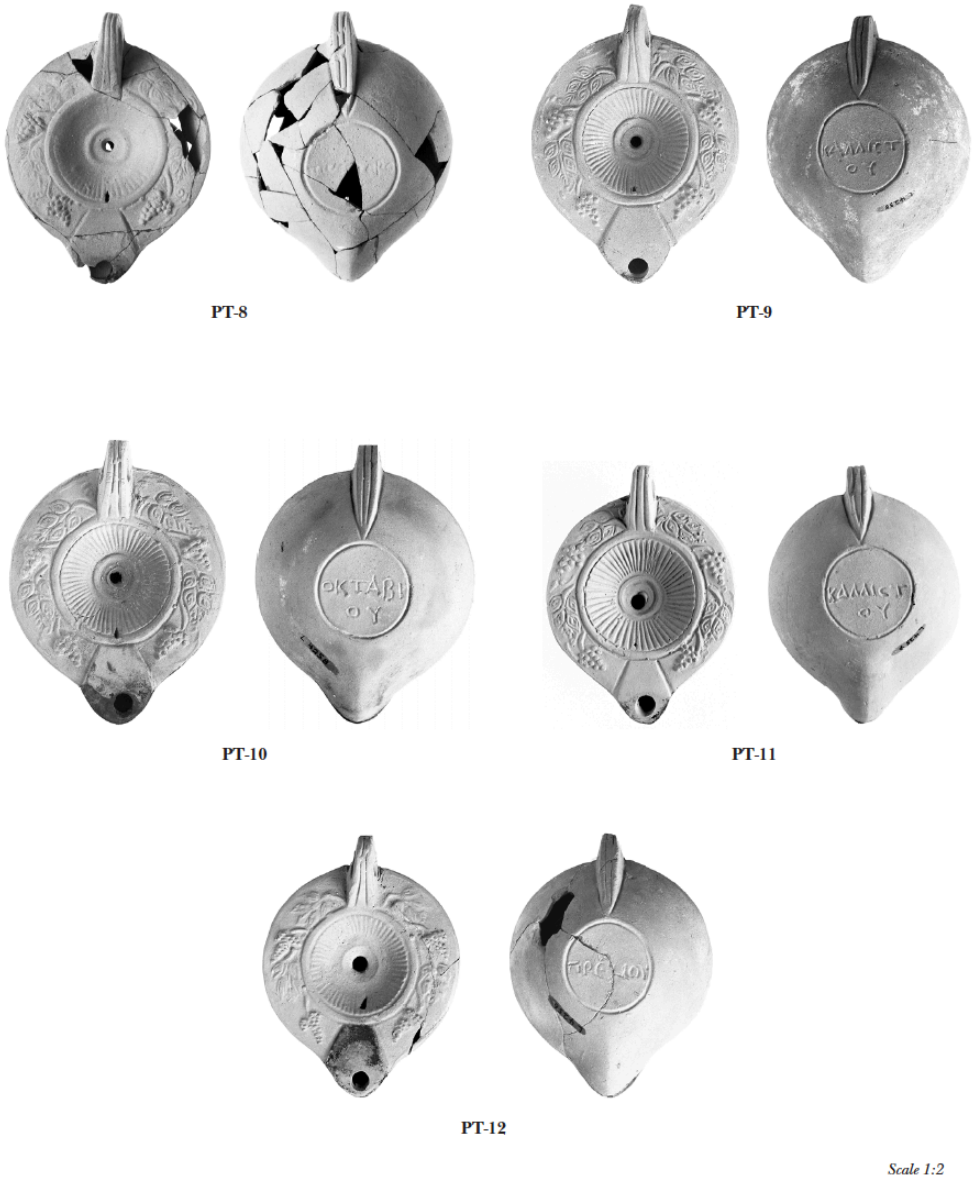

Figure 151. Corinthian vine-and-ray lamps (Slane 2017, pl. 58)

(a)

(b)

Figure 152. Relief bowl from the oilery, found below press bed 3 (Copyright owned by the Ephorate of Antiquities of Arta)

Figure 153. Rosette-discus lamp (cΠ32) (Copyright owned by the Ephorate of Antiquities of Arta)

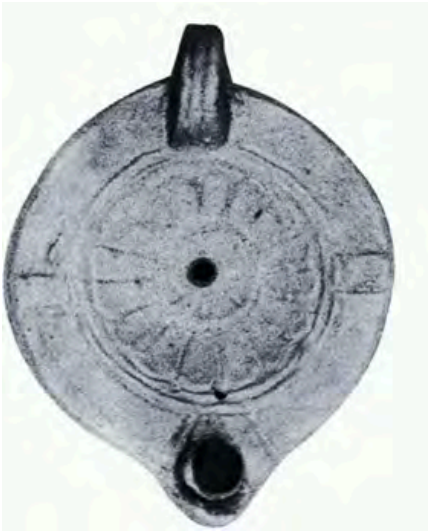

Figure 154. Rosette-discus lamp (Petropoulos 1999, pl. 38, no. M223)

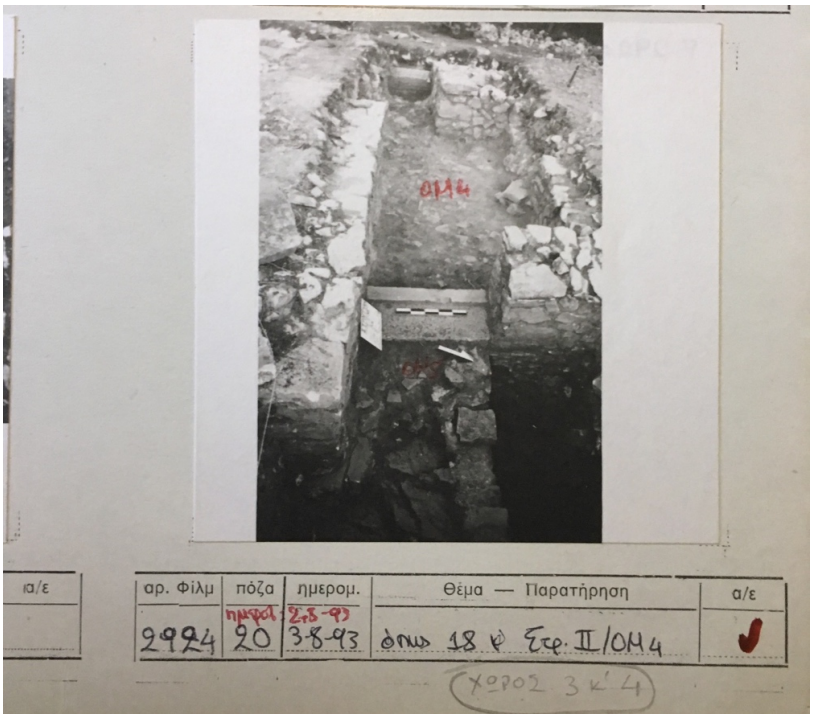

Figure 155. Strongyli, pars urbana, *a probable end-of-use layer from room 3 (OM 4), pre-excavation (Ephorate of Antiquities of Arta, Photocard)*

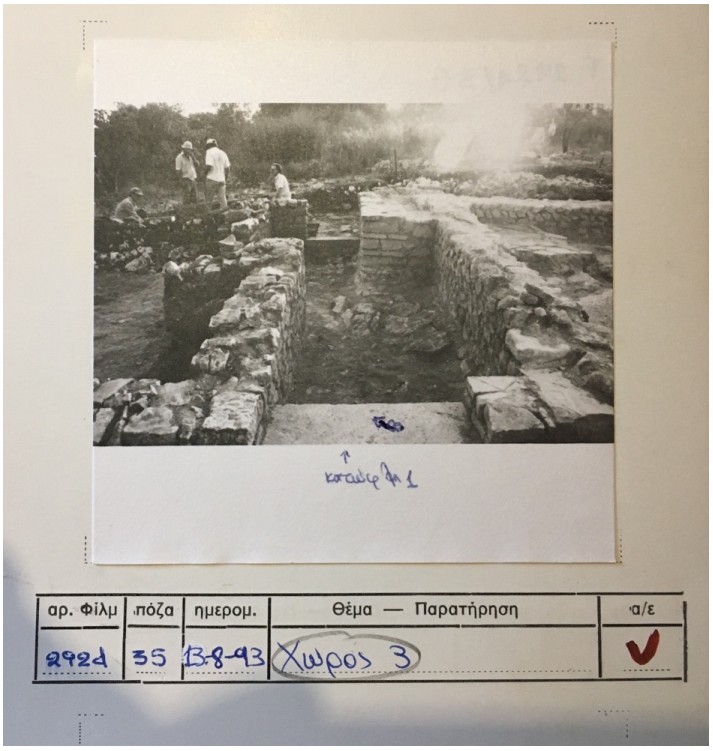

Figure 156. Strongyli, pars urbana, *room 3 at bedrock level (Ephorate of Antiquities of Arta, Photocard)*

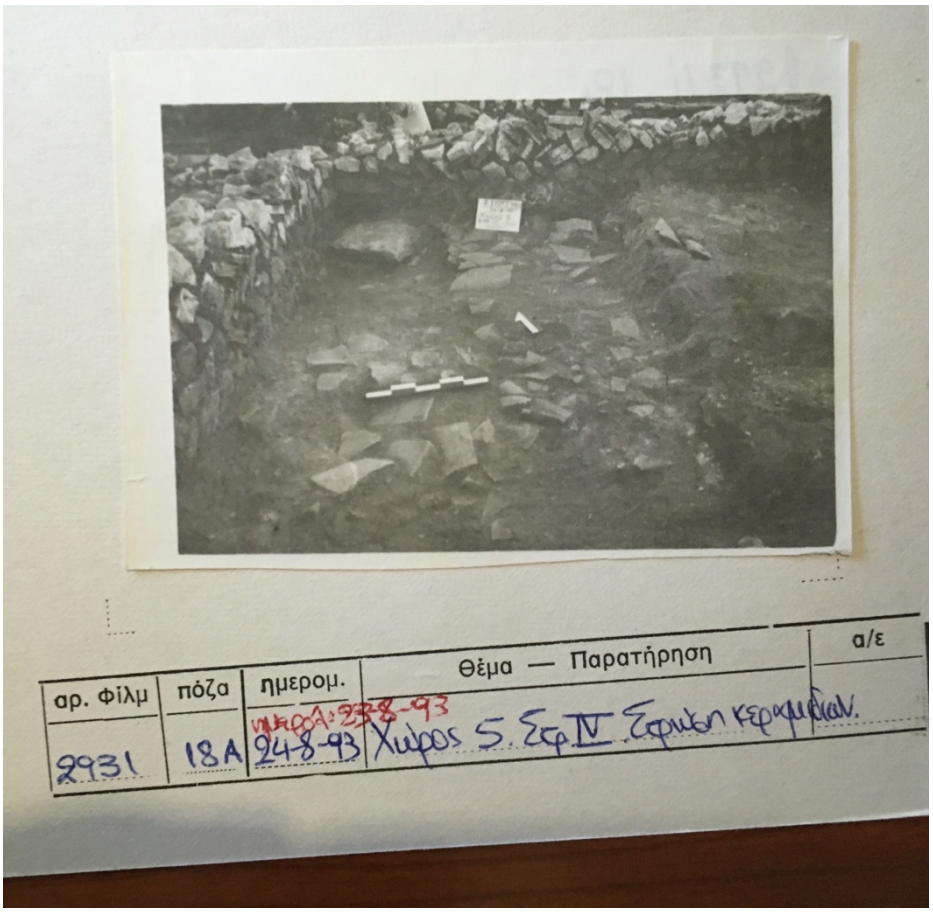

Figure 157. A probable end-of-use layer from room 5. This was excavated, revealing layers of pottery sealed beneath, such as context Str.Room5.III.7., below the tiles pictured next to the large stone in the northwest corner (Ephorate of Antiquities of Arta, Photocards)

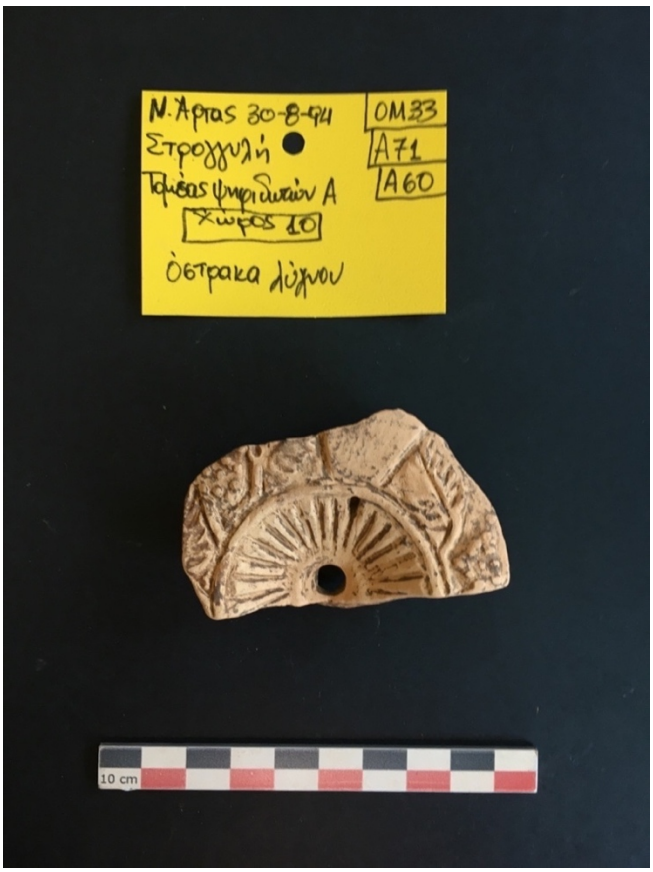

Figure 158. Strongyli, pars urbana, *vine-and-ray lamp sealed below the destruction layer of area 10 (nos. cA71) (Copyright owned by the Ephorate of Antiquities of Arta)*

Figure 159. Strongyli, pars urbana, *vine-and-ray lamp sealed below the destruction layer of area 10 (nos. cA64) (Copyright owned by the Ephorate of Antiquities of Arta)*

Figure 160. Strongyli, pars urbana, *examples of grooved rim cooking pots (Copyright owned by the Ephorate of Antiquities of Arta)*

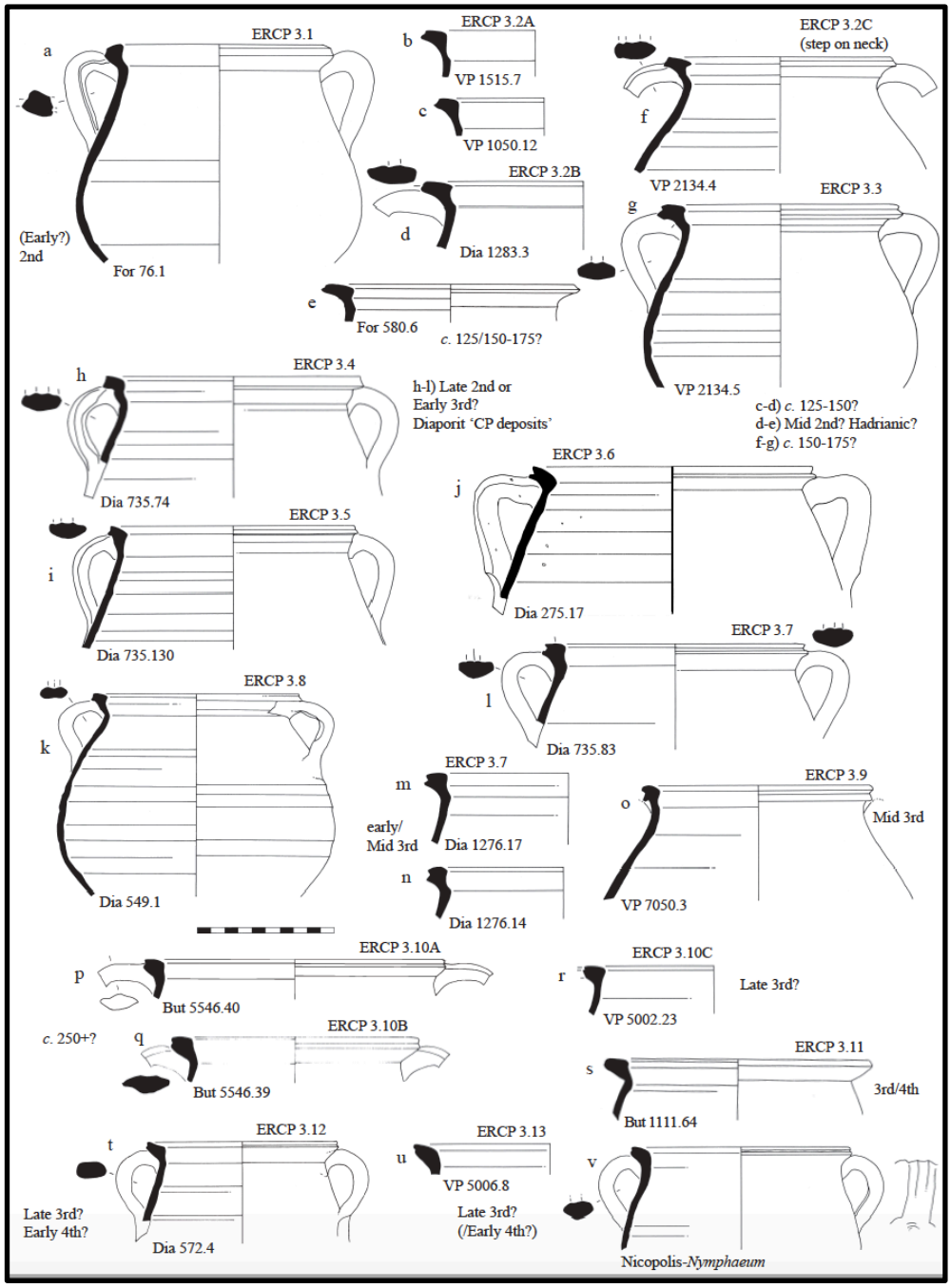

Figure 161. The development of the grooved rim cooking pot (Reynolds 2019, fig. A-5)

Figure 162. Strngyli, pars urbana, rim *fragments of an ARS dish, Hayes form 50A, from room 5; detailed views of the rim and the minute bevelling employed to round it (bottom) (Copyright owned by the Ephorate of Antiquities of Arta)*

Figure 163. Strongyli, pars urbana, *fragments of an ARS dish, Hayes form 50A, from room 5, including rim and base fragments (Copyright owned by the Ephorate of Antiquities of Arta)*

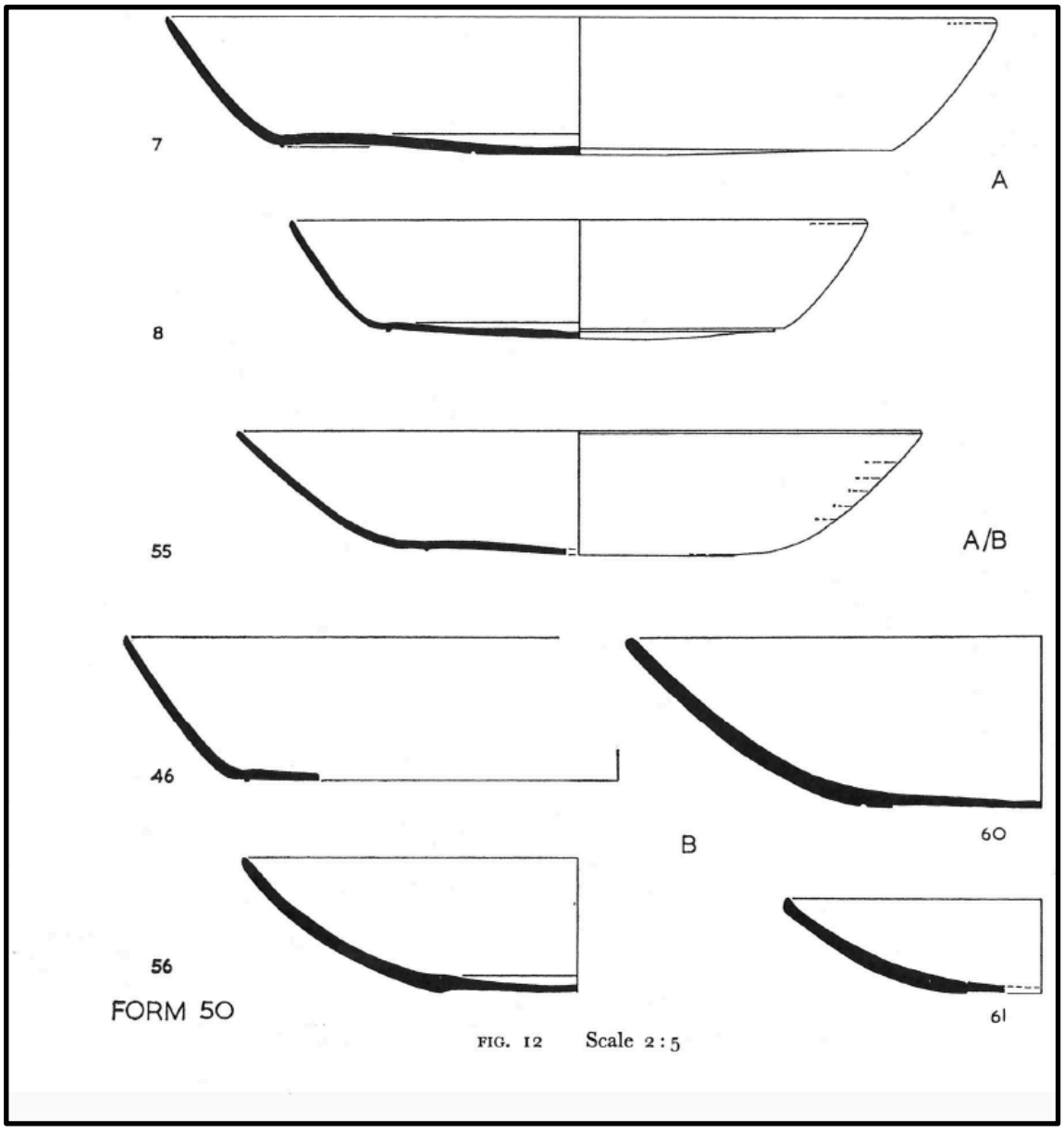

Figure 164. Drawings of ARS dishes Hayes form 50 (Hayes 1972, fig. 12)

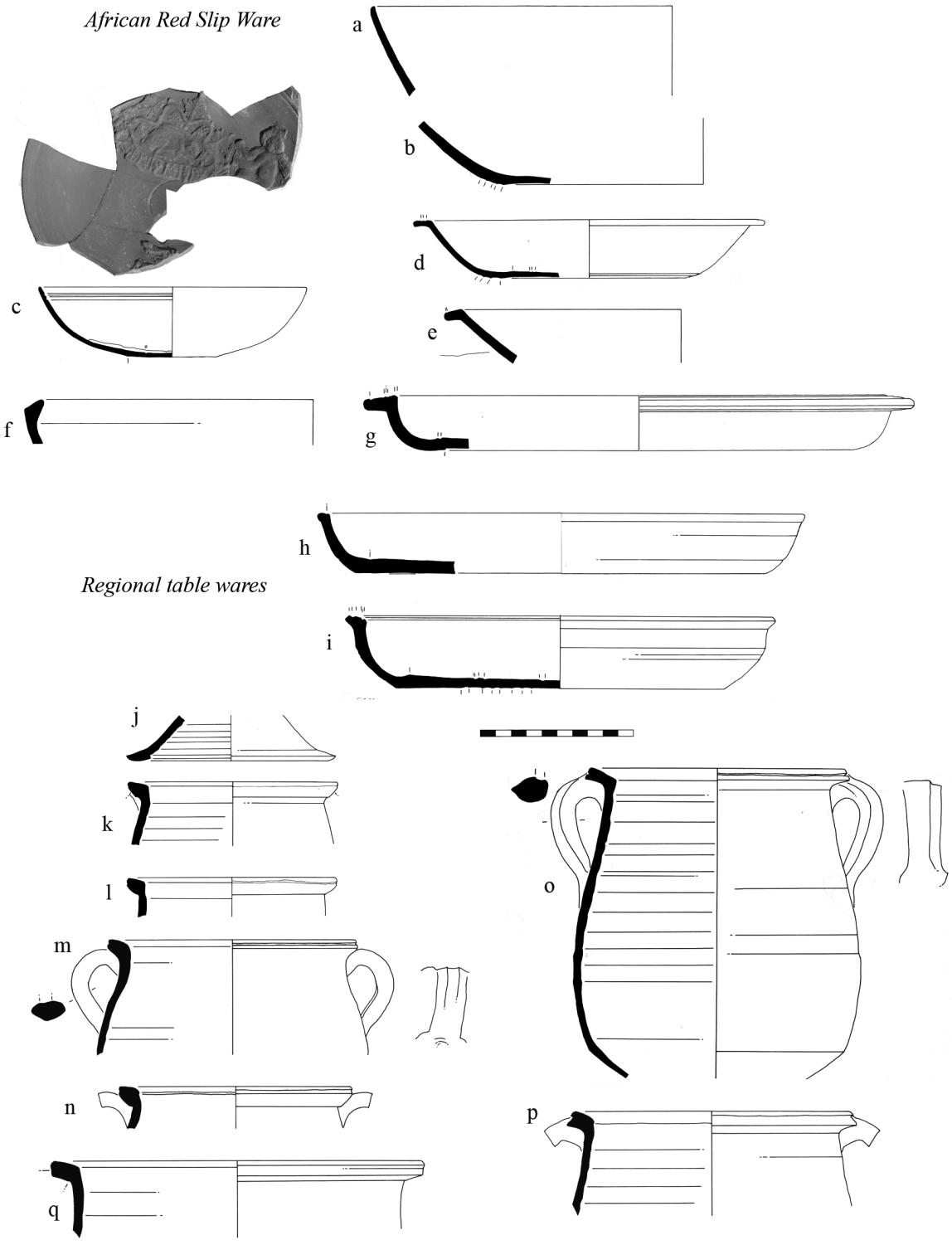

Figure 165. Tablewares (a–i) and kitchen wares from a 4th-century deposit at Nicopolis: a-b are the rim and base of a Hayes 50A, late variant (Reynolds and Pavlidis 2018, fig. 2)

(a)

(b)

Figure 166. The supporting wall of room 1, visible to the right in photo a and to the left in photo b. The room pictured in the middle of photo a is room 3, where the bedrock reached in the excavation is still visible today (Copyright Ephorate of Antiquities of Arta)

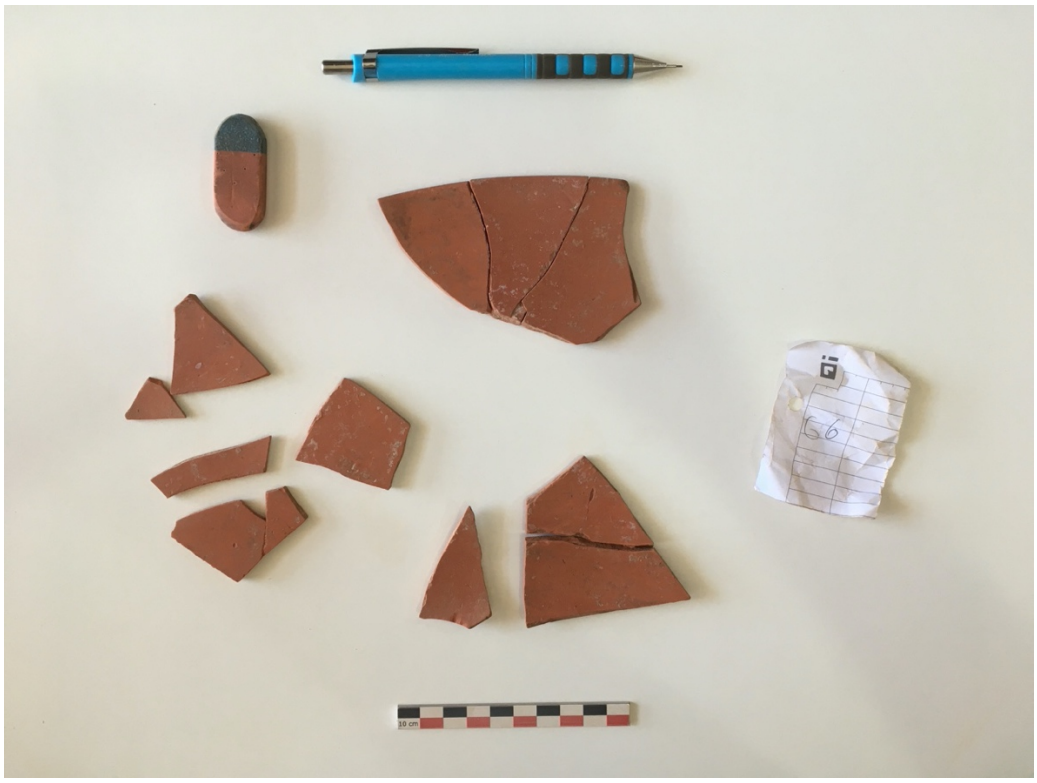

(a)

(b)

Figure 167. Fragments of an ARS 'D' ware dish, Hayes form 50 transitional from type A to B, from the destruction layer of room 1. Notice the pimply interior surface (Copyright owned by the Ephorate of Antiquities of Arta)

Figure 168. Rim of the ARS 'D' ware dish, Hayes form 50 transitional from type A to B, from the destruction layer of room 1, showing the bevelling of the rim from the interior and exterior (Copyright owned by the Ephorate of Antiquities of Arta)

Figure 169. View from Riza over hills with olive groves overlooking the Ionian sea

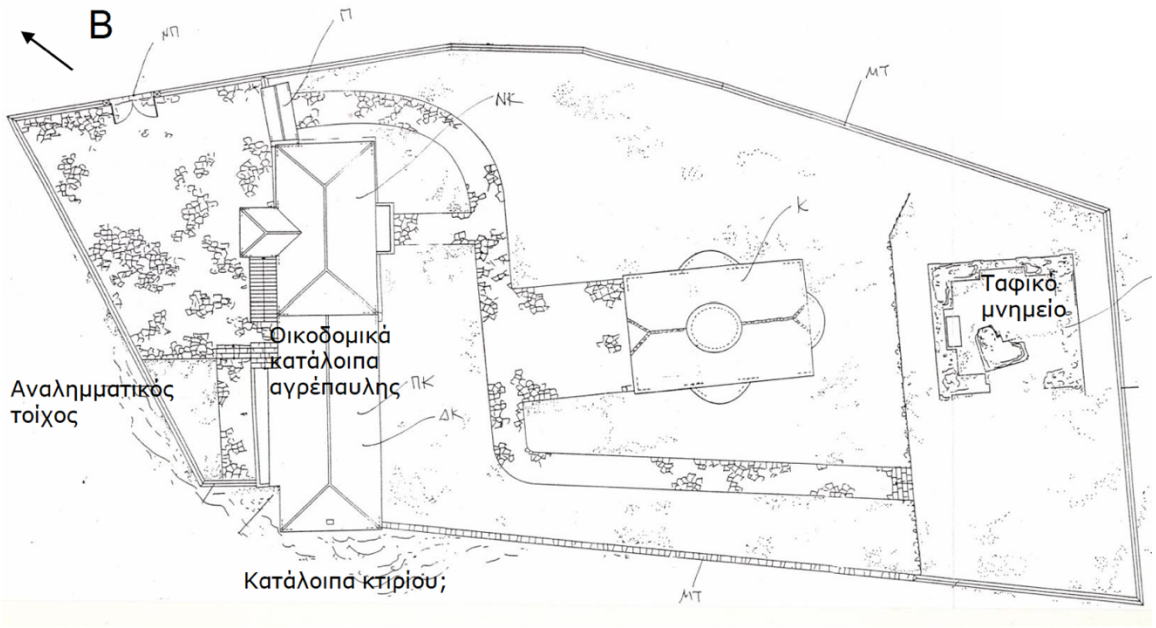

Figure 170. Agia Pelagia, plan of present-day remains indicating the location where ancient remains probably belonging to the villa were found; from right to left, noted are the remains of a retaining wall, those of the villa and of another building, and of the mausoleum *(Konstantaki 2015, pl. 56β)*

γ-δ. Καστροσυκιά, Ι.Μ. Αγ. Πελαγίας. Άποψη του Χώρου 2 και του ψηφιδωτού δαπέδου μετά τις εργασίες ανάδειξης

Figure 171. Agia Pelagia, remains of the villa's pars urbana, showing reconstructed mosaics (Konstantaki 2015, pl. 57γ-δ)

Figure 172. Agia Pelagia, retaining wall (Konstantaki 2015, pl. 59β, after Katsadima and Angeli 2001)

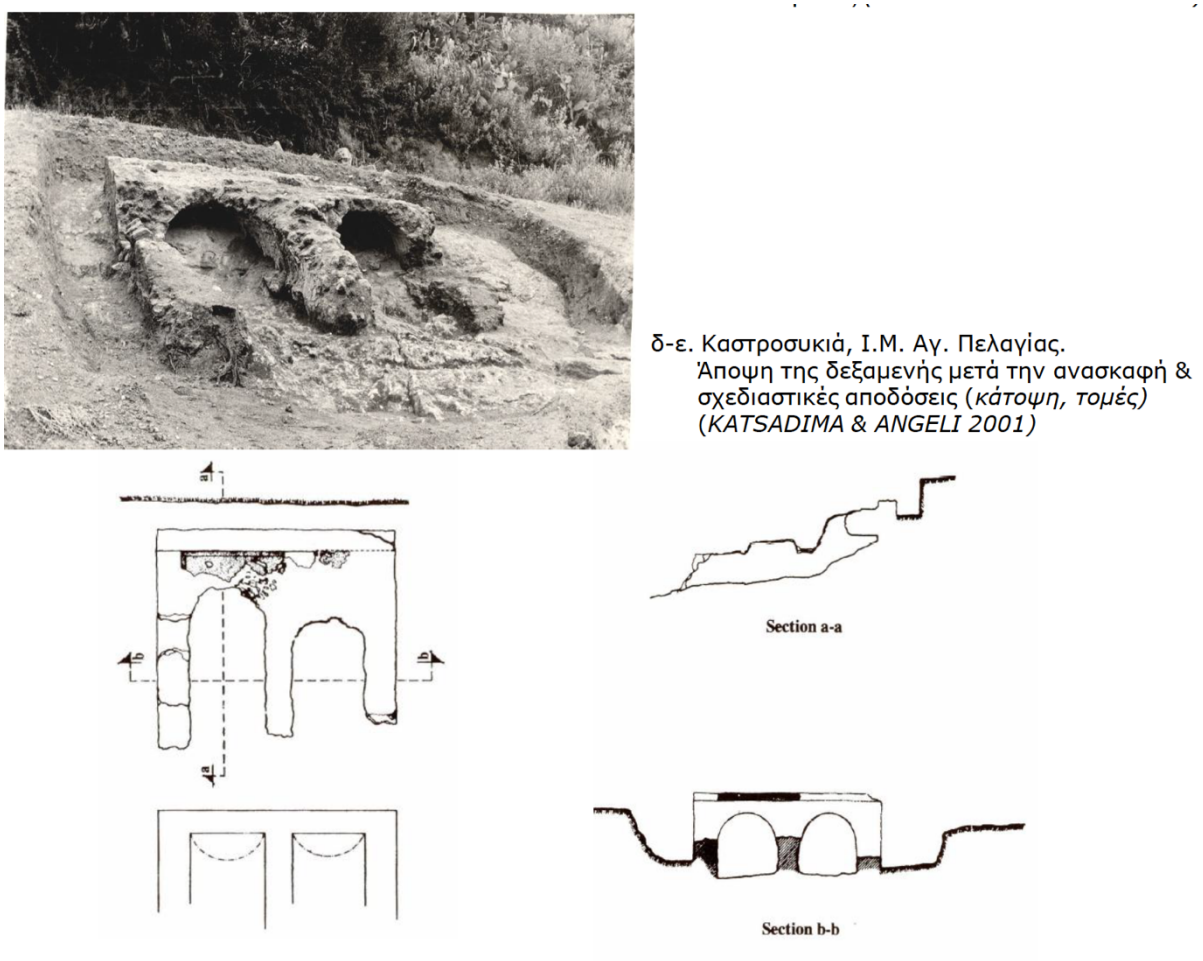

Figure 173. Covered cistern found in the vicinity of Agia Pelagia (Konstantaki 2015, pl. 59δ-ε, after Katsadima and Angeli 2001)

(a)

(b)

Figure 174. The large, open-air rectangular cistern bellow the hill at Agia Pelagia

Figure 175. Agia Pelagia, trapetum *and* orbis *found in the garden of the modern monastery, with other nearby ancient remains (Konstantaki 2015, 59ª)*

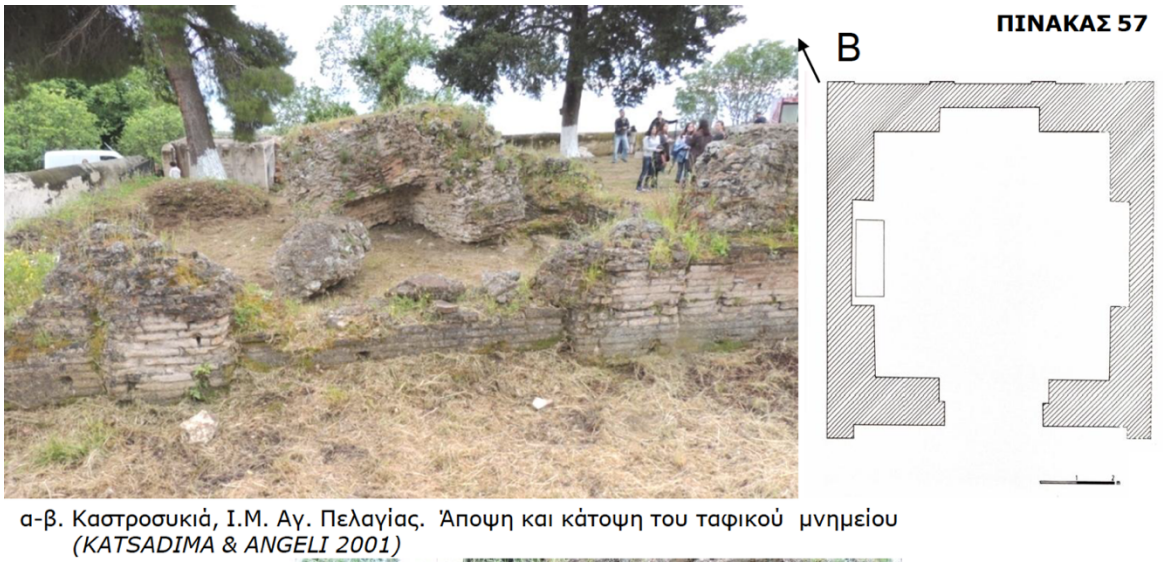

Figure 176. Agia Pelagia, mausoleum *to the left and plan of it to the right (Konstantaki 2015, pl. 57α-β, after Katsadima and Angeli 2001)*

Figure 177. Fragment of the Attic sarcophagus from Agia Pelagia in the Nikopolis Museum

Figure 178. Margarona Attic sarcophagus in the Archaeological Museum of Nikopolis

Figure 179. View of the remains of the rural complex at Almoutses (Photo courtesy of I. Katsadima and her colleagues; Copyright of the Ephorate of Antiquities of Arta)

Figure 180. Almoutses, winery area in the middle-ground (Photo courtesy of I. Katsadima and her colleagues; Copyright of the Ephorate of Antiquities of Arta)

Figure 181. Almoutses, collecting vat (Photo courtesy of I. Katsadima and her colleagues; Copyright of the Ephorate of Antiquities of Arta)

Figure 182. Almoutses, bath suite view from the northwest, showing the remains of the hypocaust in the foreground (Giouni, Katsadima, and Faklari 2012, pl. 20a)

Figure 183. Agios Georgios, mosaic from room I (top), with detail of the goblet overflowing with wine (bottom) (Kykou 2020, fig. 130 and fig. 125)

Figure 184. Kanali, reconstructed mosaic (Kyrkou 2020, fig. 110)

Figure 185. Kanali, detail of mosaic (Kyrkou 2020, fig. 109)

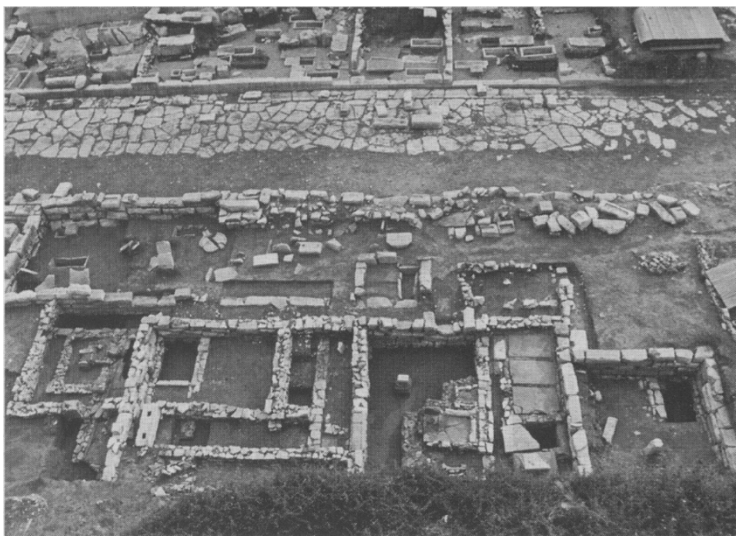

Figure 186. Garoufalia street oilery (lower half of the photo), with the main road of the ancient cemetery of Ambrakia showing (top half of the photo; Aggeli 2012, pl. 2d)

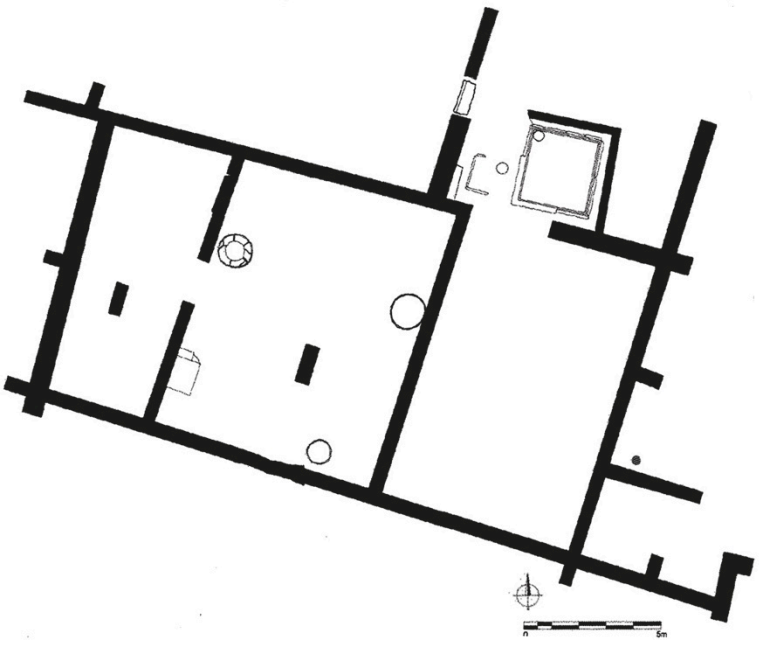

Figure 187. Vaggeli plot villa, pars rustica, *possibly an oilery, showing the two, connected (top) and storage areas with* pithoi *found* in situ *(bottom; Riginos and Sakkas 2018, fig. 12)*

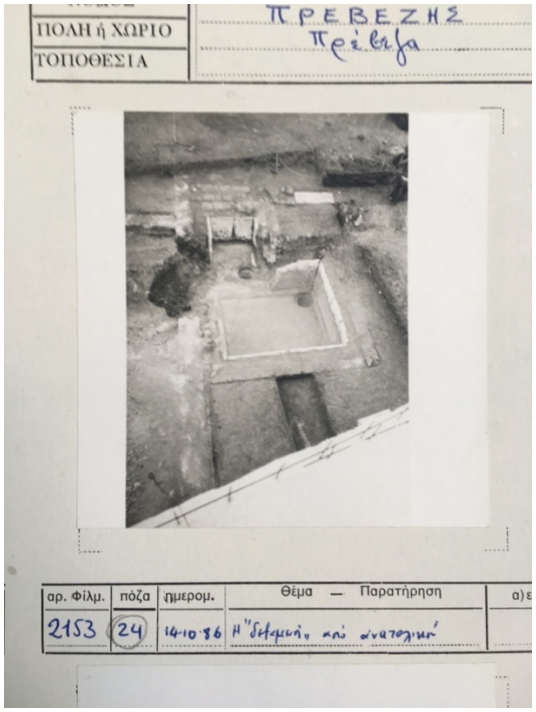

Figure 188. Vaggeli plot villa, pars rustica, vats 1 and 2 *(Copyright Ephorate of Antiquities of Preveza, Photocard)*

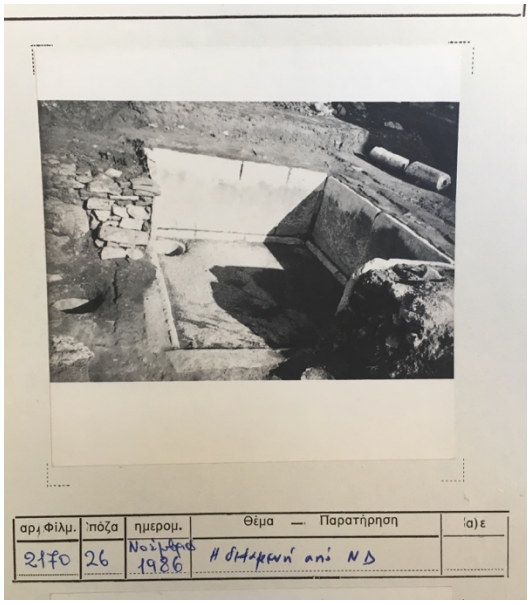

Figure 189. Vaggeli plot villa, pars rustica, vat 1 *(Copyright Ephorate of Antiquities of Preveza, Photocard)*

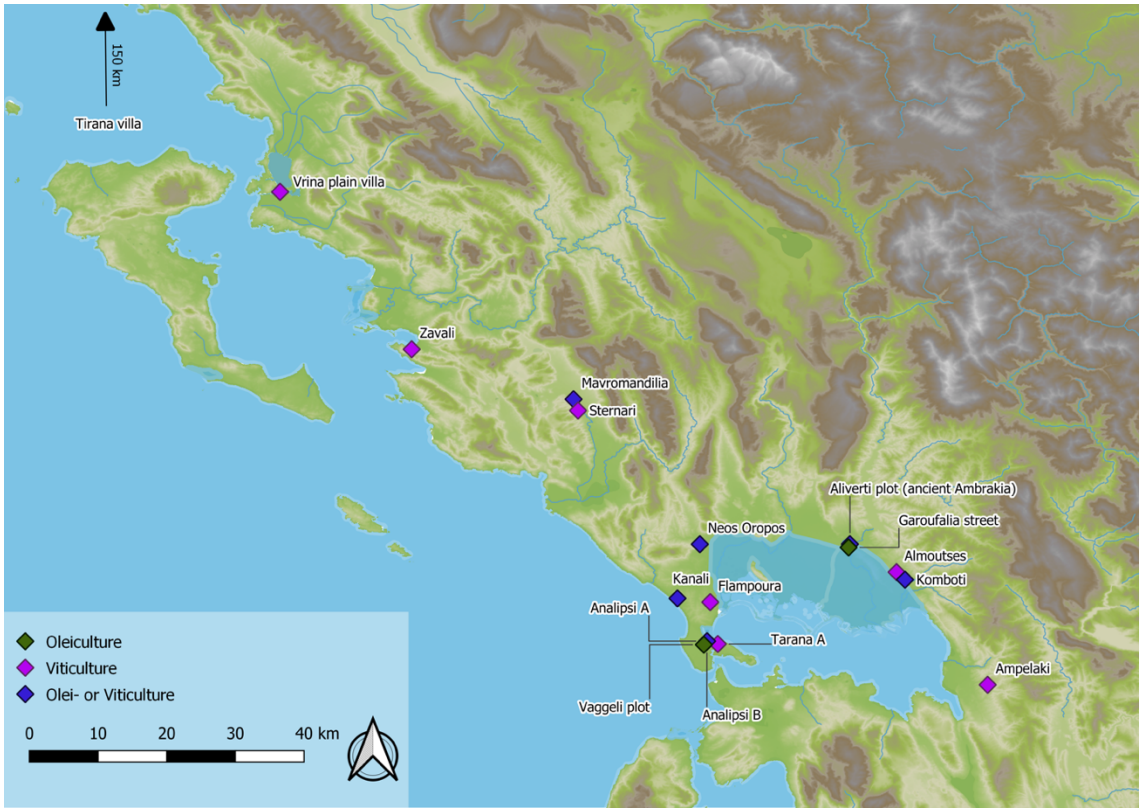

Figure 190. Map showing the location of collecting vats used in oleiculture, viticulture, or either of the two (Map made by Hallvard Indgjerd)

Figure 191. Flampoura vat, vat floor

Figure 192. Flampoura vat, vat floor, showing part of a probable Lamboglia 2 amphora *built into its floor and fragments of the* amphora, *including part of the pointed spike of its base*

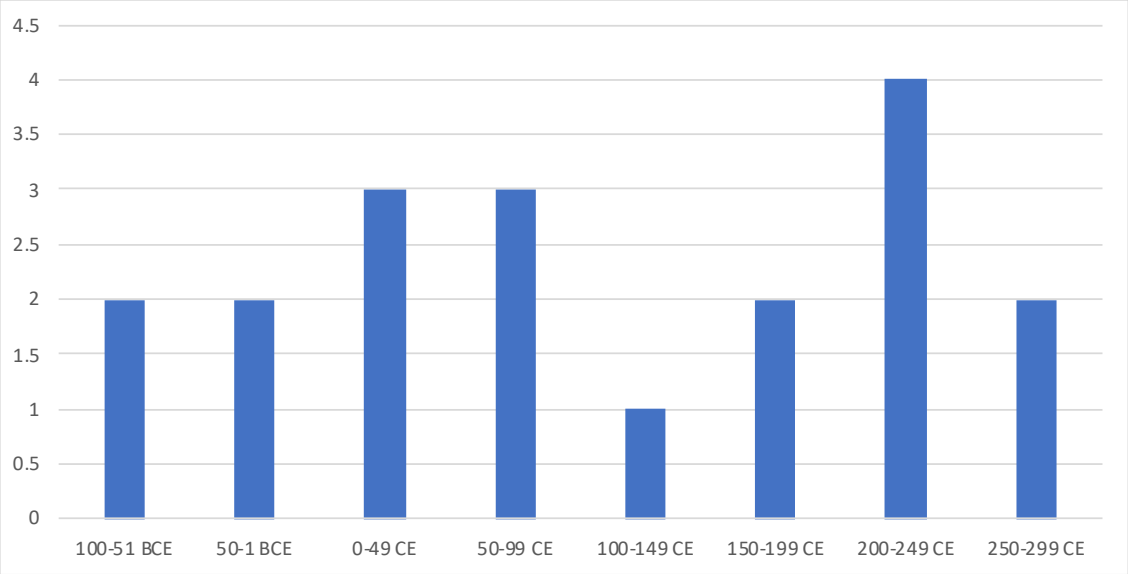

Figure 193. Number of collecting vats possibly constructed in a half-century. Note that this graph does not correspond to vats definitively constructed in a half-century; for example, those that might have been constructed over a century-long period would be counted twice on this graph.

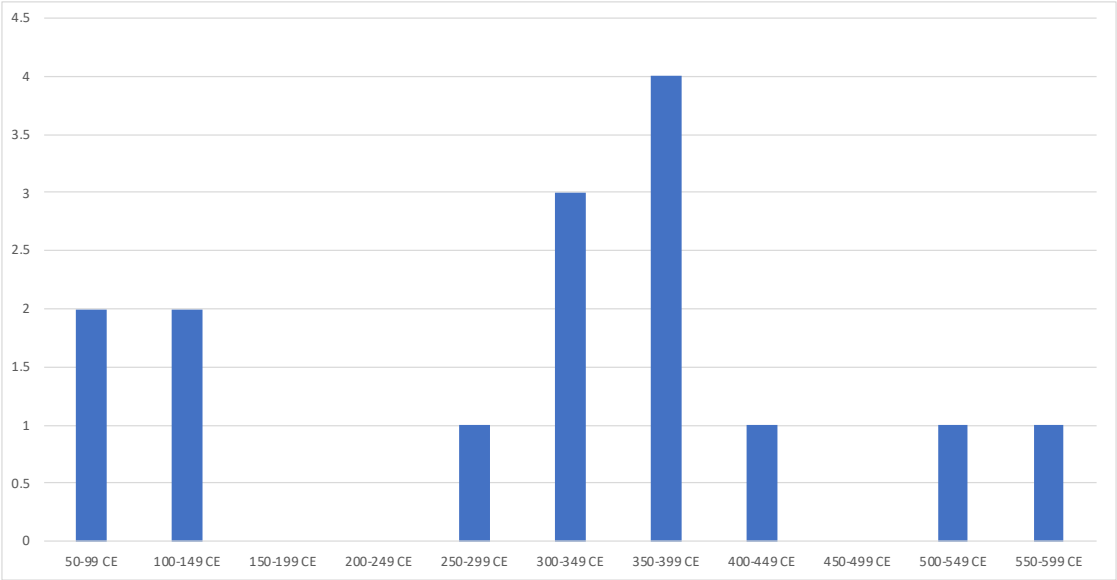

Figure 194. Number of collecting vats possibly disused in a half-century

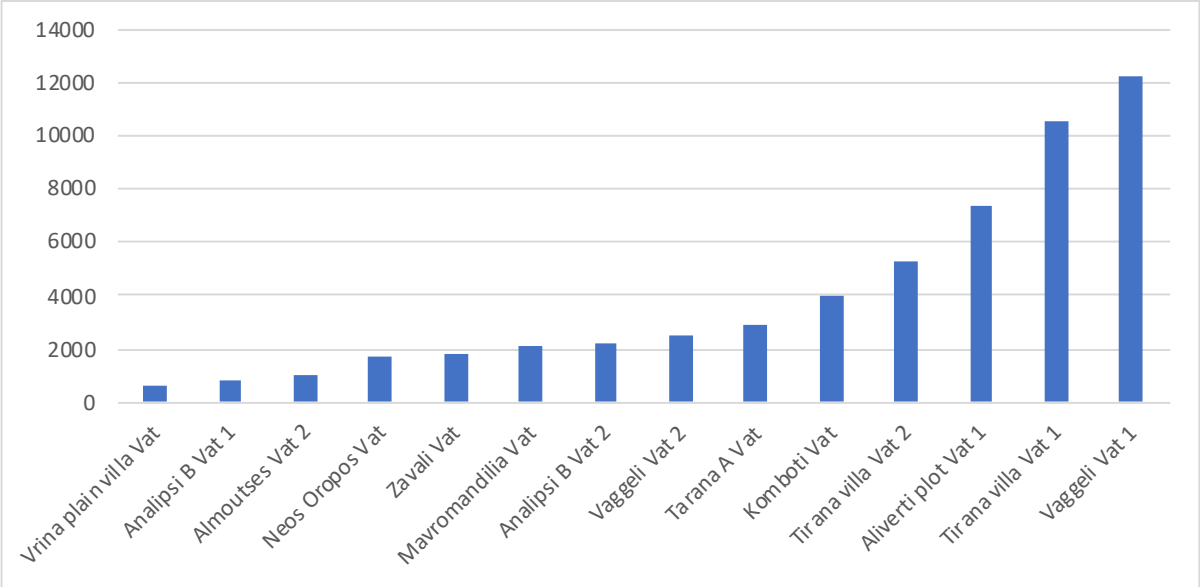

Figure 195. Estimated (minimum) volumes of collecting vats arranged in order of scale